

UC Merced

UC Merced Electronic Theses and Dissertations

Title

Effects of Microwave Radiation on Selected Mechanical Properties of Silk

Permalink

<https://escholarship.org/uc/item/7fj44148>

Author

Reed, Emily Jane

Publication Date

2013

Peer reviewed|Thesis/dissertation

UNIVERSITY OF CALIFORNIA, MERCED

Effects of Microwave Radiation on Selected Mechanical Properties of Silk

Dissertation

by

Emily Jane Reed

2013

Submitted in partial satisfaction of the requirements for the degree of

Doctor of Philosophy

Advisor: Christopher Viney, Professor, School of Engineering
Graduate Group: Biological Engineering and Small-scale Technologies
Dissertation Committee: Valerie Leppert (chair), Jay Sharping, Christopher Viney.

Portions of Chapter 2 © 2011 Wiley Periodicals, Inc.
Submitted 2013 Materials Research Society

Portions of Chapter 3 Submitted 2013 Materials Research Society

Portions of Chapter 4 © 2011 Wiley Periodicals, Inc.
© 2011 Materials Research Society

Portions of Chapter 5 © 2011 Materials Research Society

Portions of Chapter 6 © 2011 Materials Research Society
Submitted 2013 Materials Research Society

Portions of Chapter 7 © 2012 Materials Research Society

All others Chapters and subsections © 2013 Emily J. Reed

The dissertation of Emily Jane Reed, titled *Effects of Microwave Radiation on Selected Mechanical Properties of Silk*, is hereby approved:

_____ Date: _____
Christopher Viney

_____ Date: _____
Jay Sharping

Chair: _____ Date: _____
Valerie Leppert

University of California, Merced

Abstract

Title: Effects of Microwave Radiation on Selected Mechanical Properties of Silk

Name: Emily Jane Reed

Degree: Doctor of Philosophy

Institution: University of California, Merced, 2013

Committee Chair: Valerie Leppert

Impressive mechanical properties have served to peak interest in silk as an engineering material. In addition, the ease with which silk can be altered through processing has led to its use in various biomaterial applications. As the uses of silk branch into new territory, it is imperative (and inevitable) to discover the boundary conditions beyond which silk no longer performs as expected. These boundary conditions include factors as familiar as temperature and humidity, but may also include other less familiar contributions, such as exposure to different types of radiation.

The inherent variations in mechanical properties of silk, as well as its sensitivity to moisture, suggest that in an engineering context silk is best suited for use in composite materials; that way, silk can be shielded from ambient moisture fluctuations, and the surrounding matrix allows efficient load transfer from weaker fibers to stronger ones. One such application is to use silk as a reinforcing fiber in epoxy composites. When used in this way, there are several instances in which exposure to microwave radiation is likely (for example, as a means of speeding epoxy cure rates), the effects of which remain mostly unstudied.

It will be the purpose of this dissertation to determine whether selected mechanical properties of *B. mori* cocoon silk are affected by exposure to microwave radiation, under specified temperature and humidity conditions.

Results of our analyses are directly applicable wherever exposure of silk to microwave radiation is possible, including in fiber reinforced epoxy composites (the entire composite may be microwaved to speed epoxy cure time), or when silk is used as a component in the material used to construct the radome of an aircraft (RADAR units use frequencies in the microwave range of the electromagnetic spectrum), or when microwave energy is used to sterilize biomaterials (such as cell scaffolds) made of silk.

In general, we find that microwave exposure does not detract from the average mechanical properties of silk, but that it may increase the *spread* of data points around that average. Along the way, we come to a number of useful conclusions, summarized here:

Regarding silk in general

- **Storage conditions** can have a significant and enduring effect on tensile properties of degummed *B. mori* silk. Samples stored in a sealed container with

desiccant (silica gel) have a lower yield stress and yield strain than samples stored without desiccant and they also relax more rapidly in stress relaxation tests. The ability of this silk to resist plastic deformation is optimized at intermediate hydration levels. Sensitivity to the humidity levels encountered by samples prior to testing complicates the interpretation of results, and makes inter-laboratory comparisons challenging. Silk storage conditions should therefore be reported—and, ideally, standardized—to enable useful comparison between studies.

- Differences in hand-**reeling techniques** can impose changes on the silk microstructure that significantly affect the results of tensile tests. Breaking strain and toughness were lower for the samples reeled by one person in our study, and the coefficient of variation was markedly higher for those samples in all tensile properties measured (yield strain, yield stress, stiffness, breaking strain, breaking stress, and toughness). Standardization of silk reeling technique is therefore necessary.
- Under our experimental conditions, tensile properties of *B. mori* cocoon silk **annealed** for 7 hr at 140°C do not significantly differ from those of silk taken from the same cocoon but not annealed. Tempered with knowledge about the sensitivity of silk to humidity and that degradation will occur at sufficiently high temperatures, this finding suggests that silk may be used in conditions significantly above room temperature without concern about changes in mechanical performance.
- Tensile properties of degummed silk from the **inside surface** of a *B. mori* cocoon do not differ significantly from those of silk taken from the **outside surface**, provided that samples used in the comparison have similar diameters. In combination with previous studies, this finding suggests that silk from any part of the cocoon may be used without concern over introducing a new source of variability into collected data, subject to the limitation that the sample diameters should be consistent.
- Silk **color** and **cocoon size** have a small to negligible effect on fiber tensile properties.

Regarding microwave oven calibrations

- The **shape** and **aspect ratio** of the calibration vessel can have significant effects on calibration results. Thus, these should both be specified in calibration standards.
- Calibration results depend on the **position** that the calibration vessel occupies in the microwave oven chamber. Thus the calibration vessel should consistently be placed at the same location that subsequent samples will occupy.

- Use of a large **volume of water** in calibrations gives a more accurate measure of the output power of the microwave oven; conversely, use of a smaller volume of water leads to a larger thermal gradient during the calibration, resulting in increased heat loss and ultimately an underestimate of the oven's output power.
- Calibrations performed with larger sample volumes avoid the complicating effects of **standing waves** of microwave energy, thus making the calibrations more reliable.
- **Heat loss** from the calibration vessel can occur *during* calibration of a microwave oven, such that the apparent power (as measured by the calibration) is less than the true output power of the oven. Microwave oven calibration standards should be refined to take account of this heat loss, in order to give a more accurate measure of the power that samples will be exposed to during a particular microwave treatment.
- Reproducible exposure of samples to microwave radiation requires measurement, not an assumption, of the magnetron **start-up delay** time.

Regarding microwave irradiated silk

- Under the experimental conditions reported here, silk is a poor absorber of microwave energy. Thus, silk can be used as a component in materials that are subjected to microwave processing, as well as materials that are subjected to in-service microwave radiation.
- While the mean values of mechanical properties were unaffected by the microwave treatments delivered in this study, the spread of breaking strength values as measured by the Weibull modulus increased with microwave exposure. The decrease in failure predictability of individual fibers suggests that silk can more appropriately be used in a composite material for situations where it will be exposed to microwave radiation, rather than relying on individual, isolated fibers for mechanical performance.
- In situations where microwave heating does affect the mechanical properties of silkworm (*B. mori*) silk (reported elsewhere), those effects are a result of changes that take place via a specific kinetic route that depends on rapid heating and cannot be accessed by a conventional thermal anneal.

Curriculum Vitae

Education

Ph.D. in Biological Engineering and Small-scale Technologies 2013

Dissertation: “Effects of Microwave Radiation on Selected Mechanical Properties of Silk”

Research Adviser: Christopher Viney, Professor of Engineering

University of California, Merced

Materials Research Society student chapter founding member.

Graduate Student Representative, WASC Steering Committee.

Instructional Intern with the Center for Research on Teaching Excellence.

Teaching assistant for the following courses:

Introduction to Materials

Mathematical Modeling for Biology

General Chemistry I

Calculus I

Integrated Calculus and Physics

B.S. in Biological Sciences, with high honors

2007

Emphasis: Cell Biology and Development

University of California, Merced

Intern with the Center of Integrated Nanomechanical Systems.

Regents' Scholar.

Genetics Tutor.

Publications

(*Submitted paper*) Emily J. Reed, Christopher Viney (2013). “Mechanical properties of *Bombyx mori* silkworm silk subjected to microwave radiation” Journal of Materials Research

(*Submitted paper*) Emily J. Reed, Christopher Viney (2013). “Calibrating the power of a domestic microwave oven” PLOS ONE

Emily J. Reed, Christopher Viney (2012). “Does Thermal Annealing Affect the Mechanical Properties of Silkworm (*Bombyx mori*) Cocoon Silk?” Mater. Res. Soc. Symp. Proc. Vol. 1465
DOI: 10.1557/opl.2012.1197

(*Invited Paper*) Emily J. Reed, Lindsay L. Bianchini, Christopher Viney (2011). “Sample selection, preparation methods, and the apparent tensile properties of silkworm (*B. mori*) cocoon silk” Biopolymers, Volume 97, No. 6, pages 397-407. DOI: 10.1002/bip.22005

(*Invited Paper:*) Emily J. Reed, Christopher Viney (2011). “The Effect of Microwave Radiation on Tensile Properties of Silkworm (*B. mori*) Silk” Mater. Res. Soc. Symp. Proc. Vol. 1301 DOI: 10.1557/opl.2011.571

(*Invited Paper:*) Emily J. Reed, Lisa Klumb, Maxwell Koobatian, Christopher Viney (2009). “Biomimicry as a route to new materials: what kinds of lessons are useful?” Phil. Trans. R. Soc. A Volume 367, No. 1893, pages 1571–1585.

Emily J. Reed, Michael R. Dunlap, Jacek Jasinski, Christopher Viney (2007). “Microstructure, Nanostructure, and Properties of the Wasp Petiole.” Mater. Res. Soc. Symp. Proc. Vol. 975.

Acknowledgements

There are many people that have helped over the course of this work, whom I thank:

Christopher Viney- for many years of teaching and friendship.

Marian Goldsmith- for being our silkworm cocoon supplier.

Jay Sharping- for insights on the behavior of microwave radiation, and for providing select temperature and humidity data from his laboratory.

Michael Colvin- for fruitful conversations regarding statistical tests.

Christian Moe- for advice on data handling and lessons regarding the Microsoft Office suite.

Ed Silva- for assistance configuring the Instron.

Gary Reed- for adapting our customized load cell to be able to attach to the Instron crosshead.

The Lu lab- for sharing your precision balance, and water from your purification system. Also for the use of your refrigerator and microwave oven (which was not used for experiments!)

The Leppert lab- for the occasional use of your balance, and for the use of your refrigerator.

Mike Dunlap- for insight on experiments and assistance with equipment.

Mark Lutz- for providing information regarding RO water available in our laboratory.

Keith Perkins- for helpful discussions regarding electromagnetic waves.

Sheryl Barringer- for input on the state of microwave literature surrounding standing waves.

Jon Klingborg, DVM- for discussions on silk as a suture material.

Derick Whitley, DVM- for discussions on the biodegradability and biocompatibility of silk sutures.

And finally my *family* and many *friends*, especially my parents *Gary and Beverly Reed*.

Parts of this dissertation are adapted from my work published previously in conference proceedings and journal papers. References to these works are provided in footnotes throughout.

Portions of the work presented in this dissertation (on pages 38-43) have been funded by the NSF Nanoscale Science and Engineering Center: “Center Of Integrated Nanomechanical Systems” Contract grant number: SA4593

Statement of Originality and Collaboration

All experiments presented in this dissertation are original works of the author, with the exception of experiments (see pages 38 and 41) contributed by Lindsay Bianchini while working in collaboration with me. That being said, I note that most (if not all) of the experiments presented here would not have been possible without the conversations, assistance, and support from multiple sources (including my advisor, colleagues, friends, and family). Therefore, throughout this dissertation, I have chosen to use a collaborative tone (“We performed experiments...”, “Our results indicate...”) rather than individual (“I performed experiments...”, “My results indicate...”). This is also in keeping with standard scientific writing practices.

Table of Contents

Abstract	iv
Curriculum Vitae	vii
Acknowledgements.....	viii
Statement of Originality and Collaboration.....	ix
Chapter 1: Introduction	1
Silks: features, biodiversity, and applications.	1
<i>B. mori</i> silk: processing and structure.	2
<i>B. mori</i> silk: biomaterial applications.	4
Biocompatibility and aqueous processing.	4
Tailoring of surface chemistry and functional groups.....	5
Control of degradation rate.....	7
Ability to form	8
<i>B. mori</i> silk: as a pharmaceutical vector.	9
<i>B. mori</i> silk: as an engineering material.....	9
Mechanical properties—limitations.	10
Biomimetic Fiber Production	12
Mechanical properties—addressing limitations.	13
Microwave exposure.....	14
Microwave Radiation—general information	15
Chapter 2: Materials, Equipment, and Methods	17
Microwave oven.....	17
Beakers	17
Temperature measurement	17
Power calibration.....	17
Silk collection.....	18
Microwave exposure	18
Silk storage	20
Measuring silk fiber diameter	21
Mechanical tests	22

Tensometer	22
Mechanical tests: stress-strain	25
Mechanical tests: stress relaxation	26
Chapter 3: On the Statistical Treatment of Data.....	27
“Is this normal?”	27
Nonparametric statistical tests.....	28
Weibull statistics	29
Chapter 4: Sample Selection, Preparation Methods, and the Apparent Tensile Properties of Silk.....	31
Effect of Silk Location within the Cocoon.....	31
Effect of Storage Conditions	33
Effect of Handling (Reeling) by Different People’	38
Effect of Silk Color	41
Chapter Conclusions	43
Chapter 5: On Calibrating the Power of a Microwave Oven.....	45
Measuring the magnetron startup delay time	45
Effect of calibration ‘work piece’ volume	48
Effect of size and aspect ratio of calibration ‘work piece’	50
Effect of standing waves on apparent power	52
Effect of ‘work piece’ position in the microwave oven	58
Chapter conclusions	61
Chapter 6: Does <i>Bombyx mori</i> Cocoon Silk Absorb Microwave Radiation?.....	62
Chapter-specific Materials and Methods.....	62
Effect of microwave exposure times on <i>B. mori</i> silk tensile properties.....	62
Effect of water load on microwave absorption by <i>B. mori</i> silk fibers	65
Effect of strain rate on the apparent tensile properties of <i>B. mori</i> silk fibers.....	68
Effect of microwave radiation on the failure predictability of <i>B. mori</i> silk fibers.....	69
Does microwave radiation cause thermal heating of silk?.....	71
Chapter conclusions	73

Chapter 7: Does Thermal Annealing Affect the Mechanical Properties of <i>B. mori</i> silk?	74
Chapter-specific Materials and Methods.....	74
Effect of annealing on the mechanical properties of <i>B. mori</i> silk.....	74
Structure-property relationships.....	76
Effect of ambient conditions.....	77
Chapter Conclusions.....	77
 Chapter 8: Future Work.....	 79
Microwave induced enhancements.....	79
XRD analyses.....	80
Deciphering Weibull plots.....	80
Effects of annealing on crystal size.....	81
 References.....	 82

Chapter 1: Introduction

Silks: features, biodiversity, and applications.

Silks are members of a class of biological proteins that are fibrous (as opposed to globular) in nature. Other examples of fibrous proteins include collagen and keratin. All proteins are built from a primary sequence of amino acids, and in the case of fibrous proteins at least part of that sequence is repetitive [1]. Side groups of the amino acids in the primary sequence can interact with each other (either attracting or repelling), so that the primary sequence of amino acids leads to secondary and higher level structures responsible for so many of the properties of these materials.

Silks are produced by multiple members of the phylum Arthropoda, including silkworms, spiders (each producing up to six different types of silk [2]), bees [3] [4], myriapods [5] (though some of the millipede secretions may be only “silk-like” and not true proteins [6]—much about their secretions remains unexplored), embiids [7] [8], and ants [9], among others [10]. While silks from different arthropods can be quite distinct from each other in structure and performance, all seem to share several characteristics [10]: silk proteins are produced by specialized glands, are high in alanine content, contain crystals formed from secondary structures, and are mechanically strong or tough. Interestingly, fibers containing silk-like domains are also produced by some mussels (which are not arthropods) as a component in the adhesive filaments (byssus) used for substrate attachment [11] [12]. These fibers also include domains of collagen, and thus provide an example of a natural block copolymer.

The natural uses of silk are as varied as the creatures that produce them. Many are involved in providing the **mechanical support** of a habitat (radial “spokes” of spider webs, silk-lined embiid abodes [13], tropical ant nests [9], honeycomb walls [3] [4]) and **protection** (egg cases and cocoons of many species, including silkworms [14]), while others facilitate **energy dissipation** (spider major ampullate and viscid silks [15], food capture nets of caddisfly larvae [16] [17]), provide **thermal insulation** (silkworm cocoons [18]), are used to facilitate **reproduction** (wrapping material for nuptial gifts of some spiders [19] [20], webs for sperm transfer [21]), and for prey **immobilization** (some spiders wrap their prey after catching [22] [23] [24] [25]), serve as an **adhesive** (viscid silk catching spiral of spider webs [15], nest construction of some ants [9], component of the bolas swung by bolas spiders to capture prey [25]), may provide **water proofing** (as in embiid nests [13], or silkworm cocoons [26]), or even function as a gill for **gas exchange** [27] (for the air-breathing water-dwelling diving bell spider *Argyroneta aquatica*).

The artificial uses of silk have their roots in textiles. The most readily available silk for human use is that produced by the domesticated silkworm (*Bombyx mori*). The large quantity of silk produced by a silkworm during construction of its cocoon (each contains a single fiber approximately 1000 meters long [28]), coupled with the ease of raising

silkworms domestically, continues to facilitate the use of silkworm silk over other types of silks in textiles, as well as in many research efforts.

Exceptional mechanical properties have piqued interest in spider silk in recent decades (see for example reference [29] in which the authors find silk from *Caerostris darwini* to be 10 times tougher than Kevlar), but the cannibalistic nature of spiders limits the quantity of silk that can be obtained from spiders reared in captivity—they cannot be confined in small quarters the way silkworms can. Efforts to produce spider silk through alternative vectors are ongoing (bacteria [30] [31], potato and tobacco plants [32], transgenic silkworm [33] [34] [35], mammalian cells [36], and the milk of transgenic mice [37] have all been used as expression vectors), but to date all are limited in either the quantity of silk that can be economically produced, and/or the mechanical properties of the artificially spun fibers do not match those of naturally produced spider silk. Efforts to improve the quality and yield of biomimetic silks are part of the ongoing branch of biomimetic engineering; the development of this field will be spurred on by a more complete understanding of their naturally produced silk counterparts. In the interim, silkworm silk remains a viable option for more immediate engineering applications, and it is this material that will be examined as the focus of this dissertation.

Silkworm silk has been used in high quality textiles for centuries. In recent decades, its uses have expanded into the fields of engineering (e.g. as high performance fibers) and medicinal research (e.g. as a scaffold for cell growth, and as a drug delivery vehicle). In many cases, engineering and medicine have looked to silk for different properties (mechanical and chemical respectively), but those properties all share the same root: the inherent composition, processing, and structure of silk, which bears closer examination.

***B. mori* silk: processing and structure.**

B. mori silk is secreted from glands located on both sides of the silkworm's head. The silk is composed primarily of two proteins: fibroin (~75%), and sericin (~25%), with smaller amounts of other natural materials such as waxes and salts (reviewed in reference [38]). Fibroin consists of three protein components: a heavy (H) chain [39] (~350 k Da [38]), a light (L) chain [40] (~26 k Da), and the glycoprotein "P25" [41] (~30 k Da [38]), which coexist in a 6:6:1 molar ratio [42]. The H and L chains are linked by a disulfide bond, which is essential for proper secretion from the silk gland [43]. Six of the H-L dimers associate with P25 through a noncovalent interaction [44]. P25 is believed to help maintain the integrity of the complex, which totals approximately 2.3 MDa [42].

Polarized-light microscopy has indicated [45] that processing of fibroin in the silkworm is carried out through a liquid crystalline phase, which facilitates molecular alignment and flow, and helps to minimize the energy expenditure of the silkworm. Ducts containing the fibroin lead to the front of the head and merge into a single spinneret, where a single fiber (a "bave") is formed by joining the two fibroin microfibers ("brins") from the ducts. Studies of fibroin solution have indicated [46] the self assembly process

involved in drying includes a transition from microspheres (in which the hydrophobic regions of fibroin are clustered inside the microsphere, surrounded by hydrophilic regions at the surface) to nanofilaments as the solution dries. In vivo silk processing necessarily involves the concurrent motion of fibroin down the duct as the solution dries, thus influencing the final microstructure of the silk. The two brins are adhered to each other with a glue-like protein called sericin which is secreted along the outside of the brins. The sericin provides minimal contributions to the tensile properties of individual fibers (the yield and breaking strengths of sericin [47] are lower than that of fibroin), and serves instead as a matrix which keeps the fibers of a cocoon together and able to work collectively to protect the silkworm inside.

When silk fibers are collected from cocoons for study in the lab, in many cases they must first be freed from the sericin glue adhering them to the cocoon. This is done in a process called degumming. The simplest method of degumming involves boiling the cocoon in water until fibers are loosened enough to reel from the cocoon. Although it has been suggested that this method of degumming has minimal effects on the microstructure of silk (as determined from differential scanning calorimetry) [48], other studies have indicated that the mechanical performance of the fibers may still be affected (decreases in the elastic modulus [49], yield strength [50], yield strain [49], and Weibull modulus [51] have been reported). Other methods of degumming include addition of various chemicals to the bath to achieve a more complete removal of sericin, though in many cases these chemicals alter the silk fibroin as well, further affecting mechanical properties [52] [53] [54]. Ideally the degumming treatment will remove as much of the sericin as possible if fibers are intended for tensile tests, so that diameter measurements of the fiber (used in calculations of fiber strength, stiffness, and toughness) reflect the load bearing (fibroin) component only.

The microstructure of fibroin is dominated by two phases: one crystalline (capable of diffracting), and the other primarily amorphous (does not produce a discernible diffraction pattern, though some positional ordering of the chains may still exist [55]). The regions connecting the crystalline and amorphous microstructures have been called the “interphase”, and have been observed through the use of ATR infrared spectroscopy on deuterated silk [56]. The crystalline regions are thought to be responsible for the high tensile strength and stiffness of silk [51], while extensibility is attributed to the disordered regions [57]. In the crystalline regions, the amino acid chains fold back on themselves to form an antiparallel β pleated sheet (stabilized with hydrogen bonds), as deciphered through X-ray diffraction in 1955 [58]. Sheets then stack against each other to form crystals. cDNA sequencing has shown that the crystalline regions are dominated by the motif (Gly-Ala-Gly-Ala-Gly-Ser)_n [59]. Because side groups of the amino acids alternate which side of the backbone chain they lie on [58], and since Gly (every other amino acid) has a particularly small side chain (a single hydrogen atom), the antiparallel chains display a bimodal layer spacing; 5.7 Å between chains when alanine and serine are juxtaposed, versus 3.5 Å when glycines are [58].

The amorphous regions are formed from motifs that are similar to that described above, but with several modifications [59]; serine residues are replaced with tyrosine, whose

cyclic (and bulky) side group disrupts the ability of chains to pack closely. In addition, alanine is sometimes replaced by valine or tyrosine, so that the overall sequence is less regular (further hindering crystallization). Random coils are present within the amorphous region, and thermal conductivity studies [60] have indicated their end-to-end length at rest is approximately 61% of their contour length.

Details of the microstructural form silk takes on are strongly tied to the mechanical processing it receives, as well as its chemical environment. A discussion of the different forms of silk (polymorphs) that have been observed is presented in reference [61]. Regardless of the processing silk receives, the fact that it is a protein remains unchanged, as does its primary structure (the amino acid sequence).

***B. mori* silk: biomaterial applications.**

A “biomaterial” has been formally defined [62] as “*a substance that has been engineered to take a form which, alone or as part of a complex system, is used to direct, by control of interactions with components of living systems, the course of any therapeutic or diagnostic procedure, in human or veterinary medicine.*” Silk has been used as a suture material for centuries, and in that traditional capacity has acted as a biomaterial; in modern times, the biomaterial applications of silk have expanded into the realm of biomedical engineering, wherein scaffolds for cell growth can be made of fibroin, and chemically decorated to promote specific cellular behaviors (details below). In the sections below, a series of examples are given to illustrate the present usefulness as well as the future potential of silk based biomaterials. The literature is too vast to include a description of every modification and use here—it is the author’s opinion that additional examples would not help frame the reader’s perspective for the present dissertation; instead the reader is referred to several published papers (references [63], [38], [64], [65], [66]) for additional information.

Biocompatibility and aqueous processing.

A key feature of any biomaterial is that it be biocompatible with the cells or tissues it is to be in contact with. Experiments performed with silk fibroin fibers have indicated [67] they are immunologically inert as measured by macrophage response *in vitro*. There has been some confusion surrounding whether silk is capable of initiating adverse biological responses, but several studies have indicated (discussed and reviewed by Altman et al. [63]) that sericin is the main allergenic agent in silk, and it is believed that adverse reactions to silk fibers *in vivo* have been the result of incomplete removal of sericin. Thus, the biocompatibility of silk *fibroin* is considered good, provided sericin removal is complete [63] [68] [69].

Silk processing is naturally carried out in aqueous conditions (the phase through which the energy efficient transformation to solid silk occurs has been termed an “aquamelt”

[70]), which holds another advantage for biomaterial applications. Since processing of silk does not *require* the use of harsh chemicals or organic solvents [71], it is possible to altogether avoid the problem [72] of residual traces of these chemicals when using silk as a biomaterial. It is interesting to note that even when processing is carried out in aqueous conditions [71], it is still possible to achieve microstructural changes (i.e. β -sheet formation) that result in a water-stable product. This is possible thru the addition of salts in aqueous solution, which draw water molecules out of the silk structure, allowing formation of stable β -sheet structures.

Tailoring of surface chemistry and functional groups.

One specific feature of silk that makes it a useful biomaterial is the ability to functionalize (and more generally, modify) the surface. For example, by incorporating growth-promoting molecules into the surface fibroin, scaffolds made of silk can be used to facilitate growth (or other behaviors) of tissues. Many modifications to silk have been developed, historically for use in textiles (see reference [73] for a review). More recently, interest has developed in modifications that could transform the way silk is used as a biomaterial. Many modifications deal only with the surface of the silk, as that is where contact with cells and tissues will occur. Here we illustrate the potential for biomaterial applications by highlighting a variety of modification examples:

UV treatment

UV treatment of silk surfaces can be used to enhance surface hydrophilicity [74], which can be beneficial for cell adhesion and growth. The UV treatment provides high energy photons which can break the fibroin chains at the silk surface [73], forming free radicals. Reaction with atmospheric oxygen then leads to the formation of polar groups (such as -OH) at the silk surface. Because only the surface is affected, changes in crystallinity and strength of the fiber are negligible. We note however that an earlier study of photochemical reactions (as they relate to photoyellowing and phototendering of *B. mori* silk) indicates that extended UV/ozone treatments can affect the bulk of the silk material, decreasing overall crystallinity degree as indicated by Fourier transform infrared spectroscopy [75]. These authors propose this decrease is due to molecular rearrangements that accompany UV/ozone induced scission of peptide bonds. Thus, any UV treatment to alter the surface only of silk should be carried out in moderation.

Gelatin incorporation

Surface modification can be used to simultaneously decrease the inflammatory response to silk and facilitate desirable mechanical properties. As mentioned previously, problems with biocompatibility and hypersensitivity to silk is usually caused by sericin rather than fibroin. Therefore, sericin must be removed in order

to help eliminate inflammatory reactions when silk is used as a biomaterial. However, complete removal of sericin can have the unintended consequence of causing the fibers to fray, and can decrease fiber strength and stiffness [69]. In addition, the surface becomes more hydrophobic due to the removal of hydrophilic sericin. To address these problems, surface modification with gelatin has been shown to be effective both at enhancing mechanical properties, and increasing biocompatibility (as measured by rat *in vivo* inflammatory responses) [69]. The authors of the study note that the same surface modification technique (sericin free fibers were immersed in aqueous gelatin solutions for 1 hour) could be used to incorporate polysaccharides and growth factors into the silk surface for a variety of tissue engineering needs.

Calcium phosphate coating

Another silk coating that holds potential benefits is calcium phosphate. Tests performed in rat plasma show that calcium phosphate coated silk has a hemostatic effect—speeding the intrinsic coagulation times relative to both normal plasma, and plasma in contact with non-coated silk [76]. Thus, surface modified silk also holds potential as a wound dressing material. A separate study [77] has shown that coating fibroin mats with silver nanoparticles effectively inhibits the growth of certain microorganisms—another benefit for a wound dressing material.

Genetic engineering modifications

Silk proteins can be bioengineered through recombinant DNA technology for precise control of chemical features. While this modification affects more than just the silk surface, we include mention of it here since the altered surface is the primary point of interaction with any biological tissues. The transgenic potential of silkworms was demonstrated in 2000 [78] by successful genetic insertion and expression of green fluorescent protein (GFP) at multiple sites throughout the silkworm genome. Since then, efforts have expanded toward genetically engineering silkworms to produce specific motifs en mass through the silk gland. One research group has reported [79] successfully producing transgenic silkworms whose fibroin encodes the calcium binding sequence $[(AGSGAG)_4E_8AS]_4$. Porous scaffolds made from the transgenic silk were found to promote earlier mineralization and bone formation in rabbit femurs compared to those made of native silk fibroin.

Genetic engineering involving the fibroin genome can also be performed *outside* of the silkworm. The silk-elastinlike polymers (SELPs) are a good example of genetically engineered protein block copolymers based in part on silk; by alternating the $(Gly-Ala-Gly-Ala-Gly-Ser)_n$ silk fibroin sequence with $(Gly-Val-Gly-Val-Pro)_m$ elastin motifs, SELPs can be produced en mass via bacterial expression (often *Escherichia coli*). Once purified from the host, the SELP can be formed into drug delivery vehicles with controlled release times [80] (see section below on degradation rate), or used as a functionalized surface coating. In addition, the ability to incorporate biorecognition sites into the SELP sequence

gives potential for *targeted* drug delivery (see section below on silk as a pharmaceutical vector).

Chemical modifications

In addition to surface treatments, coatings, and genetic modifications, silk fibroin can also be chemically treated to decorate the surface. Graft copolymerization of vinyl monomers can provide a variety of modifications (dependent on the grafted monomer). For example, increased thermal stability and water repellency has been achieved [81] via graft polymerization of methyl methacrylate onto *Antheraea assama* silkworm silk fiber.

The presence of amino acid side chains with functional groups provides opportunities for many different chemical modifications [73]. In another case [82], silk films have been modified to promote bone tissue growth: Fibroin films were soaked in PBS buffer to facilitate surface rearrangements that would expose hydrophilic functional groups. Next, the surface side chains containing –COOH groups (as exist in aspartic and glutamic acids) were activated (with 1-ethyl-3-(dimethylaminopropyl)carbodiimide hydrochloride (EDC)/*N*-hydroxysuccinimide (NHS) solution), and brought into contact with an amine-containing peptide in PBS solution. The result is a stable amide bond between silk fibroin and the peptide. In the present case, the peptide contained the adhesion ligand “RGB”. Fibroin films decorated with RGB were found to stimulate osteoblast-based mineralization *in vitro* relative to the other modified silk films examined.

Non-covalent functionalization

A tetrapeptide that non-covalently binds silk has been identified [83] through affinity selection using phage libraries (in this process, random peptides are fused to the phage protein coat, and allowed contact with fibroin; sequencing of the adhered phage allows determination of similar peptides). The authors of the work propose that binding peptides (such as the QSW amino acid sequence they identified) can be fused with functional moieties (such as bioactive molecules or nanoparticles) to impart tailorable functionality to the silk surface. With modern molecular tools, this technique provides promise for a multitude of modifications without the need to chemically or genetically alter the silk.

Control of degradation rate.

One of the major benefits of using silk as a biomaterial is the fact that it is biodegradable [84]; in addition to all the selling points listed in the previous section, *in vivo* use doesn't require subsequent surgical removal [68], provided that the degradation rate matches what's needed at the site in question.

While materials engineers correctly refer to silk as ‘biodegradable’, medical professionals correctly refer to silk sutures as ‘non-degradable’. These two apparently conflicting viewpoints have led to some confusion over whether silk degrades *in vivo*. The confusion is alleviated when both fields understand that the medical professionals’ viewpoints are based on definitions set by the United States Pharmacopeia [84] (silk has a negligible loss of tensile strength over short time periods), whereas the language used by materials engineers is rooted in the more basic fact that as a protein, silk is susceptible to proteolytic degradation [85] (whether *in vivo*, or as a result of environmental exposure). Therefore, natural silk can properly be termed a biodegradable material, though *in vivo* the degradation occurs over longer time span than that of a “degradable biomaterial”.

There are multiple ways to tailor the degradation rate of silk. Some are as simple as modifying the bath used in a degumming treatment [53], whereas others involve reprocessing silk fibroin from solution [86] [71].

Studies performed with regenerated (reconstituted) *B. mori* silk fibroin have shown that the overall percent crystallinity of the silk can be controlled through the prevailing humidity and temperature during processing from solution [86]. In addition, when silk is used as a biomaterial, the degradation rate is known to be related to the crystal content of the silk—silks with a higher percent crystalline content take longer to degrade. Thus the processing conditions of reconstituted silk allow tailoring of the degradation rate—a useful feature for a biomaterial since the growth of some tissues requires a longer lasting scaffold than others. More recently, degradation rates of films cast from *B. mori* silk have also been linked to the length of degumming treatment (when 0.02 M Na₂CO₃ is used as the degumming solution) [53], providing another possible route to degradation rate control.

The biodegradability of silk is beneficial not only for the controlled removal of scaffolds from tissues, but also in the broader context of minimizing waste accumulation around the world; because silk is biodegradable, discarded products made from silk will not indefinitely take up landfill space.

Ability to form

Silk can readily be processed into many different forms; fibers can be bent into different shapes (e.g. knitted scaffolds [87]), regenerated silk fibroin can be cast as a membrane [88] [89], poured into a mold [90], crosslinked to form a hydrogel [91], or freeze-dried to form a sponge for tissue engineering [92], and fibroin can even be electrospun to form fibers with nanoscale diameters [93] (providing large surface areas for cell growth).

The ability to process fibroin into different forms and shapes is an important feature for a biomaterial; it allows cell-specific substrate requirements to be met (some cells need to grow as a monolayer, and thus a membrane is the appropriate scaffold, whereas others require three dimensional growth, in which case a porous scaffold is better), and also allows for the matching of mechanical requirements of different types of scaffold. Matrices composed of twisted silk cords have been used successfully in physiological cell

culture conditions as a substrate for human adult stem cell growth and differentiation [94], with a goal of tissue engineering replacement anterior cruciate ligament (ACL). The silk matrix provides mechanical properties sufficient to match the requirements of an ACL, and degrades slowly enough to allow time for new host tissue growth and gradual relinquishment of mechanical functions.

***B. mori* silk: as a pharmaceutical vector.**

The ability to attach bioactive molecules or proteins to fibroin has led to a branch of silk research investigating its potential as a drug delivery vehicle (mentioned above in the context of genetically engineered SELPs on page 6). Different preparation treatments have been examined [95], to probe which fibroin treatments allow the activity of L-asparaginase (a chemotherapeutic drug) to be retained when crosslinked to the treated fibroin. In combination with the ability to control degradation rates (through tailoring of secondary structures via processing), this allows for the controlled release of bioactive molecules or drugs.

Other experiments have aimed at genetically modifying the silkworm to produce recombinant therapeutic proteins in sericin, which can then be purified from the silk cocoons by soaking in aqueous solutions [96]. Thus, silk can be useful not only as a drug *delivery* vehicle, but also as a *production* route. The ability to tailor the chemistry of silk proteins produced through recombinant DNA technology opens possibilities for targeted drug delivery (i.e. specific to certain tissues). For an in depth review of this developing field, the reader is referred to reference [97].

***B. mori* silk: as an engineering material.**

The historical use of silk in textiles makes it easy to obtain large quantities of silk at low cost—the infrastructure for production and collection of silk on an industrial scale is already established. The ability to process silk in aqueous conditions [71] and the fact that it is biodegradable [84] allow for the use of silk as an environmentally friendly engineering material.

The inherent mechanical properties of silk [15] (in particular the high tensile strength, toughness, and elasticity) combined with its low density [98], give silk excellent potential for use in several (non-biomaterial) engineering contexts. For example: as the **reinforcing fiber** in fiber-reinforced polymer composites [99] (which traditionally have used glass, aramid, or carbon fibers—the lifecycles of which are not as environmentally friendly [100]), as a **ballistic material** (as in body armor [101] [102], or to line the cargo hold of an aircraft in case of explosion [103]), and even as a flexible **electrical material** (silk fibers can be made conductive by dyeing with the appropriate polyelectrolyte [104], or by co-electrospinning with carbon nanotubes [105]), or as a **flexible sensor** (silk substrates can be micropatterned with metallic antennae sensors, and adhered to a variety of food surfaces ranging from brittle egg shells to soft meats or even liquids. The sensors can detect the dielectric property changes that accompany ripening and spoilage, and can be used for food quality detection purposes [106]).

While there are synthetic fibers [15] that can provide higher strength (Kevlar) or greater stiffness (carbon fiber), it is the unique ability of silk to *combine* several desirable properties [107] (not only are they strong, they are *also* stiff and tough) that has kept these natural fibers in focus as a high performance material. However, several factors have limited its commercial use as an engineering material, to be discussed here.

Mechanical properties—limitations.

Variability in reported mechanical properties

The as-reported impressive mechanical properties of silk are necessarily based on averaged values, measured from multiple fibers. A perusal of the silk literature indicates that reported mechanical properties of silk cover a wide range of values. One paper reports the elastic modulus of *B. mori* cocoon silk to be 7 GPa [15], while another gives values as high as 17 GPa [108]. If silk is to be used as an engineering material (in which reliability is key for either safety or cost), it is important to understand the nature of such variability.

Some work has been done to investigate how variable the fiber mechanical properties are along the thickness direction of individual cocoon walls [109] [28] [110]. Results suggest that at least some of the variability in measurements can be attributed to fibers of different thickness; smaller diameter fibers tend to be found in the inner layers of the cocoon, and generally perform better than the larger diameter fibers in outer layers of the cocoon. Much work remains to be done to discover whether other intrinsic factors besides fiber diameter may also affect the variability of measured mechanical properties (for more on this topic, see the chapter beginning on page 31).

Mechanical properties of individual fibers are still variable even when fiber diameters are similar [111]. Thus, the variability still calls for closer examination. One study has investigated how silk differs along the entire fiber length of single cocoons [28]. The authors use a Weibull distribution function to analyze the variability of breaking strengths through the parameter β (see page 29 for a description of Weibull statistics). Lower values of β indicate higher variability. In this study the values of β measured for the ultimate tensile strength ranged from 0.94 to 1.89, significantly lower than 5.76 as measured in an earlier work performed by a different group [108] (in which the authors note that the value of β they measured is comparable to the failure predictability of glass). Values of the β are unusually high in another paper (13.46 for *B. mori* fiber) [112]. Samples in this study were intentionally taken from adjacent points along a single fiber to minimize the intrinsic scatter of data, so this may be why β is higher here than in other studies, but we also note that the sample sizes in this study (10 samples) were smaller than recommended for statistical significance (21 samples [113]), and thus some level of cautiousness in the statistic is warranted.

The variability in the parameter used to *measure* variability underscores the fact that silk behavior from one sample to the next and from one laboratory to the next can be very noisy.

This variability is not a problem in the natural setting of silkworm silk—cocoon are constructed from enough silk so that any weak points are concomitantly offset by the strength of surrounding fibers. But when silk is considered for use as an engineering material, this variability poses an intrinsic limitation to the use of individual silk fibers as engineering devices, and is therefore an important problem to be aware of.

As a final note on reliability, it is interesting to note that the health of the silkworm itself can affect the quality of silk produced, and therefore must be an important factor for production of silk with reliable properties. For example, air pollution is known to affect silkworm silk production [114]. This may be due to nutritional effects on food sources (the leaves of Mulberry trees), and calls for closer examination of how pollution may affect the mechanical properties of silk produced in different environments.

Moisture affects mechanical properties

There are multiple studies indicating that moisture affects the stiffness (Young's modulus; elastic modulus) of silk: the elastic modulus of *Antheraea pernyi* silkworm silk tested at 25 °C drops abruptly as relative humidity increases above 80% [115]. The elastic modulus of *Bombyx mori* silk fibers is also affected by moisture. The elastic modulus of samples tested under water in one study [116] was $\frac{1}{4}$ what it was in dry conditions. In addition, regenerated silkworm silk fibers were *considerably* more compliant when tested in water versus those tested in air (when immersed, the elastic modulus decreases to $\frac{1}{50}$ of its value in dry conditions), though some improvement may be possible by including a postspinning wet-stretching process to improve alignment of molecular chains [116].

Stiffness is not the only property affected by moisture. An unrelated study has shown that toughness can change with humidity [117], and again other studies have observed that the overall shape of stress-strain curves may be related (in part) to the moisture content within the silk [118], or in the surroundings [119]. In addition to these observations from the literature, we encounter the effects of moisture in our own experiments. We develop a framework for understanding the interplay of moisture and mechanical properties beginning on page 33. Standardization of ambient humidity during testing will be an important step towards minimizing the variation in reported mechanical properties of silk.

Silk is a viscoelastic material

Most structural engineering materials (if not all) are necessarily expected to be able to support loads over long time periods. Although silk is a strong material, it is also a viscoelastic material, and therefore will creep or experience stress relaxation over time when loaded [120] [103]. In spider silk, creep is known to occur even when the load is significantly less than that required to initiate yield in a conventional mechanical test – and can be exacerbated by moisture [121]. A model to describe the mechanical behavior of silk has recently been developed using viscoelastic theory and observations from

tensile tests performed in conjunction with x-ray diffraction [57]. The viscoelastic deformation of silk provides an important means of energy dissipation in the context of naturally spun and used silk (e.g. when a flying bug is intercepted by a spider's web), but it will be necessary to overcome this limitation before silk can be used alone as a long term load bearing material.

Biomimetic Fiber Production

The ideal biomimetic, artificially spun engineering counterpart to naturally spun silk would emulate the average (or better) mechanical behavior, and minimize performance variability (to allow more confidence in the final product). It is hoped that by controlling the spinning conditions (including the dope composition, orifice diameter, flow rate, and ambient conditions), reproducible mechanical behavior of fibers may be achieved.

Some attempts to produce artificially spun silk (by wet-spinning regenerated silk fibroin) have yielded fibers that are brittle and have poor mechanical properties compared to their natural counterparts [122]; the addition of a post-spinning draw step can provide some improvement by increasing chain alignment, and possibly decreasing the number (or magnitude) of flaws in the nanocrystals of the fiber [122]. In some cases it has been possible to achieve toughness that is comparable to that of natural *B. mori* silk [123], though the study does not include a discussion about how economical the production route is (e.g. time and cost), and other properties (tensile strength, breaking strain) do not match those of natural silk.

One group, noting that most artificial wet spinning techniques involve organic solvents that are either toxic or too expensive for use in industrial processes, has experimented with a dry spinning technique [124]. In combination with a post-spinning treatment in ethanol [125], the dry spun fibers had a higher breaking strain than cocoon silk, though other properties such as the breaking stress were significantly lower than that of cocoon silk.

With the advent of microfluidic devices, Hu et al. [126] have noted that the scale of ducts involved in the silkworm gland is comparable to channels of the microfluidic devices. Their experiments with the microfluidic production of regenerated silk allowed them to achieve solution concentrations across the microfluidic device similar to those found across the silkworm gland—providing a step towards biomimetic processing of silk. Mechanical tests on the end result have yet to be published in order to compare with naturally spun fibers. Viney and Bell [127] have raised the question of whether the 'green' (aqueous) processing carried out at near-equilibrium conditions (as in the silkworm) is necessarily tied to slower production rates—limiting the feasibility of mass producing a true biomimetic counterpart to silk at economical rates. To the author's best knowledge, the question remains to be addressed in the literature.

Lessons from B. mori silk

One thing we do know about production rates is that they affect the mechanical properties of native silk. Engineering experiments carried out by forcibly silking *B. mori* silkworms

at different rates [128] (by drawing the silk fiber directly from the silkworm head instead of collecting it from a cocoon) have indicated that higher rates of collection lead to fibers with a higher breaking strength (though they are more brittle than fibers collected at slower speeds). Separate biological experiments have led to the observation that there is an intrinsic physiological control of spinning rate in native silkworms; the neurohormone corazonin is believed to influence the silkworm spinning rate [129], and plays diverse roles in many other physiological functions of arthropods (e.g. accelerates the heartbeat of cockroaches [130]). These discipline-specific studies (engineering and biology) may be usefully combined to provide some insight on the spinning of reconstituted silk: The natural control that is in place for spinning rates of silk suggests that efforts to increase the spinning rate of reconstituted silk will require an input of energy in some form, if a fiber similar to the natural counterpart is desired as the outcome.

In addition to spinning rates, the conditions under which fibroin is processed can be used to alter the microstructure and mechanical properties of silk. An experiment published in 2009 [131] demonstrated that processing conditions are nearly as important as amino acid sequence for achieving desired mechanical properties in silk fibers. Silkworm fibroin solutions were processed via a wet spinning process with an immersion postspinning draw. The resulting microstructure of the silkworm fibroin more closely resembled that of spider silk (in terms of the crystalline fraction, and size, orientation, and degree of anisotropy of nanoglobules). Mechanical properties of these fibers more closely resembled spider silk too—even to the extent of supercontracting when immersed in water (supercontraction is a reduction in the length of spider silk fibers in humid environments, with the potential of reverting to a “ground state” [123]). Therefore, it is possible to tailor mechanical properties through spinning conditions.

Mechanical properties—addressing limitations.

We have discussed three broad categories of limitations to the use of silk as an engineering material (variability of mechanical properties, moisture sensitivity, and the propensity to creep). Here we consider some possibilities for overcoming these limitations.

With a forward looking mindset, it is appropriate to note that the advent of molecular modeling has opened the way to a deeper understanding of the properties of silk as a direct consequence of molecular interactions of fibroin chains and their surroundings [132] [133], (to be discussed at several points throughout this dissertation). As this better understanding continues to grow, it will become possible to design conditions for the use of silk that do not *trigger* the limiting behaviors of silk. Additionally, it will become more feasible to design a biomimetic counterpart to silk that does not include the features which currently result in the limiting behaviors of silk.

While the fields of molecular modeling and biomimetic fiber spinning have promising futures, they are likely to take some time to develop to the point where fibers comparable

to natural silk can be economically produced on an industrial scale. In the meantime, it is prudent to attempt to mitigate as many of the limitations of natural silk as possible.

To accomplish the goal of improving natural silk fiber reliability, it will first be necessary to understand the origins of variability in the reported mechanical properties. Before the origins of variability can be deciphered, it is necessary also to minimize *externally* imposed variability in data; that is, variability introduced as a consequence of the experimental techniques used rather than due to the inherent properties of silk. We spend a chapter (beginning on page 31) investigating several potential sources of variability in data, and use our findings to minimize the noise in our own experiments.

While humidity is known to affect the behavior of silk, there is also some indication that conditioning silk yarn in high relative humidity *prior* to testing may help reduce variation in mechanical data (this effect is more pronounced in wool than silk [134]). We take a step in this direction in our own experiments by using consistent storage conditions prior to any mechanical testing (discussed in the chapter beginning on page 31).

There is one solution that addresses both the variability of mechanical properties and the moisture sensitivity of silk, and that is to use silk as a composite material rather than as a standalone engineering material. A natural analogy can be taken from the combs of honeybees. Over time, silk (produced by the honeybee larvae) is incorporated into the walls of the honeycomb, greatly enhancing the strength and stiffness of the comb [3]. Because the silk fibers in this natural composite are surrounded by hydrophobic wax, the fibers are isolated from moisture fluctuations.

B. mori silk fibers can be used in an analogous way in engineering materials. For example, by incorporating silk as the reinforcing fiber in epoxy based composites, the silk will be shielded from moisture variations (because it is encased in epoxy), and the presence of *multiple* fibers in a load transferring epoxy matrix will allow stronger fibers to carry the load where weaker ones would otherwise fail.

Microwave exposure.

The use of silk in fiber reinforced epoxy composites (for example in lightweight sandwich structures for automotive or aviation applications [135] [136] [137]) leads to situations in which silk may inadvertently be exposed to microwave radiation. The rate at which epoxies cure can be significantly increased by heating. Microwave radiation can provide a rapid, energy efficient, and inexpensive means of heating epoxy [138].

Microwave exposure of silk may occur in a biomaterial context as well. Microwave induced argon plasma treatments have been used successfully to sterilize bacteria [139] (*Escherichia coli* and methicillin-resistant *Staphylococcus aureus*) and to degrade mycotoxins [140] (aflatoxin B1, deoxynivalenol, and nivalenol), and hence another paper reports [73] that microwave-induced argon plasma treatment could be used to sterilize silk fibers at relatively low temperatures. As such, it may prove a convenient way to sterilize silk fibroin scaffolds prior to cell seeding or *in vivo* use.

Given that microwave radiation is used in many different types of materials processing [141] [142] (other examples include sintering of ceramics, vulcanization of rubber, chemical syntheses, food processing, and even waste remediation), it is reasonable to consider that it might also affect silk in some way. In cases where the mechanical properties of silk are being relied upon, understanding the consequences of microwave radiation is necessarily important.

A 2004 study carried out in Scotland [103] showed that microwave radiation can enhance many of the tensile properties of silkworm (*Bombyx mori*) and spider (*Nephila clavipes*) major ampullate silk. As this was a preliminary study, only a few samples of each type were studied, and many of the details of the experimental procedures were not standardized or recorded. Further work is needed to follow up on the reproducibility of the microwave effects reported in this study.

Given the prevalence and usefulness of microwaves (not only in materials processing, but also as used in communications and radar), their presence in the world is not likely to subside in the near term. This dissertation therefore is devoted to exploring the effects of microwave radiation on the mechanical properties of silkworm (*B. mori*) silk.

Microwave Radiation—general information

Microwave radiation includes frequencies of the electromagnetic spectrum ranging from 0.3 GHz to 300 GHz [143]. Corresponding wavelengths therefore range from 1 cm to 1 m (see Figure 1). Within this range, higher frequencies (wavelengths from 1 cm to 25 cm) are commonly used for RADAR, and lower frequencies (wavelengths from 25 cm to 1 m) for telecommunications. All commercially available domestic microwave ovens use a frequency of 2.45 GHz—one of several frequencies designated for use in industry, science, and medicine to avoid interfering with communication frequencies [143] [144].

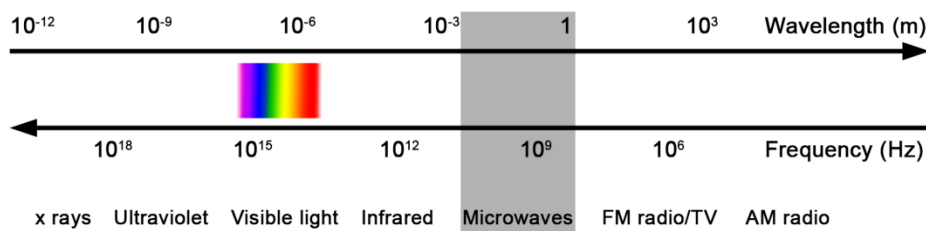


Figure 1 Diagram showing the position of microwaves in the electromagnetic spectrum relative to other types of electromagnetic waves. Label positions (compiled from references [145] and [143]) are intended to be approximate only.

Given that the photon energy at 2.45 GHz is so low (approximately 1.0×10^{-5} eV), microwaves are not energetic enough to cleave bonds (the energy of a hydrogen bond is

on the order of 0.2 eV [144]), and therefore cannot directly induce chemical changes. However, the rotational vibrations induced within molecules can result in a *buildup* of thermal energy great enough to initiate chemical changes. In some cases the rapid heating rate achievable by microwaving can even allow better kinetic control over reactions than could be achieved by conventional (conductive) thermal heating; selectivity between competing reactions can be induced [144].

Sources of microwave energy range from household (domestic) microwave ovens that may deliver a pulsed power output, to laboratory microwave processors that deliver power continuously, allow precise temperature control, and can be run for weeks at a time. The latter is an item of specialty lab equipment, likely to be purchased only when long term microwaving experiments are planned. For laboratories that only perform occasional or short term experiments involving microwaves (such as ours), the domestic microwave oven is a useful, accessible option.

Before the effects of microwave radiation on silk can be explored quantitatively, it is necessary to be able to calibrate the source of the microwave radiation. Therefore, we spend a chapter (beginning on page 45) exploring factors that affect the calibration of microwave ovens. Using the conclusions that we draw, the results of mechanical tests performed on microwave irradiated silk can be interpreted with greater confidence (discussed in the chapter beginning on page 62).

Chapter 2: Materials, Equipment, and Methods

This chapter provides general descriptions of materials, equipment, and procedures used throughout this course of study. Any modifications to these procedures are described in the chapters themselves.

Microwave oven^a

A Panasonic microwave oven equipped with a rotating turntable (“The Genius Premier”, Model No. NN-S969BA, Danville, KY) was used for all procedures involving microwave exposure. This particular microwave oven is equipped with an inverter system, which allows continuous power delivery at a given wattage (rather than a pulsed delivery, in which the quoted wattage is actually a time averaged value). Before any experiment (or calibration) was performed, the magnetron was ‘warmed up’ [146] by running the oven with a 1 L beaker full of water in it for 3 minutes.

Beakers^a

KIMAX® Kimble borosilicate glass beakers (glass type “KG-33”) were used to hold water during all calibrations of the microwave oven.

Temperature measurement^a

Water temperature was measured with a HANNA Instruments thermistor thermometer (Minitherm HI 8753). The probe of the thermometer was used to quickly stir the water just before the temperature was recorded. In cases where the water was deeper than the length of the probe, a glass rod was used instead to stir the water.

Power calibration^a

When a known volume (V) of water is heated in a microwave oven for a given magnetron run time (t), the resulting temperature rise (ΔT) can be used to estimate the apparent power (P) of the microwave source via the following equation [147]:

$$\begin{aligned} P &= (\Delta T) V c \rho / t \\ &= (\Delta T) V c \rho / (t_{set} - t_{delay}) \end{aligned}$$

Equation 1

where c and ρ respectively are the specific heat and the density of water, t_{set} is the set time selected on the microwave oven, and t_{delay} is the magnetron startup delay time. To obtain P in watts (J/s), we measure ΔT in °C, time in seconds, and volume in mL; we used 4.18 J/(g.K) and 0.997 g/mL respectively for the specific heat and density of water [148], and assumed that both were constant within the temperature range of our

^a As presented in our paper entitled “Calibrating the power of a domestic microwave oven” (submitted 2013, [PLOS ONE](#)).

experiments. In every case, the microwave oven power level was set to 100 (i.e. full power).

Silk collection^b

Bombyx mori silkworm cocoons were obtained from Marian Goldsmith, Department of Biological Sciences, University of Rhode Island. As provided, these cocoons had been cut open at one end to remove the silkworm pupa, so it was possible for us to retrieve silk from both the inside and outside surfaces.

Cocoons were degummed by boiling individually for about 30 min in ~1 L of water. The exact timing has been found to be unimportant with respect to the effect on microstructure, for boiling times of up to 7 h [48]. While the cocoon was still wet, lengths of silk were teased from it by hand with tweezers. The cocoon was held gently with the fingers of one hand, and with the other hand tweezers were used to grasp a silk fiber and pull gently until resistance increased noticeably (usually when a “knot” was encountered), at which point scissors were used to cut the fiber at the point of resistance. Vinyl gloves (Finish FactorTM) were worn during this procedure. The lengths of silk were then taped at their ends to a piece of black paper for temporary storage, with the tape serving as a useful grip for subsequent handling.

The collected silk was cut into shorter lengths (~70 mm), and a small piece of tape (or a Post-it® note) was attached to each end for handling. Samples that were to be microwave irradiated were taped loosely across the hole of a black cardstock frame (see section below on **Microwave exposure**). Otherwise, samples were stored prior to mechanical testing according to the section below on **Silk storage**.

Microwave exposure^c

The microwave oven power level was set to 100%, which corresponds to 788 ± 12 W according to our calibrations (see the chapter beginning on page 45). For some experiments (identified explicitly throughout), a 200 mL “load” (or “sink”) of water was included in the oven, in a 2 L beaker with the top covered in plastic wrap (to prevent steam from escaping) and centered on the turntable. This water load was introduced as a precaution to protect the magnetron [142] from potentially damaging build-up of microwave energy inside the oven.

The cardstock frames with silk attached were positioned to lean against the beaker, so that the lengths of silk were only in contact with air, approximately 1 cm above the glass

^b As presented in our 2012 paper “Sample Selection, Preparation Methods, and the Apparent Tensile Properties of Silkworm (*B. mori*) Cocoon Silk” (see Reference [111])

^c As presented in our paper entitled “Calibrating the power of a domestic microwave oven” (submitted 2013, [PLOS ONE](#)).

turntable (see Figure 2a). After every minute of microwave exposure, the water load was replaced with a fresh 200 mL of water at room temperature, and the turntable was cooled back to ambient if warm to the touch.

Experiments were also conducted without a water load, initially as a control to determine whether the presence of the water had an effect on the results; recalibration of the oven confirmed that there was no detrimental effect on the power output. Cardstock frames supporting samples that were microwave irradiated without including a water load were placed in a triangular configuration around the center of the turntable (Figure 2b), so that again the silk was approximately 1 cm above the glass. Microwave burst length was either 30 s or 60 s (minus the startup delay time), as noted throughout. After each microwave burst, the turntable was cooled back to approximately ambient temperature if it had become warm.

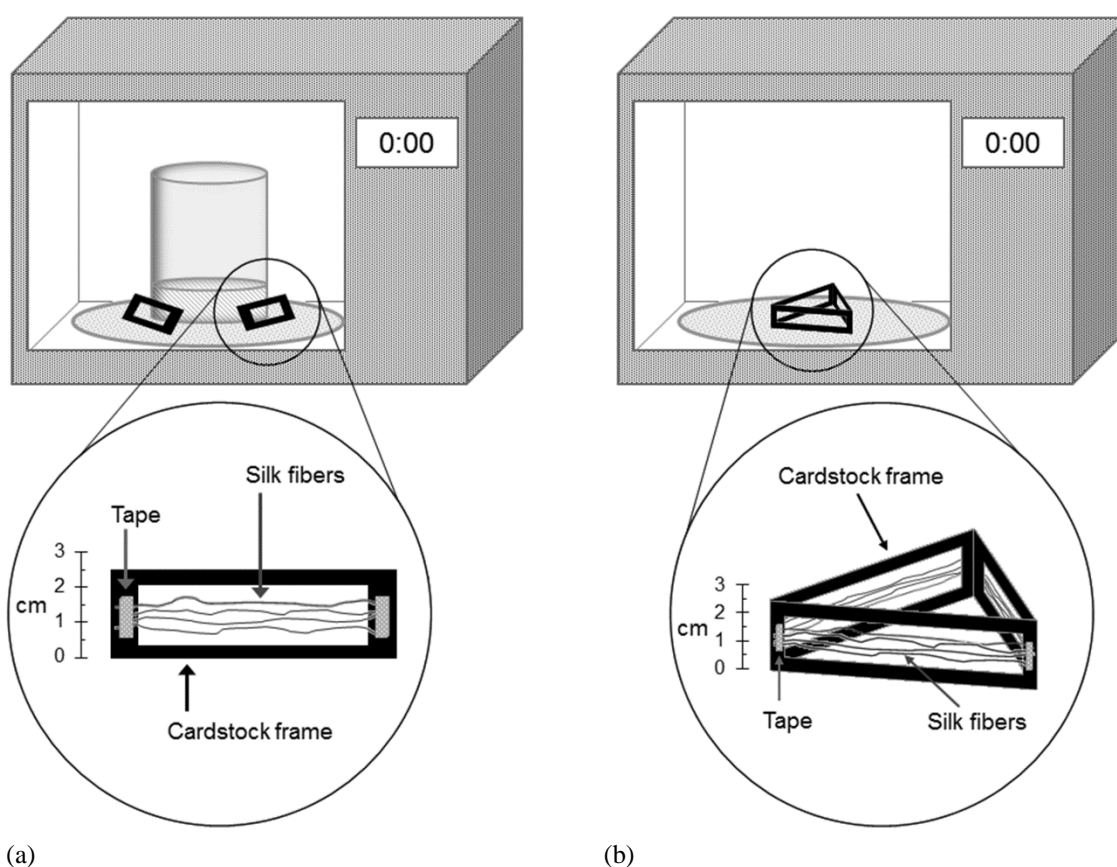


Figure 2 Schematic representation of silk fibers ready for exposure to microwave radiation: (a) with a water load included in the microwave oven as a “sink” for excess microwave radiation, and (b) without such a water load.

After microwaving, silk fibers were removed from the cardstock frame, and stored prior to mechanical testing according to the section below on **Silk storage** .

Silk storage^d

Silk samples (~70 mm long) were attached with cyanoacrylate glue (Loctite® Super Glue Gel) across a hole in a black cardstock support (Figure 3), so that the gauge length of the silk in mechanical tests was 55 mm (constrained by the dimensions of the punch used in making the holes; a previously noted lack of consensus on preferred gauge length [107] persists to the present day). This method of mounting samples on cardstock supports is similar to an existing protocol in the literature [108]. The supports with their attached silk were stored in airtight plastic boxes, resting silk-side up in the grooves of a paper “accordion”, so that each silk sample was only in contact with its cardstock support; in some cases (where noted throughout the chapters), silica gel desiccant was included in the box, below the paper accordion to ensure that no direct contact occurred between the desiccant and the silk.

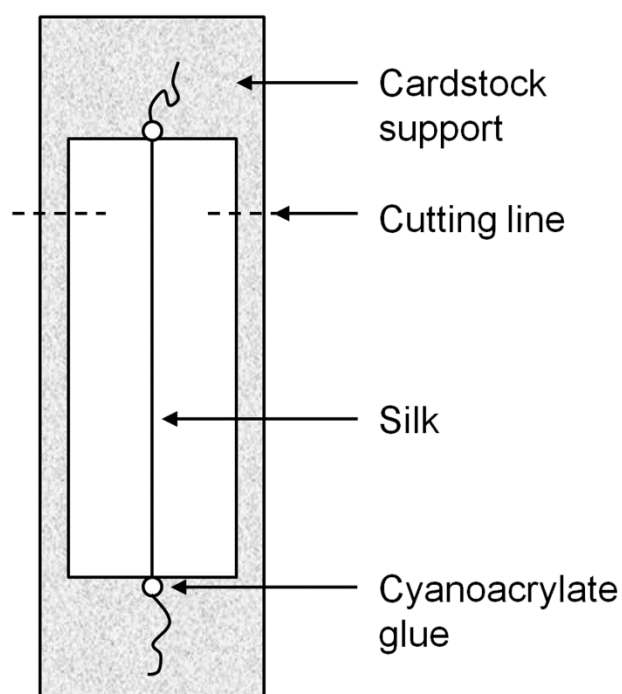


Figure 3 Silk sample glued to a cardstock support. The gauge length of the sample is defined by the distance between points of attachment to the cardstock support—i.e. the length of silk spanning the hole in the cardstock support, between the dots of cyanoacrylate glue.

^d As presented in our 2012 paper “Sample Selection, Preparation Methods, and the Apparent Tensile Properties of Silkworm (*B. mori*) Cocoon Silk” (see Reference [111])

Measuring silk fiber diameter^e

Fraunhofer diffraction of the beam from a pen-style green laser pointer (RadioShack®, cat. no. 63-132, wavelength $\lambda = 532 \pm 10$ nm) was used to measure the apparent diameter of silk samples (Figure 4).

This technique offers several attributes that favor its use for characterizing the diameter of silk. It has the advantage of quickly sampling the diameter of many different points in an approximately 1 mm region of the fiber (corresponding to the beam diameter), so that averaging accrues efficiently when diffraction is performed at several locations along the fiber. With polarized light microscopy or SEM, it would take significantly longer to acquire a similarly well-averaged result. Another advantage of Fraunhofer laser diffraction is the absence of a substrate (glass slide and cover slip; carbon adhesive tab) that could damage the sample; transfer into the tensile test is straightforward. Also, the sample is not subjected to potentially damaging radiation, and there is no need to focus the optics to ensure that the imaged “edges” are indeed the boundaries of the sample. Fraunhofer laser diffraction has been explored in detail as a means of measuring spider silk diameter [149].

To ensure effective averaging and thus minimize the possible problem of perspective affecting the diameter measured, eight measurements were taken from each sample, at locations spaced ~5 mm along the sample length. An average diameter d was calculated:

$$d = \lambda / \sin [\tan^{-1}(x_{\text{average}}/y)]$$

where x and y are defined in Figure 4. The above equation is obtained from a standard result for the first-order node in single-slit Fraunhofer diffraction ($d = \lambda / \sin \theta$), with the geometry of the present experiment defining θ as $\tan^{-1}(x_{\text{average}}/y)$.

^e As presented in our 2012 paper “Sample Selection, Preparation Methods, and the Apparent Tensile Properties of Silkworm (*B. mori*) Cocoon Silk” (see Reference [111])

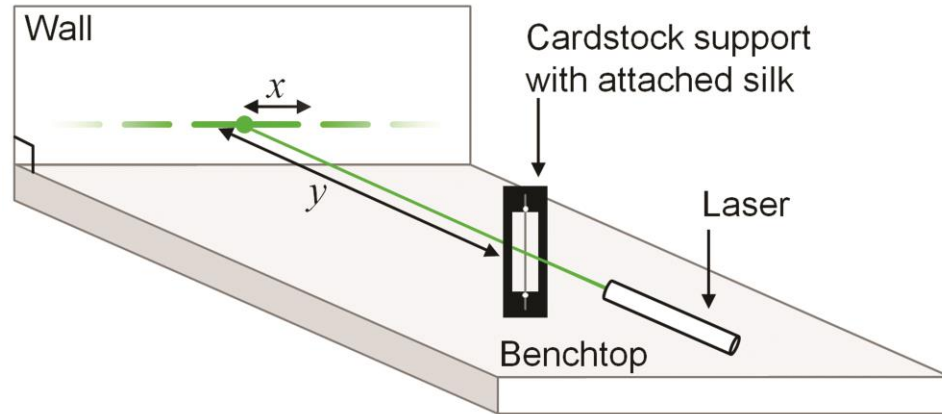


Figure 4 Schematic representation of Fraunhofer diffraction used to measure the diameter d of silk samples; x is the distance measured on the wall from the direct beam of the laser to the first dark node. The distance y between the sample and the wall was fixed at 1 m. The laser beam is normal to the plane of the wall, so that x and y are perpendicular to each other.

Mechanical tests

Tensometer

A 3369 Instron Tensile Tester (tensometer) was used to perform all mechanical tests on silk fibers. The tensometer was equipped with a 0.5 N cantilever load cell (Model S-100, Strain Measurement Devices Ltd., Bury-St-Edmunds, UK), which was attached to a moveable crosshead as shown in Figure 5.

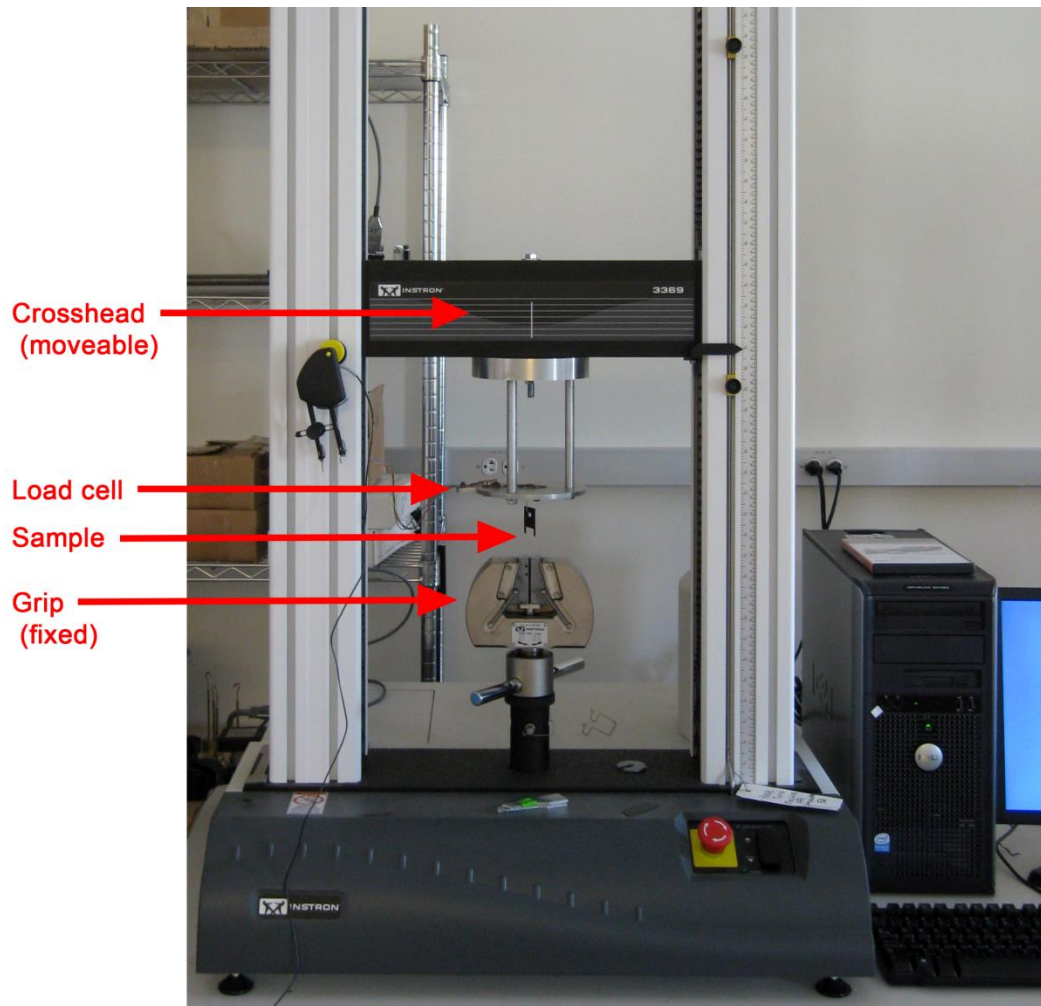


Figure 5 Instron tensile tester equipped with a 0.5 N cantilever beam load cell.

Samples on their cardstock supports were mounted vertically from a hook placed at the end of the cantilever beam (Figure 6), and secured at their base to a grip whose position was fixed. Prior to the start of each test, both sides of the cardstock support were cut (see also Figure 3), so that all of the force during the test was transmitted through the silk fiber. This arrangement allowed forces transmitted through the silk to be detected via deflection of the cantilever beam.

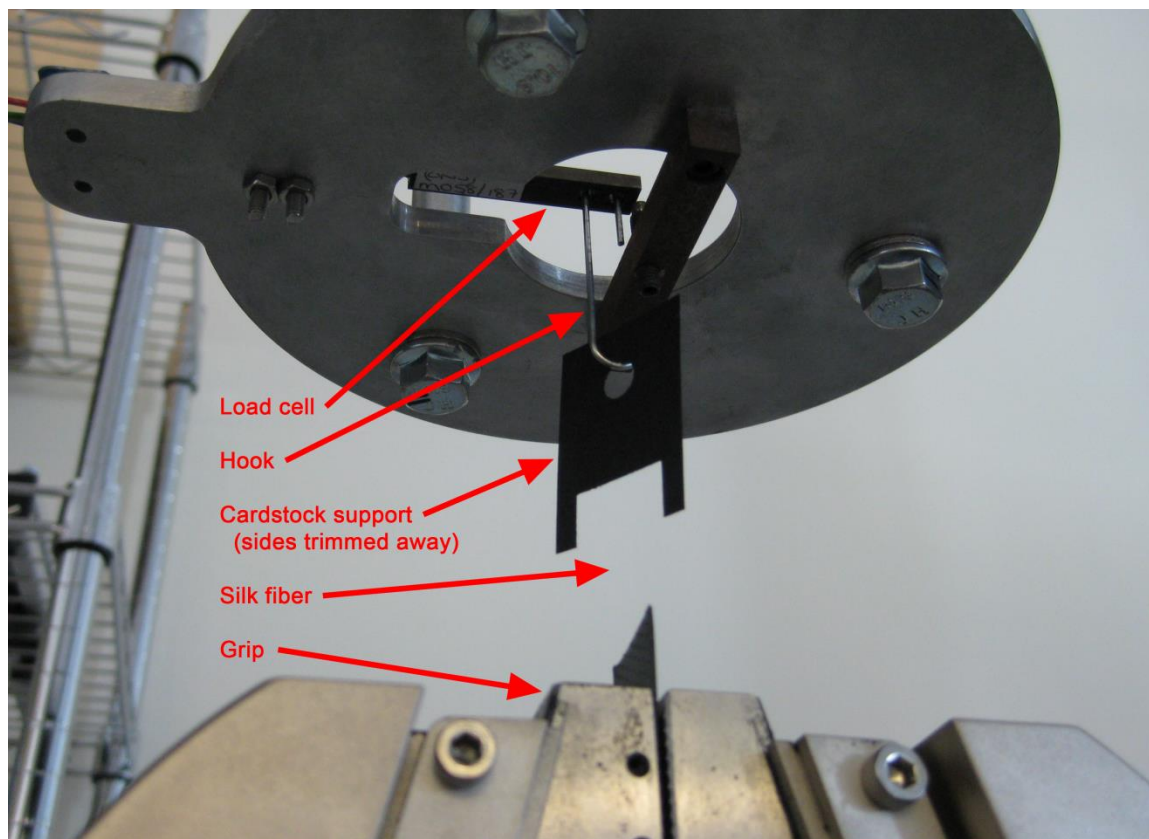


Figure 6 View of the connection between the sample (mounted on a cardstock support) and the cantilever load cell.

Each time the tensometer was powered on, the system was allowed a 30 minute warm-up time prior to the start of any tensile tests, in accord with the manufacturer's recommendations. In addition, the load cell was recalibrated each time the machine was powered up, and as needed throughout the day if the zero-load reading between tests seemed to change (this rarely happened).

The accuracy of the equipment and experimental setup were tested by performing a calibration with a series of weights whose masses were known (by measuring on an external balance). In every case, the load measured by the tensometer agreed closely with the load computed from the mass via Newton's second law (see Figure 7). This was true even for the smallest mass tested (0.619 g; 0.006 N; much less than the forces typically measured during a tensile test performed on *B. mori* silk fiber), indicating that the resolution provided by the equipment was sufficient for measuring the loads encountered at points of interest during tensile tests performed on silk fiber.

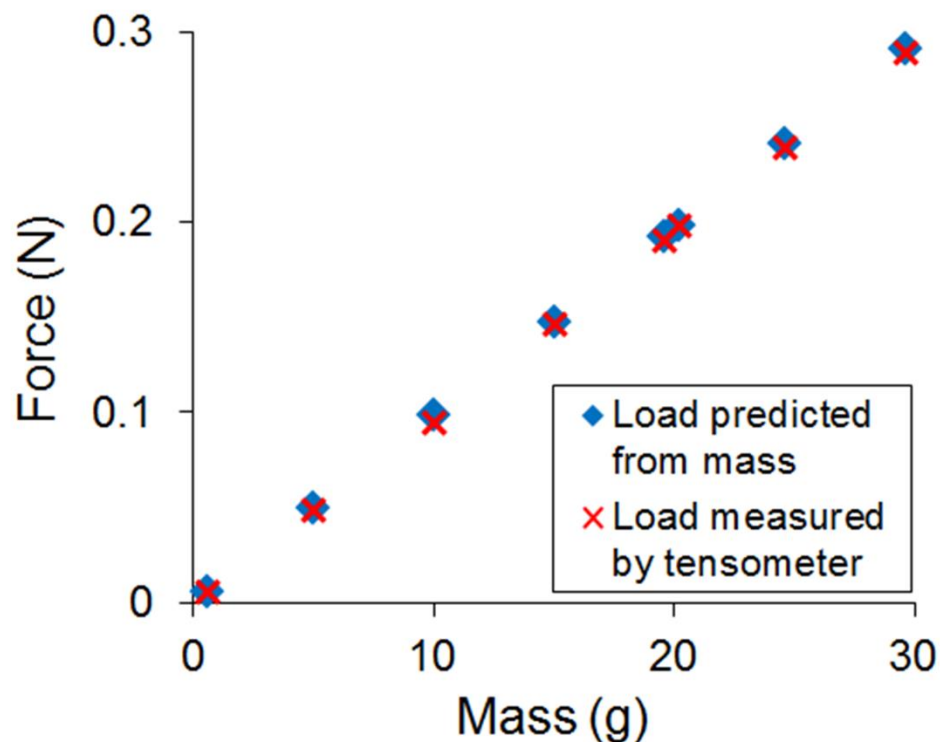


Figure 7 A comparison of loads as measured by the calibrated tensometer when weights are hung from it, and as predicted by Newton’s second law based on the known masses of the weights.

Mechanical tests: stress-strain^f

For all stress-strain tests, the gauge length of the silk fiber was 55 mm (defined by the size of the punch used in preparing the cardstock supports), and the crosshead speed was 0.275 mm/min, corresponding to a nominal strain rate of 0.005 min^{-1} (or $8.33 \times 10^{-5} \text{ s}^{-1}$).

Load versus extension data were collected via Instron’s Bluehill® 2 software. Microsoft Office Excel was used to rescale and plot the data in terms of nominal stress and nominal strain, and to calculate numerical values of mechanical properties.

To define the yield point (ϵ_y, σ_y), we have opted to use a conventional 0.2% strain offset yield criterion, wherein a line is extended upwards from 0.002 on the strain axis, parallel to the initial linear region of the graph, to intercept the data at the point (ϵ_y, σ_y).

^f As presented in our paper entitled “Mechanical properties of *Bombyx mori* silkworm silk subjected to microwave radiation” (submitted 2013, [JMR](#))

Mechanical tests: stress relaxation^g

Prior to each stress relaxation test, ε_y was found by performing a constant strain rate (stress-strain) tensile test on silk fiber taken from the same cocoon as the material to be used in the stress relaxation test. Next, a 55 mm gauge length sample was elongated at a rate of 0.275 mm/min (unless otherwise noted) to an extension of $0.6\varepsilon_y$. Time dependent load was then measured at that fixed elongation for 1200 s and re-scaled to obtain stress relaxation data.

^g As presented in our paper entitled “Mechanical properties of *Bombyx mori* silkworm silk subjected to microwave radiation” (submitted 2013, [JMR](#))

Chapter 3: On the Statistical Treatment of Data

The goal of any experimental design is inherently to produce data; that data must then be *interpreted* if useful information is to be gleaned from the experiment. In order to provide the most benefit, data interpretation must be carried out in an unbiased manner, and this is where statistics come in to play. Our experiments with silk are no exception; thus, the present chapter is devoted to considering statistical tests appropriate to our needs.

When comparing two sets of data (such as may be collected from an experimental group and a control group), the question arises: at what point are the two sets of data considered *significantly* different from each other? Ordinarily, parametric statistical procedures (such as a t-test) are preferred for answering this question, because their results are more powerful than nonparametric statistics: with a given number of data points, a parametric test is less likely to miss a significant difference when comparing two groups of data [150]. However, for sample sizes less than 30 (as is the case in many silk tensile experiments—each sample takes several hours to prepare and test), parametric tests require that the population from which samples were taken should be normally distributed. In the case of tensile tests performed on silkworm silk, there are many systematic (nonrandom) contributions to the values of properties measured (for example, the variable draw ratio imposed by motion of the silkworm's head during spinning), so it is not appropriate to assume that the distribution will be normal. Therefore, the first step in our data analysis is to test whether the data comes from a normal distribution.

“Is this normal?”

Normality can be assessed by generating a normal probability plot, in which the observed data are plotted against scaled values (“Z-scores”) that would be expected if the data came from a normal distribution [150]. Observed data that follow an ideally normal distribution will yield a normal probability plot that is linear. If the plot is significantly *nonlinear*, the distribution of the data cannot be considered to be normal. When our data are presented in normal probability plots, they are found to be nonnormal in several cases. A representative plot is shown below (Figure 8), constructed from data presented in a later chapter (in Figure 30).

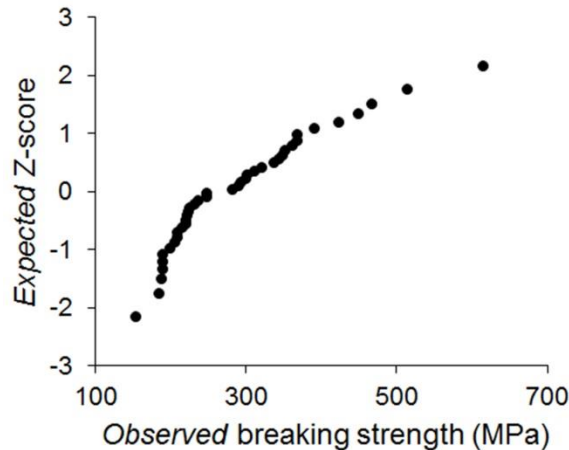


Figure 8 Normal probability plot constructed with breaking strength data collected from silkworm silk that has been microwave irradiated. Nonlinearity indicates the data does not follow a normal distribution.

The curvature displayed in the normal probability plot (Figure 8) indicates the data does not follow a normal distribution, and therefore parametric statistical tests are not appropriate for our needs. Thus, we turn our attention to *nonparametric* statistical tests.

Nonparametric statistical tests

Nonparametric statistical tests make no assumptions about the type of distribution a data set comes from. Therefore, there is no need for the data to be normally distributed. There are two nonparametric tests that stand out as applicable to our needs:

The Mann-Whitney test: for comparing two population medians based on independent samples.

Data from two sample groups (A and B) are combined and ranked in ascending order. The sum of the ranks of sample A is compared to the sum of the ranks of sample B. Given equal sample sizes, the rank sums of A and B should be the same if A and B came from populations with identical medians. To make the comparison more practical, a test statistic is used that takes account of the number of samples in A and B. A test statistic that is too large or too small indicates that sets A and B likely came from populations with different medians. Critical values for the test statistic are tabulated [150] and assigned based on the level of confidence desired. Unless otherwise noted, Mann-Whitney tests performed here were two-tailed, and results are given at the 90% confidence level.

The Kruskal-Wallis test: for comparing three or more sets of independent samples.

Similar to the Mann-Whitney test, data from all sample groups are first combined and ranked in ascending order. The sum of the ranks for each sample group is determined, and compared through a test statistic that takes account of the number

of data points in each sample group. A low test statistic indicates the sums of ranks were similar (when sample size was taken into account), and that the samples all likely came from the same distribution. A large test statistic indicates there is a difference in one or more of distributions from which the samples came. Kruskal-Wallis tests are designed to be right tailed, so a single critical value for the test statistic is all that is needed to be able to interpret the test. Critical values are tabulated [150], and are chosen based on the level of confidence desired. Unless otherwise noted, our tests were performed at the 90% confidence level.

For comparison with the nonparametric statistics, means, standard deviations, and coefficients of variation (“CV”; standard deviation divided by the mean) are provided in Figures throughout this dissertation.

Weibull statistics^h

In cases where the tests described above reveal no significant differences between sample groups that have received different treatments, the possibility remains that the *spread* of the property values may be different between the groups. Practically, a change in the spread of the breaking strengths translates to a change in the predictability of failure – in other words it is a measure of the reliability of the material. To quantify the failure predictability, we use Weibull statistics, in line with previous studies performed on silk [108] [28]. Using the two parameter Weibull distribution [113], the probability of fracture at stress σ is given by:

$$F(\sigma) = 1 - e^{-\left(\frac{\sigma}{\eta}\right)^\beta}$$

Equation 2

where β is the Weibull modulus (also known as the shape parameter of the distribution), and η is the scale parameter (equivalent to the stress at which 63.2% of samples will have fractured). The distribution function can be rearranged so that the data can be plotted as a straight line (if indeed the data belong to a Weibull distribution):

$$\ln \ln \left\{ \frac{1}{1-F(\sigma)} \right\} = \beta \ln(\sigma) - \beta \ln \eta$$

Equation 3

Here $\ln \ln \left\{ \frac{1}{1-F(\sigma)} \right\}$ is plotted as the vertical axis, and $\ln(\sigma)$ as the horizontal axis. Then, β can be read from the plot as the slope. A higher Weibull modulus corresponds to more predictable behavior.

^h As presented in our paper entitled “Mechanical properties of *Bombyx mori* silkworm silk subjected to microwave radiation” (submitted 2013, [JMR](#))

To calculate the probability of failure, $F(\sigma)$, the breaking strengths are first ranked from smallest to largest. Then, for the i th of n samples, we used the median rank approximation (Equation 4), as this has been deemed more appropriate than other methods [151].

$$F(\sigma) = (i - 0.3)/(n + 0.4)$$

Equation 4

Once the plot is created, a linear regression can give the best fit line to the data, the slope of which is the Weibull modulus, β .

Chapter 4: Sample Selection, Preparation Methods, and the Apparent Tensile Properties of Silk

Before beginning an examination of the effects of microwave radiation on silk mechanical properties, it is first appropriate to determine and eliminate any obvious sources of noise in data. Significant variation in data could hide effects that we are trying to observe, or alternatively could by chance make it appear there is an effect when in fact there is none.

First we identified potential sources of noise that we believe are common to research laboratories where silk is reeled by hand from silkworm cocoons. Sources of noise can be categorized as either intrinsic (inherent to the silk as it was made by the silkworm) or extrinsic (imposed on the silk at some point after production by the silkworm). Here we investigate two factors that are intrinsic (the color of the silk, and the part of the cocoon wall from which the silk was collected), and two that are extrinsic (how the silk was handled, and how the silk was stored prior to tensile testing).

By quantitatively identifying which factors have a significant effect, and which ones are relatively unimportant, we hope that unnecessary statistical variation in data can efficiently be minimized—not only in the present work, but also across different laboratories.

Effect of Silk Location within the Cocoonⁱ

Figure 9 shows comparison plots of properties measured from silk taken from the outside of a cocoon and silk taken from the inside of a cocoon. A total of 16 samples were tested (eight from the outside and eight from the inside). All samples were collected by one person from the same white cocoon, and no desiccant was used during sample storage. In an attempt to minimize the effects of daily temperature and humidity variations while the tensile tests were being performed, successive tests alternated between samples from the inside and outside surfaces of the cocoon. At the 90% confidence level, none of the tensile property comparisons revealed a significant difference between the two locations of sample collection.

ⁱ As presented in our 2012 paper “Sample Selection, Preparation Methods, and the Apparent Tensile Properties of Silkworm (*B. mori*) Cocoon Silk” (see Reference [111])

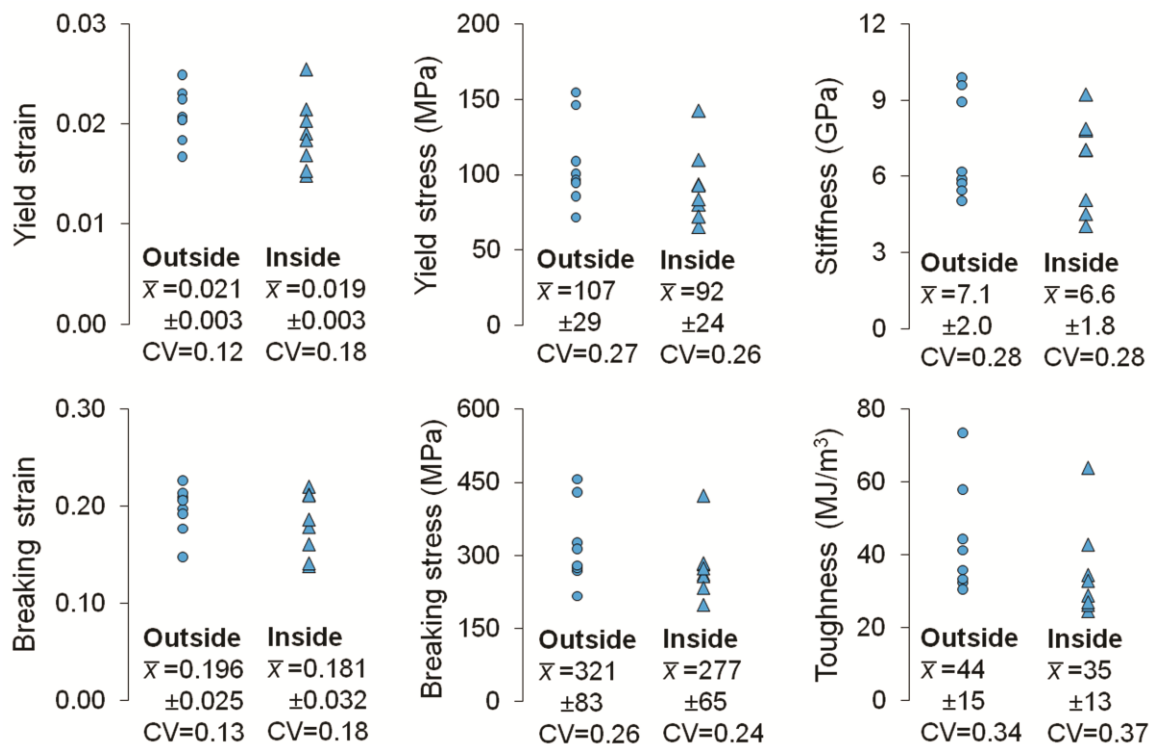


Figure 9 Comparison of tensile properties of silk samples taken from the outside and inside surfaces of a cocoon. The mean (\bar{x}) \pm standard deviation is given below each set of samples (in the same units as the plotted data), along with the coefficient of variation (CV). The ambient testing temperatures for outside and inside samples were 21.2 ± 0.4 °C and 21.1 ± 0.4 °C, respectively, and the relative humidities were $45 \pm 3\%$ and $46 \pm 4\%$, respectively.

Previous authors [28] [110] have reported on the variability of *B. mori* silk mechanical properties within a single cocoon, and also when comparing silk from different cocoons. They concluded that *silk diameter* is an important factor, with thinner samples correlating to better performance. The authors report that, for the particular cocoons used in one study [28], the silk from the “middle” of the wall tends to be the thickest, exhibiting the poorest stiffness, yield strength, and ultimate tensile strength. However, we note that the same research group has also published results on *B. mori* silk implying that the fiber at the outer surface of the cocoon is thickest [109]. It is not stated whether samples described in these different studies were collected by the same person, or whether the samples were stored, or tested under comparable conditions. Our study adds to this work by explicitly comparing silk samples of similar diameters from the inner and outer surfaces of cocoons, to see if these two regions exhibit similar or different tensile properties. Our eight samples from the inner surface had a diameter of 18.4 ± 1.2 μm (mean \pm standard deviation), and the eight samples from the outer surface had a diameter of 19.4 ± 2.0 μm .

The fact that we observe no significant differences in our comparison is consistent with the claim that mechanical properties are diameter dependent, and that fibers of a given diameter should therefore have similar microstructures [28]. This correlation is also consistent with the principles of processing—microstructure—property interdependence in synthetic fiber production, where the final fiber diameter after spinning and drawing dictates the degree of molecular alignment and the consequent mechanical properties of the product. Interestingly, when layers of silk are peeled from a cocoon and tested, the inner layers are found to have a higher stiffness and ultimate tensile strength [109]. However, since we observe no significant differences when testing individual fibers, the differences in layer properties must be the result of factors such as fiber alignment, layer density, and whether fibers in a particular layer happen to be thick or thin.

Effect of Storage Conditions^j

Figure 10 shows comparison plots of properties measured from silk stored without desiccant (eight samples) and with (nine samples). All samples were taken by one person from the outside of the same white cocoon. Data plotted from silk stored without desiccant are the same as in Figure 9. At the 90% confidence level, differences in yield strain and yield stress were observed.

Because our results demonstrate that storage conditions affect the yield point, we performed an additional property comparison in the form of stress relaxation tests (Figure 11). Nine samples were tested from each storage condition.

^j As presented in our 2012 paper “Sample Selection, Preparation Methods, and the Apparent Tensile Properties of Silkworm (*B. mori*) Cocoon Silk” (see Reference [111])

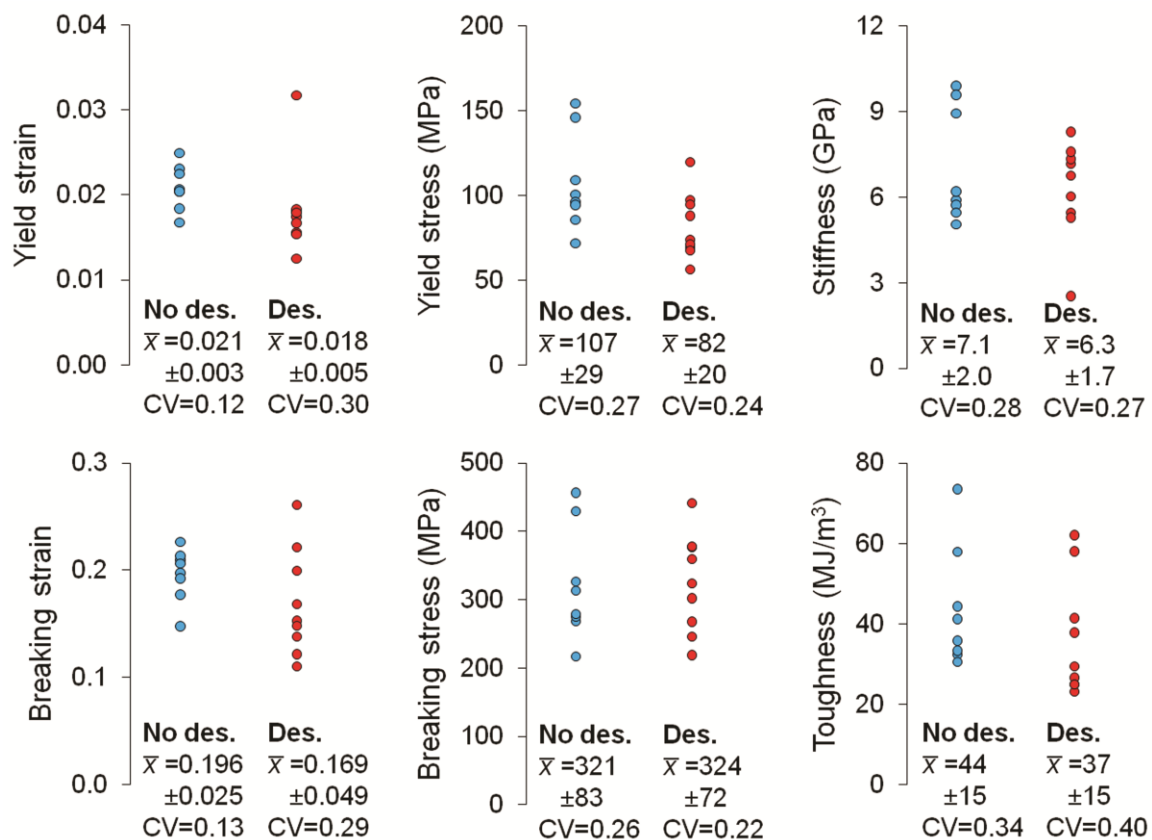


Figure 10 Comparison of tensile properties of silk samples stored without desiccant (No des.) and with desiccant (Des.). The mean (\bar{x}) \pm standard deviation is given below each set of samples (in the same units as the plotted data), along with the coefficient of variation (CV). The ambient testing temperatures for samples that had been stored without and with desiccant respectively were $21.2^{\circ}\text{C} \pm 0.4^{\circ}\text{C}$ and $21.0^{\circ}\text{C} \pm 0.6^{\circ}\text{C}$, and the relative humidities were $45\% \pm 3\%$ and $45\% \pm 4\%$.

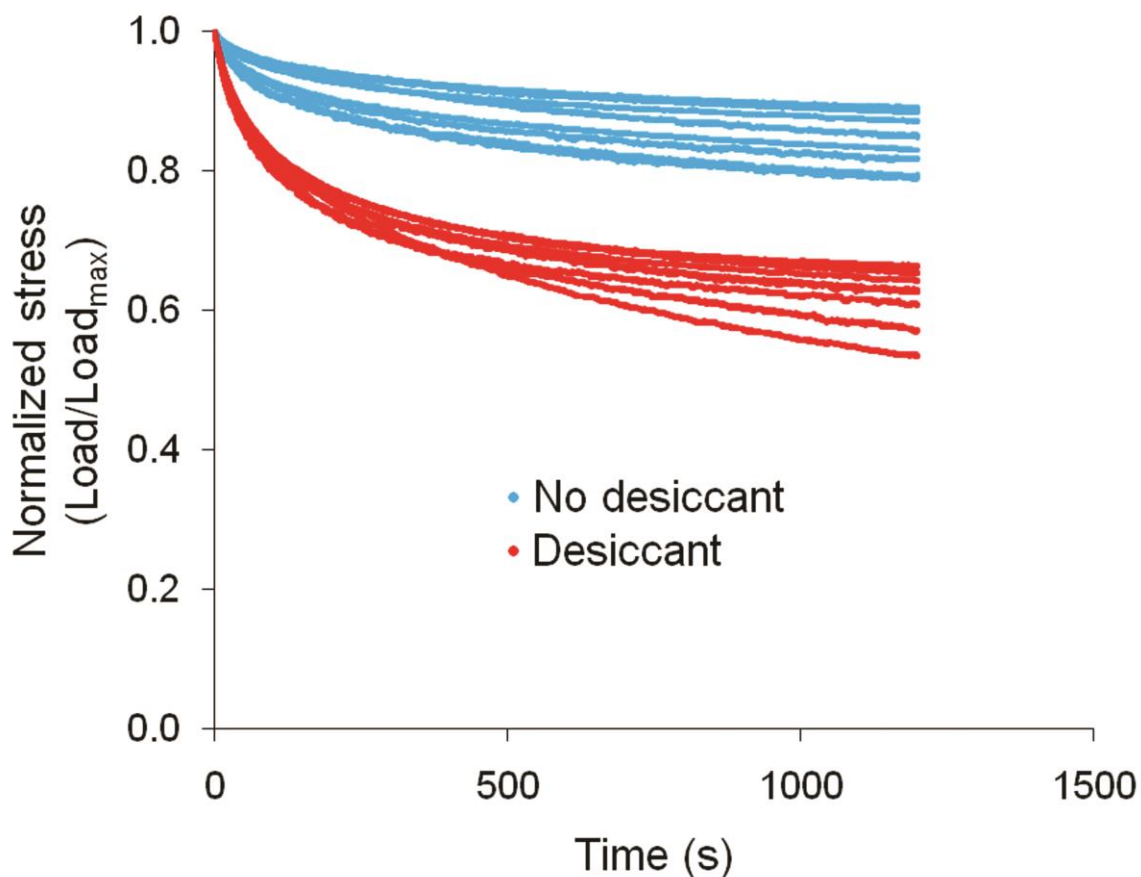


Figure 11 Comparison of stress relaxation in samples that had been stored without desiccant and with desiccant. Ambient testing temperatures for samples that had been stored without and with desiccant were $21.3 \pm 0.4^\circ\text{C}$ in both cases, and the relative humidities were $34 \pm 6\%$ in both cases.

Atmospheric humidity is known to affect the microstructure and properties of many silks (the supercontraction of spider dragline [152] [153] [154] [155], the molecular structure of films of regenerated (reconstituted) *B. mori* silk fibroin [86], and the elastic modulus of *Antheraea pernyi* silk [115]). Therefore, in any study of silk mechanical properties, it is important to record the ambient humidity at the time of testing. One study [134] has indicated that conditioning silk yarn at 100% relative humidity prior to testing will affect the shape of stress–strain curves subsequently produced (relative to silk yarn that has not been conditioned at high humidity), but in general we observe that the literature lacks studies of how storage conditions prior to mechanical testing might affect the mechanical properties measured for silk fibers.

For tensile tests performed on silkworm silk fibers submerged in water (the extreme case of high ambient humidity), it has been reported [156] that breaking strain increases when compared to silk tested under ambient conditions in air, while stiffness, strain at the

proportional limit, and tensile strength all decrease. It was concluded that water disrupts hydrogen bonds in the amorphous phase of silk, thereby acting as a plasticizing agent.

Our present results Figure 10 do not reveal any decrease in breaking strain when samples are stored with desiccant—a condition that should cause the silk to be less plasticized. Also, the samples that had been stored with desiccant exhibited a lower yield strain and yield stress, and they relaxed more rapidly under a given extension than samples stored without desiccant (Figure 11); these three observations suggest that removal of water leads to an increase in plasticization. Concern about the apparent contradictions with the previous work leads us to reevaluate how the accessible amorphous regions of silk might be altered when ambient humidity is changed.

In combination with the previous work [156], our present results suggest that there is an intermediate level of hydration for optimizing mechanical properties. This idea is consistent with modeling work [132] that predicts the existence of an optimal cluster size of interchain (polymer-polymer) hydrogen bonds (3–4 bonds/cluster) to maximize the shear strength of a protein material (regardless of whether the material is crystalline or amorphous). We therefore propose that, in the case of silkworm silk, the following relationships pertain for hydration level, microstructure, and plasticization:

1. In water-free silk (an ideal state, not practically accessible), the amorphous regions will have maximum density; the protein chains will be in close contact throughout the microstructure, and will establish large clusters of interchain H-bonds in excess of the number needed for maximum strength. Since only those polymer–polymer H-bonds at the ends of a cluster participate in resistance to shear loading [132], only a small number of the H-bonds in a unit volume of material will contribute to shear strength (Figure 12, point A).

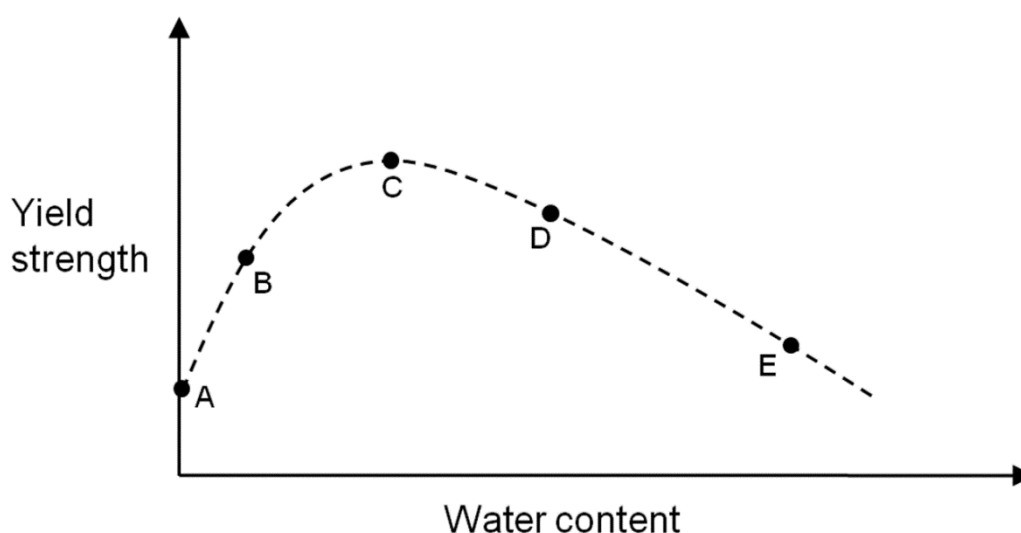


Figure 12 Proposed qualitative relationship between hydration level and yield strength of silk. Points labeled (A-E) denote features discussed in the text.

2. Silk that has been stored in a desiccator will contain less water than silk under normal ambient conditions, but will not be water-free. The size of clusters of H-bonds will be smaller than in water-free silk, but there will be more clusters, as some of the polymer–polymer H-bonds that would have been present in water-free material have been replaced by H-bonds involving water. The accompanying increase in the collective number of hydrogen bonds that are at the ends of clusters will result in a stronger material (Figure 12, point B).

3. At increasing levels of hydration, the size of H-bond clusters will be further reduced, and the number of clusters will be correspondingly increased, so that the total number of polymer–polymer H-bonds contributing to strength eventually reaches the optimal value (Figure 12, point C). The hydration level corresponding to maximum strength must lie below that associated with normal ambient conditions (Figure 12, point D), because the partial dehydration of *B. mori* silk in ethanol leads to a decrease in plasticity [156].

4. At sufficiently high levels of hydration, the number of polymer–polymer H-bonds, and the size of H-bond clusters, will drop below the values required for maximum strength (Figure 12, point E). This is the result that we would expect from immersing silk in water.

Thus we see how both an increase and an appropriately large decrease in the level of hydration, relative to the hydration under normal ambient conditions, can lead to a weaker material, and the apparent contradiction is resolved.

The strengthening effect of water is not unique amongst natural polymers. Many kinds of cellulosic fiber (cotton, linen, jute, and ramie) perform better in the presence of water, displaying both increased tensile strength and increased elongation to break. It has been suggested that this improvement is caused by water molecules allowing a more uniform distribution of load [157].

Our discussion presumes that water lost from silk stored in a desiccator is not significantly regained during the time that it takes to transfer the sample to the Instron and conduct the tensile test. Given the small sample diameter (small diffusion path; fiber diameter is $\sim 20\ \mu\text{m}$), this presumption bears closer examination. The loss of adhered water from the amorphous regions when samples are placed in the desiccator would lead to a densification of the amorphous regions, as H-bonding between protein and water is replaced by protein–protein H-bonds. We propose that this densification makes it more difficult for water molecules to subsequently reenter the amorphous structure. As a result, the effects of storing silk in a desiccating environment can persist over the time scale of one of our tensile tests, even after the silk is reintroduced into the more humid laboratory environment; although the diffusion distance for water attempting to penetrate an individual silk fiber is small, rehydration is kinetically limited by the network of densely packed, hydrogen bonded protein chains. In contrast, if the amorphous regions are

already partially hydrated, then penetration by additional water can be accommodated relatively easily by the ability of these regions to swell.

These kinetic considerations demonstrate a need to take account of a sample's exposure to humidity both prior to and during testing. To the best of our knowledge, the sensitivity of reeled silk to storage conditions (as distinct from testing conditions) has not been assessed previously in the literature. Sensitivity to both current and past ambient humidity levels complicates the interpretation of results of mechanical tests from different laboratories, and makes inter-laboratory comparisons challenging. Identifying a range of storage and testing humidity levels (and temperatures) over which variation in mechanical properties of *B. mori* silk is minimized should therefore be a priority. To achieve this goal on a practical timescale will require multilaboratory collaboration. These optimal conditions may be significantly different from the conditions that prevail naturally in a particular location where the silk is being characterized.

Insects and spiders produce many different kinds of silk, each optimized for use in a particular environment. It is therefore unlikely that the range of ambient conditions identified for minimizing variations in *B. mori* silk behavior will apply to other types of silk. An appropriate range of storage and testing conditions should therefore be considered in each case.

Recombinant silk research might also benefit from such a careful treatment. We have used data published on one such material—a recombinant spider silk [36]—to obtain the coefficients of variation for breaking stress and breaking strain (both estimated from the published stress vs. strain plots), and for toughness (calculated from published numerical data). The coefficients of variation were 0.17 (breaking stress), 0.54 (breaking strain), and 0.61 (toughness), with corresponding values that we obtained from *B. mori* silk under nominally similar but not explicitly identical circumstances (no controlled storage conditions) being 0.25, 0.15, and 0.35, respectively. The evident convoluting effect of silk type on data variability underlines the need for specific standardization of conditions.

Effect of Handling (Reeling) by Different People^{k,1}

Figure 13 shows comparison plots of properties measured from silk hand-reeled by two different people, from the same white cocoon. Silk was collected and pooled from both the inside and outside of the cocoon. Ten samples were collected by each person, and all samples were stored with desiccant. At the 90% confidence level, differences in breaking strain and toughness were observed.

^k Data presented in this section were obtained in collaboration with Lindsay Bianchini as she interned in the Viney lab in 2010.

¹ As presented in our 2012 paper “Sample Selection, Preparation Methods, and the Apparent Tensile Properties of Silkworm (*B. mori*) Cocoon Silk” (see Reference [111])

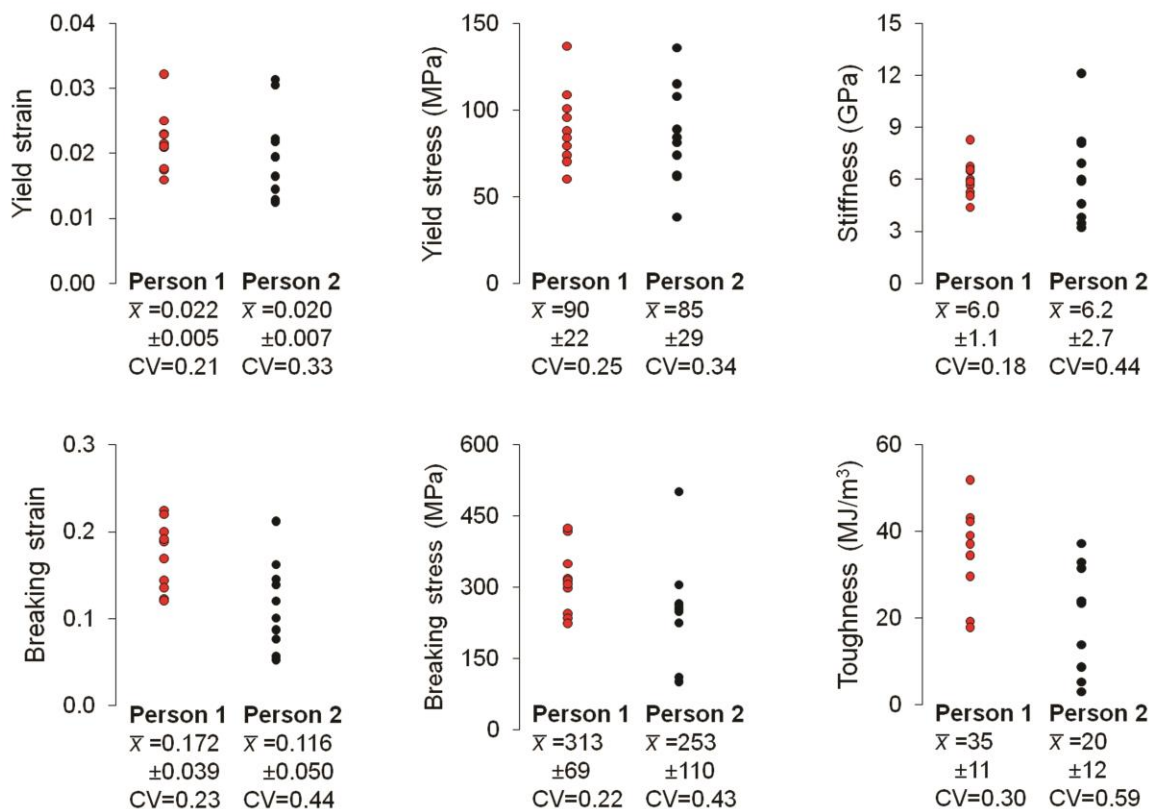


Figure 13 Comparison of tensile properties of silk samples collected by two different people. The mean (\bar{x}) \pm standard deviation is given below each set of samples (in the same units as the plotted data), along with the coefficient of variation (CV). The ambient temperature and humidity during testing were approximately 23°C and 54% respectively.

Most publications regarding the mechanical properties of silkworm silk do not provide detailed information about how the material was handled during collection for study. However, we expect that this handling could alter the values of mechanical properties that are measured in the subsequent tensile tests.

A finite (minimum) force is required to reel silk from the cocoon. This minimum force will fluctuate as the fiber is reeled, depending instantaneously on the amount of residual sericin at the point where the fiber is being detached from the rest of the cocoon. Although silk is famed for its high strength, the force needed to produce permanent deformation of single fibers is small, because single fibers have a small cross-section. Thus, in attempting to apply the minimum force needed to collect material, it is likely that the person reeling the silk will at times exceed the force corresponding to the yield stress. The resulting plastic deformation will work-harden the material, altering the tensile properties. Even in the context of being “careful”, different people will have different sensitivities and different reaction times in regard to overshooting the minimum force for reeling, and so we must consider the possibility that the measured properties of the silk will depend on the person who did the reeling.

An analogy can be made between plastic deformation inflicted during reeling and the plastic deformation imposed on a polymer fiber during a postspinning draw. The latter type of treatment has been shown to affect the tensile properties of both spider drag line [158] and regenerated *B. mori* silk [122].

Results from an experiment comparing silk hand-reeled by two researchers (“Person 1” and “Person 2”) have been presented in Figure 13. Breaking strain and toughness were significantly lower for Person 2, even at the 95% confidence level. Other properties displayed no significant differences. For all properties measured, the coefficient of variation was larger (in some cases twice as high) for the samples reeled by Person 2, who had less experience at hand-reeling than Person 1. Practice at handling silk is therefore beneficial for reducing variability that is not intrinsic. The two individuals nominally carried out the same procedure, so we suppose that the differences in reproducibility reflect differences in (i) how these researchers perceived what constitutes a noticeable increased resistance to reeling, and (ii) their natural reaction times.

Interestingly, although plastic deformation would be expected to affect the yield strength and stiffness of samples, neither property measured in silk reeled by Person 1 is distinguishably (statistically) different from the corresponding property measured in silk reeled by Person 2. This outcome may simply be a consequence of the natural and imposed variability in these properties combining to mask a change in the mean values of the properties.

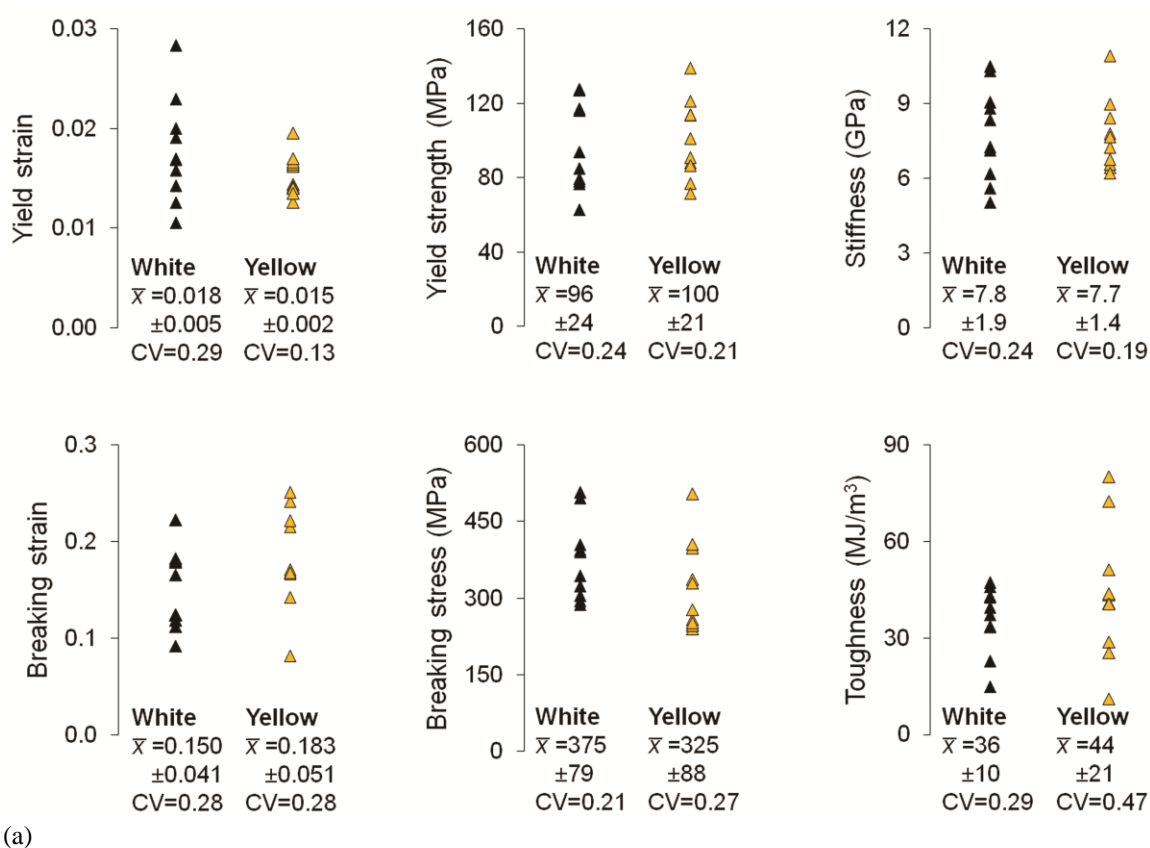
So why are breaking strain and toughness affected? Additional insights may be obtained by considering the behavior of naturally spun spider drag line silk [159]. In that material—which does not require reeling—variability increases in tensile properties measured at larger strains. For example, the coefficient of variation for the breaking strength (necessarily measured at maximum strain) was more than twice that for initial stiffness (which is measured at small strains). Since there is a wide range of values that can be achieved naturally in the properties that characterize the later stages of viscoplastic deformation, the authors note the opportunity for tailoring those properties for particular applications, if the mechanism behind the variability can be discovered. Moreover, it was observed that the conventional tensile properties are not statistically correlated with one another, suggesting the possibility of controlling specific tensile properties independently of one another via appropriate processing.

If silkworm silk behaves similarly to spider silk, the effect of some processing mechanisms, either natural or inadvertently imposed by reeling, might only become apparent in the later (plastic) regions of stress–strain plots. Such behavior would explain why we observe differences in the properties measured late in the deformation procedure (namely breaking strain and toughness), and not in properties measured early on (namely elastic modulus and yield point). Breaking stress is also measured at maximum deformation, but it is a property that we would not expect to see affected by plastic deformation (as inflicted by different styles of handling). It is therefore not surprising that the samples reeled by Person 1 and Person 2 give statistically indistinguishable results for that particular property.

To eliminate reeling techniques as a source of inter-laboratory differences and intra-laboratory variability in the behavior of silk, a purely mechanical device for reeling could usefully be developed and adopted.

Effect of Silk Color^{m, n}

Figure 14 shows comparison plots of properties measured from white and yellow silk. Two experiments were performed; in both cases 10 samples of each color were collected by the same person, primarily from the inner surface of the cocoon, and all silk was stored with desiccant prior to tensile testing. At the 90% confidence level, none of the tensile property comparisons revealed a significant color-dependent difference in the first experiment. In the second experiment, only the yield strength was significantly different.



^m Data presented in this section were obtained in collaboration with Lindsay Bianchini as she interned in the Viney lab in 2010.

ⁿ As presented in our 2012 paper “Sample Selection, Preparation Methods, and the Apparent Tensile Properties of Silkworm (*B. mori*) Cocoon Silk” (see Reference [111])

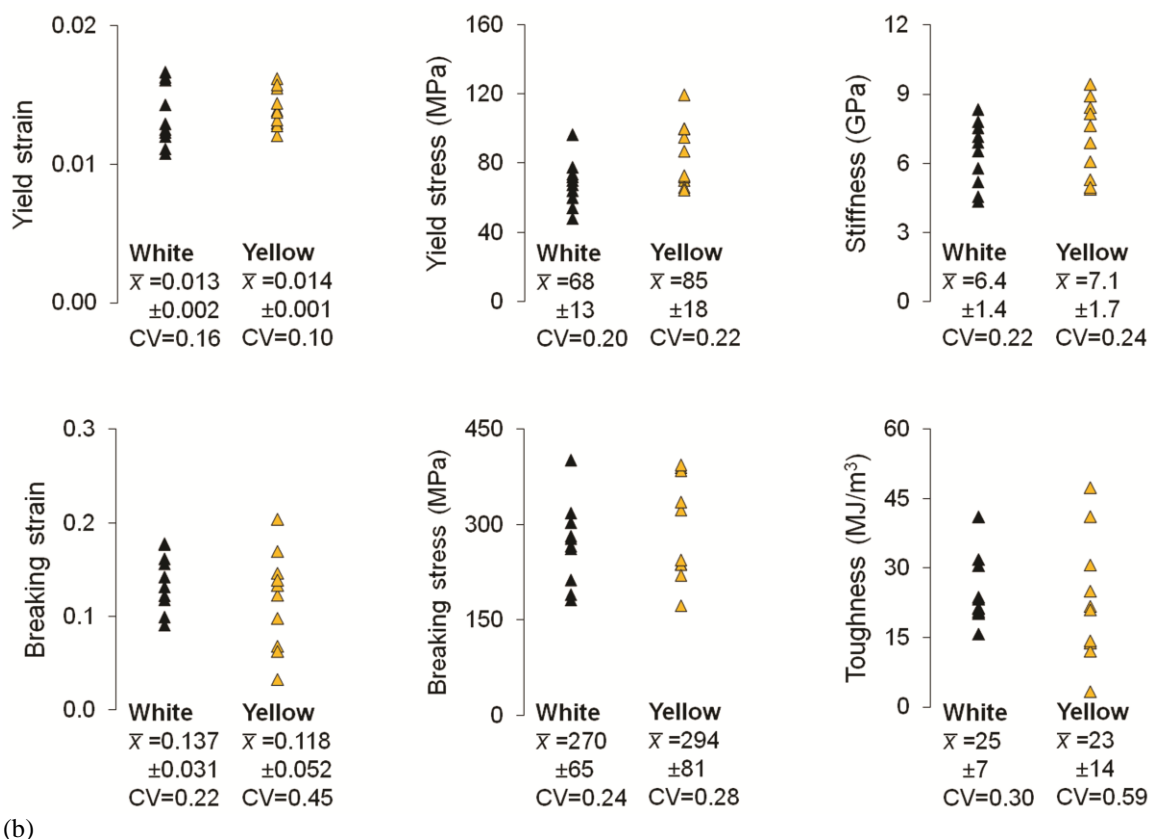


Figure 14 Comparison of tensile properties of silk samples taken from white cocoons and yellow cocoons. The mean (\bar{x}) \pm standard deviation is given below each set of samples (in the same units as the plotted data), along with the coefficient of variation (CV). (a) Comparison of representative white and yellow cocoons (one of each, without regard given to cocoon size). The ambient temperature and humidity during testing were approximately 22°C and 47% respectively. (b) Comparison of similarly sized white and yellow cocoons. The ambient temperature and humidity during testing again were approximately 22°C and 47% respectively.

Silk is spun naturally in a variety of colors. Carotenoids and flavonoids are the two main types of pigment that are known to contribute to the color of *B. mori* silk [160] [161] [162]. Larvae that inadequately absorb dietary carotenoids produce cocoons with white silk [163]. In contrast, a single spider is capable of producing more than one color of silk, even when fed the same diet consistently: the color of major ampullate silk collected from *Nephila clavipes* kept in captivity (and fed only crickets) sometimes changed suddenly from white to yellow during forcible silking [164]. It was noted in this study that surface morphology and tensile properties are unaffected by the color change.

While there are reports that describe the interplay of silkworm genetics and silk color [160] [163] [165], the literature appears to lack studies that look for a correlation between the color and tensile properties of silkworm silk. Given that both the color and the mechanical properties of silk are determined by composition, the possibility of such a correlation must be addressed. It is worth noting that some researchers [160] [162]

identify sericin as the principal locus for pigment accumulation, in which case the effect on tensile properties should be minimal. However, we observe that our yellow cocoons retain their color after the degumming treatment, indicating that at least some of the pigment remains.

We performed two experiments comparing the properties of yellow silk with those of white silk. In the first comparison (Figure 14a), we observed no significant differences in any of the tensile properties measured. The possible complicating effects of different sample diameters (see discussion starting on page 32) were minimized by checking that the diameters were similar: $15.7 \pm 2.0 \mu\text{m}$ for white silk, and $15.1 \pm 3.4 \mu\text{m}$ for yellow silk. However, we observed that in our supply of cocoons, the white ones were typically larger than the yellow ones, so we subsequently considered whether cocoon size might also be an important variable, reflecting different levels of quality of silk production by the silkworm. We therefore performed a second experiment (Figure 14b), comparing white and yellow silk collected from similarly sized cocoons. Diameters were again similar: $15.8 \pm 2.0 \mu\text{m}$ for white silk, and $16.8 \pm 3.8 \mu\text{m}$ for yellow silk. This second experiment showed yield strength to be higher for the yellow cocoon silk, with no significant effect on the other properties measured.

These preliminary results suggest at most a minor role for both silk color and cocoon size in affecting the tensile properties of silkworm silk. Their contribution is small in comparison to that of other factors such as handling style and storage conditions.

Chapter Conclusions^o

- 1) Interpretation of the extensive existing literature on silk mechanical properties must take account of the reality that the sample handling, storage, and testing environments are not standardized and are usually not reported.
- 2) Tensile properties of degummed silk from the inside surface of a *B. mori* cocoon do not differ significantly from those of silk taken from the outside surface, provided that samples used in the comparison have similar diameters. In combination with previous studies, this finding suggests that silk from any part of the cocoon may be used without concern over introducing a new source of variability into collected data, subject to the limitation that the sample diameters should be consistent.

^o As presented in our 2012 paper “Sample Selection, Preparation Methods, and the Apparent Tensile Properties of Silkworm (*B. mori*) Cocoon Silk” (see Reference [111]), and in our 2011 proceedings paper “The Effect of Microwave Radiation on Tensile Properties of Silkworm (*B. mori*) Silk” (see Reference [175]).

- 3) Storage conditions can have a significant and enduring effect on tensile properties of degummed *B. mori* silk. Samples stored in a sealed container with desiccant (silica gel) have a lower yield stress and yield strain than samples stored without desiccant, and they also relax more rapidly in stress relaxation tests. The ability of this silk to resist plastic deformation is optimized at intermediate hydration levels. Sensitivity to the humidity levels encountered by samples prior to testing complicates the interpretation of results, and makes inter-laboratory comparisons challenging. Silk storage conditions should therefore be reported—and, ideally, standardized—to enable useful comparison between studies.
- 4) Differences in hand-reeling techniques can impose changes on the silk microstructure that significantly affect the results of tensile tests. Breaking strain and toughness were lower for the samples reeled by one person in our study, and the coefficient of variation was markedly higher for those samples in all tensile properties measured (yield strain, yield stress, stiffness, breaking strain, breaking stress, and toughness). Standardization of silk reeling technique is therefore necessary.
- 5) Silk color and cocoon size have a small to negligible effect on tensile properties.
- 6) Extrinsic factors (storage conditions, reeling by different people) have a more significant effect than intrinsic differences (location of sample in cocoon wall, color of sample) on tensile properties. Accordingly, we propose that effort should be prioritized on standardizing the extrinsic factors, so that results of studies from different laboratories can be more usefully compared.

Chapter 5: On Calibrating the Power of a Microwave Oven^P

To study the effect of microwave radiation on silk in any detail, it is necessary to quantify how much radiation the silk is receiving in a given experiment. Therefore, considerable time and effort was given toward understanding how microwave oven power measurements are taken, and developing a calibration procedure that was appropriate to our needs.

Because of the limited control of internal conditions when a domestic microwave oven is used for experiments, it is important to be able to characterize the power output of individual ovens. To this end, ASTM Standard F 1317 – 98 prescribes [166] a calibration procedure wherein the power output of the oven is determined by measuring the temperature change when a beaker of water is microwaved. The standard *assumes* that there is a delay of 3 seconds from the time that the “start” button is pressed on a microwave oven to the time that the magnetron activates; here we *measure* the delay time. The standard specifies the use of 1000 mL water in a 2000 mL beaker (or alternatively a 2 L polystyrene foam container). We questioned whether using 1000 mL of water gives the most accurate measure of the oven’s output power. Moreover, we wondered if the shape, aspect ratio and placement of the container used to hold the water might influence the calibration. Here we present a series of experiments to investigate which factors can affect calibration results significantly. Our findings are applicable not only for the experiments we describe in the next chapter (beginning on page 62), but also for any experiments that involve the calibration of domestic microwave ovens.

Measuring the magnetron startup delay time

When the “start” button is pressed on a microwave oven, there is necessarily a finite delay until microwave radiation is released into the main cavity of the oven. This delay is due to the time required for the magnetron to become active. While ASTM Standard F 1317 – 98 *assumes* a delay of 3 seconds, we opted to *measure* the startup delay of our oven, so as to not introduce unnecessary error into subsequent calculations.

Figure 15a shows the relationship between t_{set} and the change in temperature (ΔT) of 1000 mL of water that was heated from ambient in a 2000 mL beaker centered on the turntable; these volumes are consistent with the existing ASTM Standard F 1317-98 [166]. The unconventional choice of plotting the dependent variable (ΔT) horizontally

^P As presented in our paper entitled “Calibrating the power of a domestic microwave oven” (submitted 2013, [PLOS ONE](#)). Portions are also presented in our 2011 proceedings paper “The Effect of Microwave Radiation on Tensile Properties of Silkworm (*B. mori*) Silk” (Reference [175])

and the independent variable (t_{set}) vertically was made so that a routine linear regression (which allows extrapolation of the y-intercept of the plot) could be performed on the data to obtain t_{delay} and the standard deviation in t_{delay} . The extrapolation gives $t_{delay} = 2.409$ s, which is significantly different from the 3 s delay assumed by ASTM Standard F 1317-98. Note that we used only the first minute of data (points plotted in red) for the extrapolation, because heat losses contribute increasingly to the data as t_{set} increases.

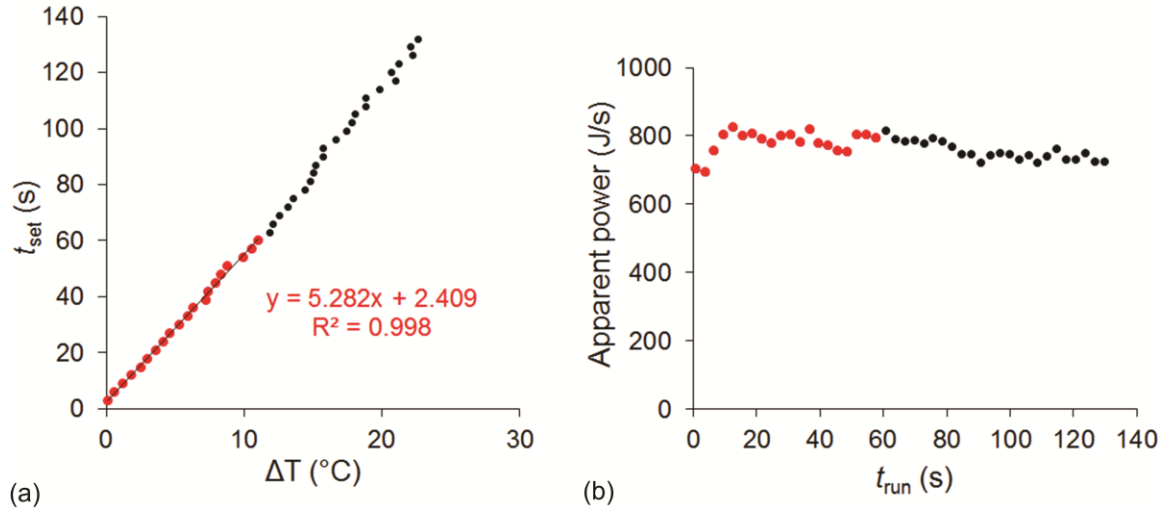


Figure 15 (a) Measurement of microwave oven startup delay time t_{delay} . For each data point collected, the water was initially at room temperature. Linear regression was performed with qtiPlot version 0.9.9-rc6 on the first minute of data (points plotted in red). The y-intercept of the plot is at $t_{delay} = 2.409 \pm 0.395$ s, i.e. 2.4 ± 0.4 s if only significant figures are retained. This value differs markedly from the 3 s delay assumed by the ASTM Standard (F 1317 – 98). (b) Microwave oven power plotted as a function of t_{run} , applying Equation 1 to the data plotted in (a) and using $t_{delay} = 2.409$ s.

If we neglect heat losses, $\Delta T = A (t_{run}) = A (t_{set} - t_{delay})$, where A is a constant. Substituting this expression for ΔT into Equation 1 gives:

$$\begin{aligned} P &= A (t_{run}) V c \rho / (t_{run}) \\ &= A V c \rho \end{aligned}$$

Equation 5

Thus, the power calculated from Equation 1, using experimental values for ΔT and t_{set} along with the extrapolated value of t_{delay} , should be independent of $t_{run} = (t_{set} - t_{delay})$. However, a plot of the calculated (apparent) power vs. t_{run} is not horizontal, but instead has a small negative slope, as is evident in Figure 15b.

Larger values of t_{run} are associated with a larger thermal gradient between the sample and its environment, leading to increased heat flux (loss) from the water. Also, larger values of t_{run} afford more opportunity for heat loss because more time elapses before the final temperature of the water can be measured. Hence the measured ΔT – and the

corresponding value of apparent power – will be less than the true value, and the discrepancy will be an increasing function of t_{run} , consistent with the negative slope of the plot in Figure 15b. More formally, this trend can be described by referring again to Equation 1 and taking into account a non-linear dependence of ΔT on t_{run} . For small departures from linearity we can neglect third- and higher-order terms and write $\Delta T = A (t_{run}) - B (t_{run})^2$, where A and B are constants. Now substitution into Equation 1 gives:

$$\begin{aligned} P &= [A (t_{run}) - B (t_{run})^2] V c \rho / t_{run} \\ &= C - D t_{run}, \text{ where } C \text{ and } D \text{ are constants.} \end{aligned}$$

Equation 6

Thus, the relationship between P and t_{run} is a straight line with a nonzero (negative) slope as seen in Figure 15b. Extrapolation of this line to the y-intercept should provide a measure of the true microwave oven power output P_{true} . The ability to neglect third- and higher-order terms in the expression relating ΔT to t_{run} requires us to impose an upper limit on the domain of values on which the extrapolation is performed. To strike a balance between setting this limit too high (which would capture more of the unwanted, increasingly nonlinear data) and too low (which would reduce the amount of data on which to base the extrapolation), we chose the limit at $t_{run} = 60$ s.

Our extrapolation-based method for measuring the power output requires that we also impose a *lower* limit on the domain of values on which the extrapolation is performed. Strictly, P is approached as the *limiting* behavior of Equation 6 as $t_{run} \rightarrow 0$, and not by considering what happens *at* $t_{run} = 0$ (since zero t_{run} would have to correspond to zero power output). Additionally, we see in Figure 15b that the two data points closest to the origin are somewhat separated from the overall trend of the data. The reliability of small t_{run} ($= t_{set} - t_{delay}$) values is questionable because the ± 0.4 s uncertainty in t_{delay} carries over into a ± 0.4 s uncertainty in t_{run} . The first two data points in Figure 15b (and Figure 15a) are for $t_{set} = 3$ s and 6 s respectively, i.e. $t_{run} \sim 0.6$ s (± 0.4 s) and 3.6 s (± 0.4 s) respectively. For these data points, the uncertainty represents more than 10% of their value, and so we cannot justify their inclusion. We therefore performed an iteration of the preceding analysis, in which the extrapolations for finding the delay time (Figure 16a) and the true power of the microwave oven (Figure 16b) are now limited to the domain $5 \text{ s} < t_{run} < 60 \text{ s}$.

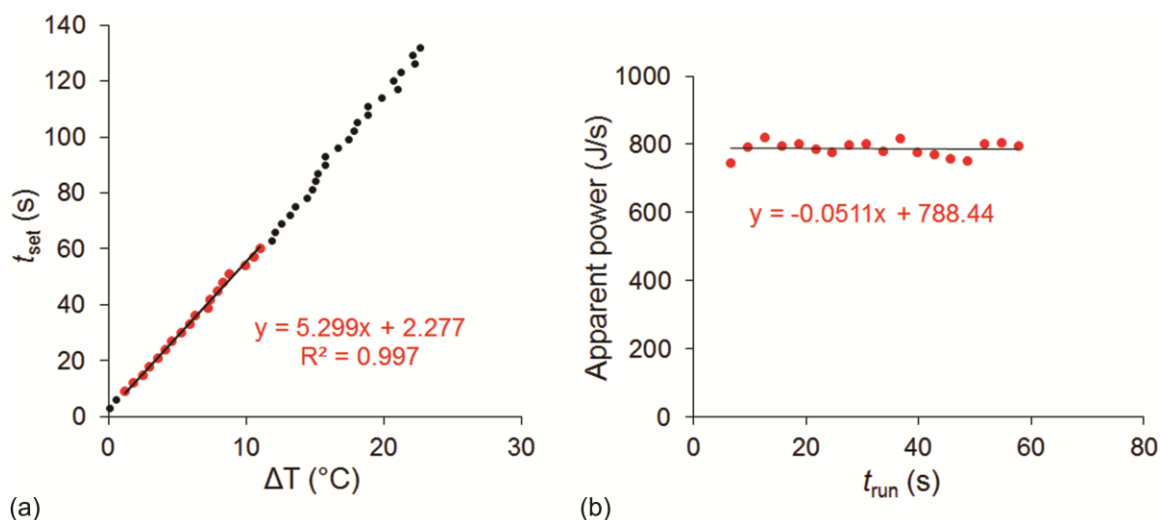


Figure 16 (a) Improved measurement of microwave oven startup delay time t_{delay} . For each data point collected, the water was initially at room temperature. Linear regression was performed with qtiPlot version 0.9.9-rc6 on data in the range $5 \text{ s} < t_{run} < 60 \text{ s}$ (points plotted in red). The y-intercept of the plot is at $t_{delay} = 2.277 \pm 0.515 \text{ s}$, i.e. $2.3 \pm 0.5 \text{ s}$ if only significant figures are retained. (b) Microwave oven power plotted as a function of t_{run} , applying Equation 1 to the data plotted in (a) and using $t_{delay} = 2.277 \text{ s}$. Linear regression was used to find the y-intercept and so obtain a measurement of true output power $P_{true} = 788 \pm 12 \text{ W}$.

We obtained a revised measurement of $t_{delay} = 2.277 \text{ s}$ ($2.3 \pm 0.5 \text{ s}$), and a measurement of $P_{true} = 788.4 \text{ W}$ ($788 \pm 12 \text{ W}$). This measurement of P_{true} is significantly higher than the value of 755 W that we obtained by following the calibration procedure detailed in ASTM Standard F 1317 - 98, which does not take account of heat losses that occur during the calibration.

Effect of calibration ‘work piece’ volume

An experiment was performed to test whether the *amount* of water used as the ‘work piece’ during calibration was important. ASTM Standard F 1317 – 98 calls for 1000 mL of water (in a 2 L beaker), so we chose to test an array of volumes about this value. Figure 17a shows how ΔT changes as a function of the volume of water microwaved. In every case, the water was placed in a 2 L beaker, and the microwave oven set time was 12 s (a value chosen to ensure that none of the samples—including small ones used in later experiments—reached the boiling point). The corresponding plot of the oven’s apparent output power (Figure 17b) confirms that larger values of ΔT (associated in this case with microwaving smaller volumes of water) lead to an underestimate of the oven’s power.

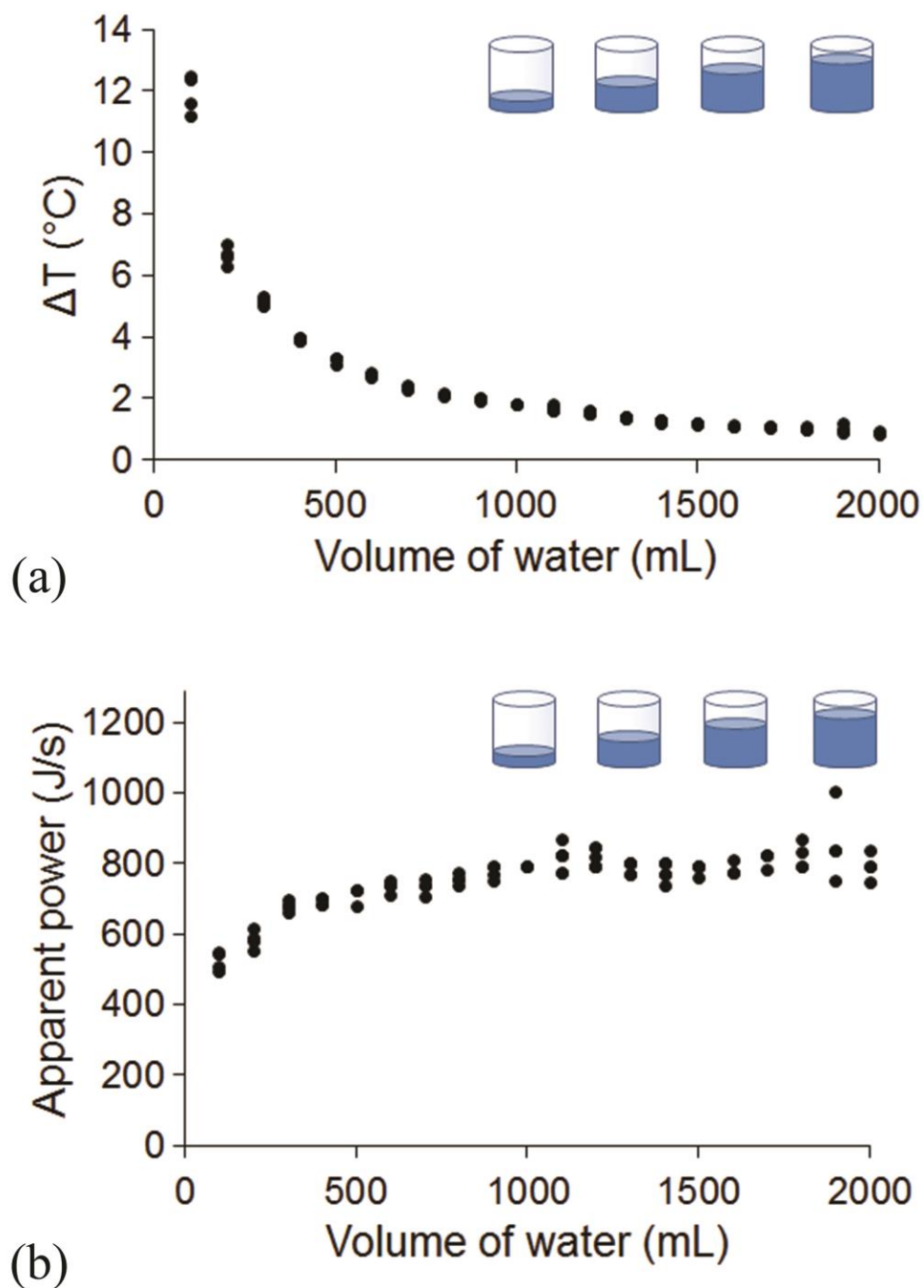


Figure 17 (a) Temperature increase caused by microwaving different volumes of water in a 2 L beaker for a set time of 12 s. A minimum of four trials were performed (and plotted here) for each volume of water tested. (b) Corresponding estimates of the microwave oven output power, obtained with Equation 1.

Qualitatively, we recognize several factors that contribute to the observed results: (1) As already noted, objects that are hotter will transfer heat to their surroundings more quickly than objects that are only slightly above room temperature. (Therefore, since small

volumes are raised to higher temperatures by a given dose of microwave radiation, they also lose more heat before the temperature can be measured) (2) A smaller volume of water also provides relatively more surface area from which heat can escape into the surroundings before the temperature is measured. (3) A larger volume of water provides a larger cross sectional area for microwaves to interact with (and subsequently be volumetrically absorbed), so that fewer are 'lost' to other mechanisms (such as travelling back up the waveguide), thus resulting in a higher measured apparent power. A *quantitative* analysis would require considerations of the heat transfer mechanisms involved, including both heat transfer into the body of water from microwave energy, and also heat loss from the surface of the water into the surrounding glass and air, and will not be performed here. Even so, our qualitative analysis alone makes it apparent that calibrations performed with a larger 'work piece' will give a more accurate measure of the output power of the oven.

Effect of size and aspect ratio of calibration 'work piece'

In the experiment summarized by Figure 17, changing the volume of water in the 2 L beaker also changes the aspect ratio (and so the distribution) of the volume of water. It is therefore appropriate to consider whether the distribution of the water might affect the calibration. As an approximation, we could try to obtain different volumes of water with comparable aspect ratios by half-filling a series of beakers that have different sizes. However, beakers of different sizes can have significantly different aspect ratios; for example, the circumference-to-depth ratio of our 2000 mL beakers is 2.21, while our 250 mL beakers, from the same manufacturer, have a circumference-to-depth ratio of 2.50. Using a 2000 mL beaker containing 1000 mL water as a reference (beaker circumference / water depth = 4.97), we can determine the water depth required for a comparable circumference-to-depth ratio in a different beaker as: beaker circumference / 4.97. On that basis, we performed three calibrations on each of the following sample volumes (beaker sizes in parentheses): 1000 mL (2000 mL), 537 mL (1000 mL), 294 mL (600 mL), 124 mL (250 mL), 49 mL (100 mL), 30 mL (50 mL) and 13 mL (20 mL).

Figure 18a shows that the apparent power still increases with increasing water volume, even when the aspect ratio of the filled volume remains constant. Therefore, the absolute volume of water used in the calibration *is* important.

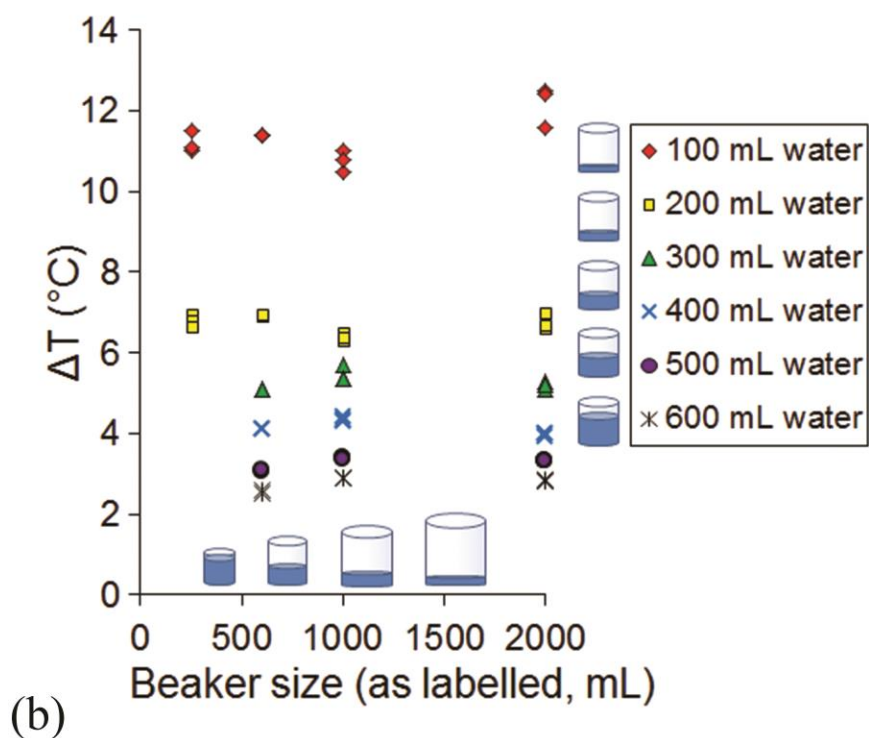
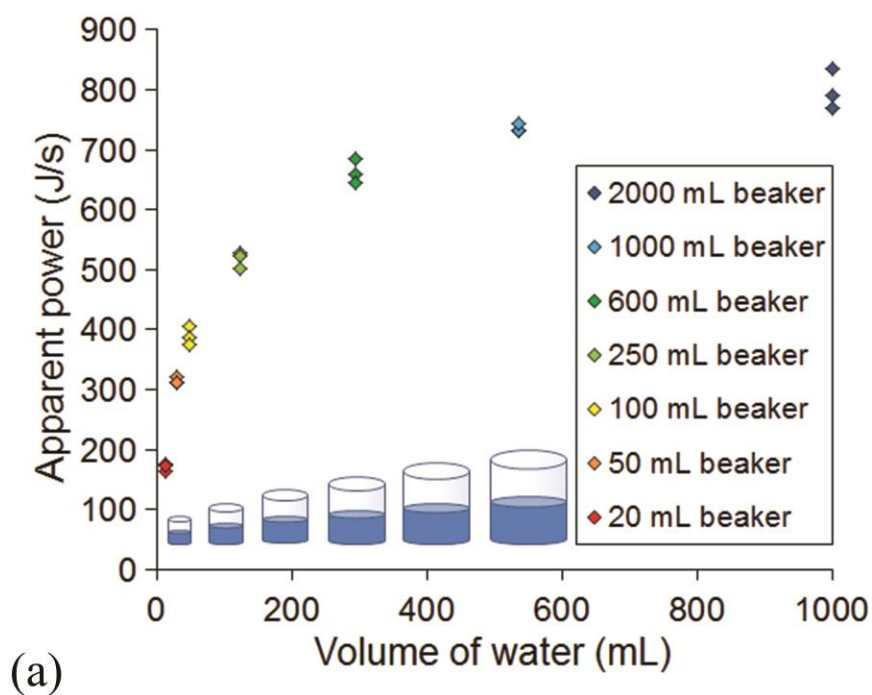


Figure 18 (a) Estimated microwave oven output power (using Equation 1) as a function of water volume and beaker size (fixed aspect ratio). (b) Temperature increase caused by microwaving fixed volumes of water in different sizes of beaker (different aspect ratios). The microwave oven timer was set to 12 s in all cases.

Additionally, if a fixed volume of water is heated for a set time in beakers of different sizes (Figure 18b), then that volume's *distribution* is observed to have an effect on ΔT , too. Figure 18b indicates that if smaller water volumes (200 mL or less) are used, ΔT experiences a minimum when the water is heated in the 1000 mL beaker; however, if larger water volumes (300 mL or more) are used, ΔT instead shows a maximum when the water is heated in that beaker. Heating anomalies in samples that are small in at least one dimension have been described as a consequence of standing waves of microwave energy arising in the sample [167] [168]. The water distribution effect that we observe in Figure 18b might also be explained by this mechanism. To investigate the significance of standing waves as a factor in our calibrations, we turn to experiments involving small beakers with small volumes of water.

Effect of standing waves on apparent power

For *large* volumes of water, most of the microwave energy will have been absorbed by the time the wave has traveled all the way through the sample and reached the far boundary where a reflection may occur. But, for *small* volumes (or large volumes that are spread thin), there may be enough energy left in the wave for it to reflect several times and result in a standing wave of microwave energy. Therefore, we expect any effects of standing waves to be more pronounced in small beakers.

The ΔT vs. volume plot that we obtain from microwaving water in a small (50 mL) beaker is shown in Figure 19a. At 25 mL water, the temperature gain is larger than expected based on the trend exhibited by larger and smaller water volumes. The peak persists when additional measurements are taken around 25 mL (Figure 19b), and becomes amplified in the corresponding plot of apparent power vs. water volume (Figure 19c). The peak in Figure 19a,b,c cannot be explained solely by the presence of a "hot spot" inside the oven; if that were the case, not only would the 25 mL data point be elevated, but also all subsequent data points at volumes larger than 25 mL, since the apparent 'hot spot' locus would still be occupied by water in those cases. To further demonstrate this point, Figure 19d shows results of an experiment in which the same beaker and same volumes of water were used, but with the beaker raised by 10 mm in the oven. To raise the beaker, a 10 mm wide strip of cardstock paper was curled into a spiral, so that the weight of the beaker was supported by the walls of the spiral. We observe that the peak in the data remains at ~25 mL. Had a hot spot somehow been contributing to this peak, we would expect to see the peak shifted to a volume of water 10 mm below the 25 mL level, closer to 15 mL.

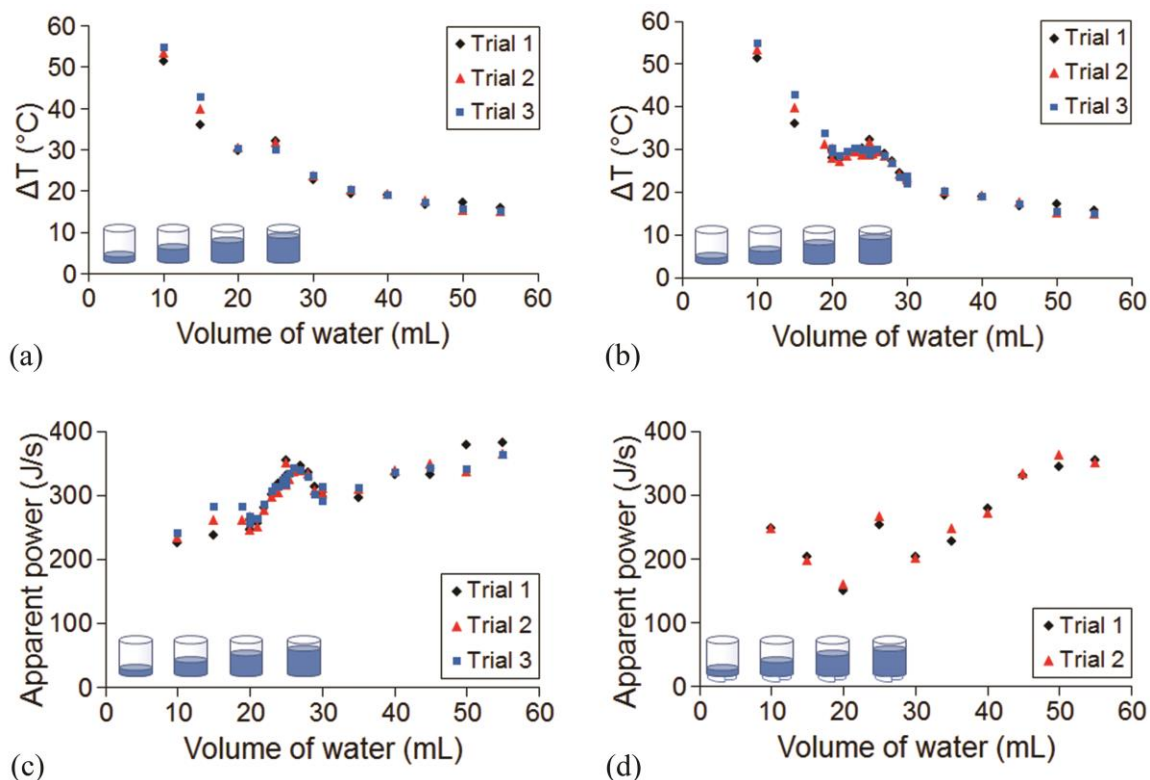


Figure 19 (a) Temperature increase caused by microwaving fixed volumes of water in a 50 mL beaker. (b) Additional data collected in the vicinity of the anomalous peak at ca. 25 mL. (c) Corresponding estimates of the microwave oven output power, obtained with Equation 1. (d) The effect of raising the beaker by 10 mm. The microwave oven timer was set to 12 s in all cases.

To check whether the observation of anomalous peaks was a special result of the particular dimensions of the 50 mL beaker, experiments were also performed in which small volumes of water were heated in a 100 mL beaker (Figure 20). The change in beaker size did not eliminate the occurrence of anomalous peaks. Rather, additional peaks appeared when 12.5 mL and 35 mL of water were used.

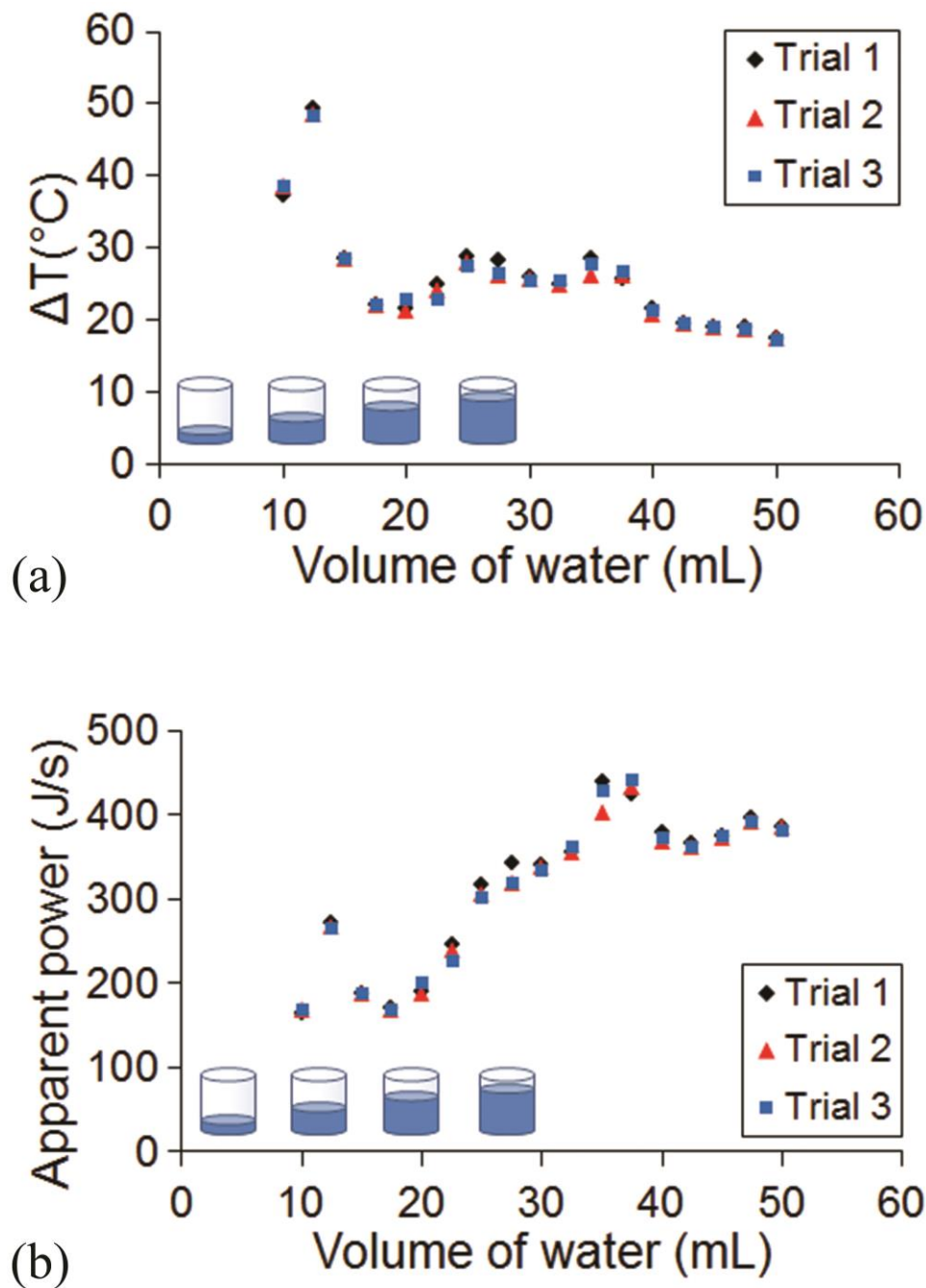


Figure 20 (a) Temperature increase caused by microwaving fixed volumes of water in a 100 mL beaker. (b) Corresponding estimates of the microwave oven output power, obtained with Equation 1. The microwave oven timer was set to 12 s in all cases.

Standing waves have been used previously [167] [168] in an explanation of heating anomalies in tall cylinders of water (where the diameter was small enough to sustain such a standing wave) and in thin slabs of agar gel. The local extremes of temperature (and

apparent power) in Figure 19 and Figure 20 led us to consider whether a similar phenomenon, occurring in the vertical direction at specific volumes of water, could explain our results. Here we show a brief analysis of the dimensional conditions necessary for standing waves to occur in water:

If a standing wave is to be accommodated between two surfaces (interfaces), the distance (d) between the two surfaces must be an integral number of half wavelengths [169]:

$$d = (m/2) \lambda_w$$

Equation 7

where m is an integer, and λ_w is the wavelength of the microwaves in water.

This distance can be calculated once the following relationships are noted:

$$\lambda_w = c/(n_w \nu)$$

Equation 8

where c is the speed of light in a vacuum, and n_w is the refractive index of water at the microwave frequency (ν ; 2.45 GHz).

The Maxwell Relation can be used to find n_w :

$$n_w = |\epsilon|^{1/2} \quad (\text{Maxwell Relation})$$

Equation 9

where $|\epsilon|$ is the magnitude of the complex dielectric constant (ϵ); it can be expressed in terms of the real (ϵ') and imaginary (ϵ'') parts of ϵ :

$$|\epsilon| = [(\epsilon')^2 + (\epsilon'')^2]^{1/2}$$

Equation 10

Appropriate values of ϵ' and ϵ'' at 25°C were obtained from the CRC handbook [170]. As a first approximation, we neglect the temperature dependence of ϵ . Then, Equation 7 through Equation 10 can be combined to show that the distance between interfaces required for a standing wave is found to be approximately:

$$d = m * 0.69 \text{ centimeters}$$

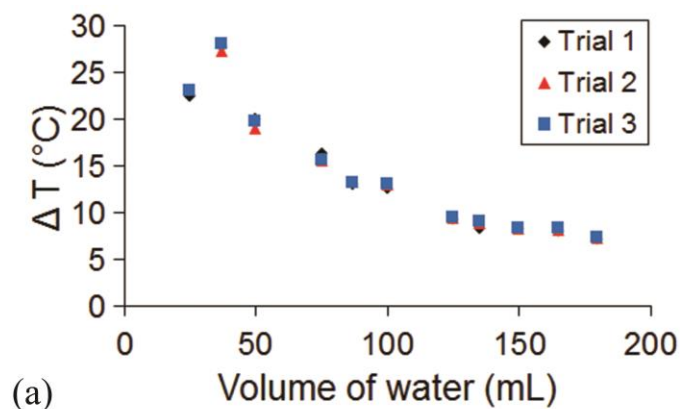
Equation 11

The smallest predicted d values are therefore 0.69, 1.38, and 2.07 cm (when m equals 1, 2, and 3 respectively). Each time a peak was observed in the apparent power as measured with the 50 mL and 100 mL beakers (Figure 19 and Figure 20), we measured the approximate depth of water present by dipping a toothpick into the beaker, and then measuring how far up the toothpick was wet. In the 50 mL beaker (Figure 19), the peak at 25 mL corresponds to a water depth of approximately 2.2 cm. In the 100 mL beaker

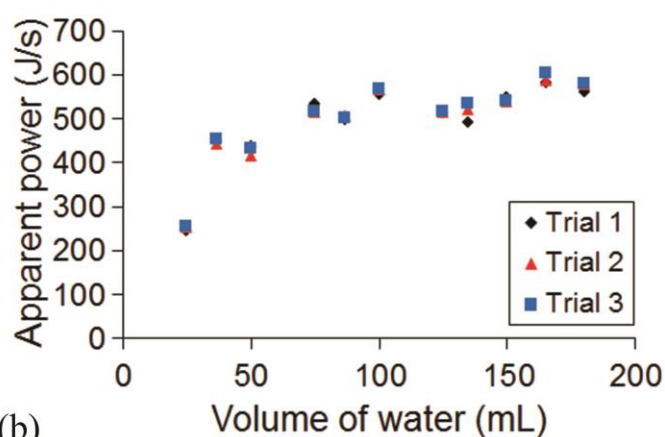
(Figure 20), the peaks at 12.5, 25, and 35 mL correspond to estimated water depths of 0.9, 1.5, and 2.2 cm respectively. While each of these depths is similar to a value of d predicted by Equation 11, in all cases the measured water depth is more than a millimeter deeper than the values predicted by Equation 11. The difference may be attributed to systematic errors, principally introduced by the measurement technique. Water “climbs” the toothpick as a result of meniscus forces and also “wicks” along the grain; both of these effects should contribute independently of the depths being measured. Also, dipping the toothpick into the water causes the water level in the beaker to rise slightly; this effect will be most noticeable when the depth being measured is large.

The oven chamber itself introduces another complicating factor that may influence our results: because conventional microwave ovens are multimodal chambers with reflective walls, standing waves may be established in directions other than the vertical, so that a consideration of only the vertical standing waves is an oversimplification. In particular, the parallel beaker walls could provide for a number of horizontal standing waves to be established, given microwaves entering at appropriate angles.

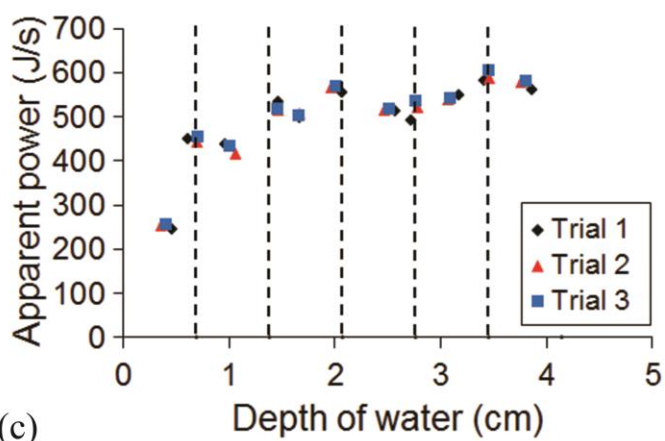
To increase the likelihood of standing waves only being established vertically in the water, we used an Erlenmeyer flask in an additional set of tests. Instead of taking a cylindrical shape, the water thus conforms to the conical shape of the flask – ensuring that the only parallel boundaries of the water are those at the top and bottom, the spacing of which can be altered by changing the volume of water in the flask. Results are shown in Figure 21.



(a)



(b)



(c)

Figure 21 (a) Temperature increase caused by microwaving fixed volumes of water in a 300 mL Erlenmeyer flask. (b) Corresponding estimates of the microwave oven output power, obtained with Equation 1. (c) Microwave oven output power plotted as a function of the depth of water used in the Erlenmeyer flask; depths that may accommodate standing microwaves (Equation 11) are indicated with dashed lines. In all cases the microwave oven timer was set to 12 s.

As can be seen in Figure 21c, apparent power is generally higher at water depths close to predicted standing wave conditions, and lower at intermediate depths. The experiment with the Erlenmeyer flask thus demonstrates the validity of our brief analysis and approximations.

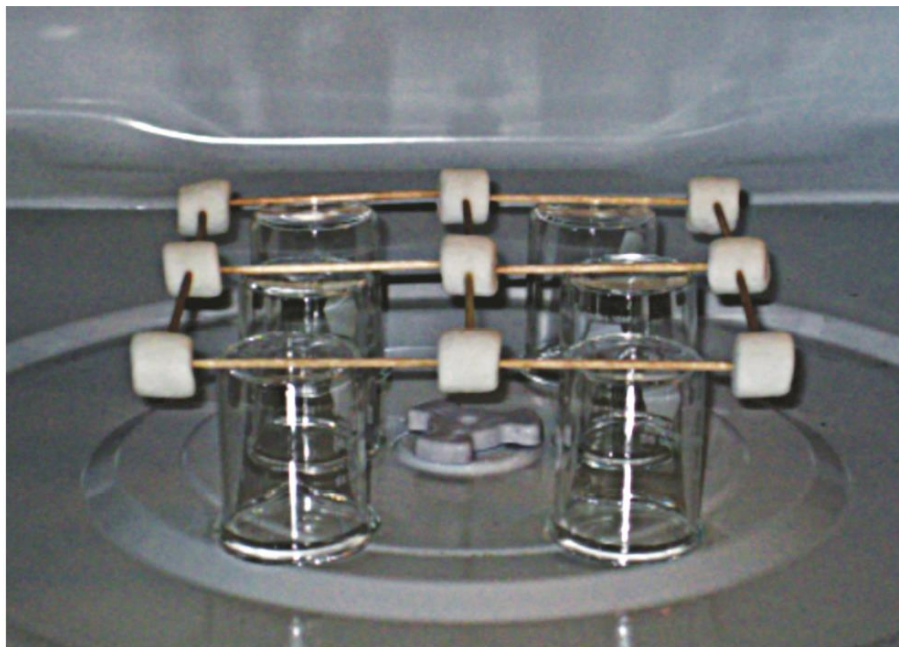
For microwave heating of samples with known dielectric properties, this analysis can be applied to determine appropriate sample dimensions to either promote or avoid standing waves, depending on the user's desired heating rate for the sample. A benefit of standing waves with constructive interference is that samples heat up more quickly, thereby making more efficient use of the microwave energy supplied. Concurrently, the possibility of standing waves significantly affecting results when small samples are used suggests once again that larger sample volumes are more appropriate for calibration purposes.

Effect of 'work piece' position in the microwave oven

Having considered the consequences of microwave energy behavior *within* the sample, it is also appropriate to consider microwave energy behavior *surrounding* the sample and its effect (if any) on calibrations. The well known existence of 'hot spots' in microwave ovens is a practical demonstration of the fact that microwave energy is not uniformly distributed throughout the oven chamber. Thus, as a final consideration we explore the effect of sample placement on calibration results.

The horizontal power distribution in the oven can be explored [171] with a grid of marshmallows, as shown in Figure 22. Marshmallows at "hot spots" start to expand after just a few seconds of microwave exposure (see the middle and middle-left marshmallows in Figure 22b); they start to 'deflate' as soon as the microwave source is turned off.

Therefore, there are actually two sets of standing waves pertinent to our results: those established by the boundaries of the sample itself, and those established by the reflective walls that bound the microwave chamber. The latter are responsible for so the called "hot" or "cold" spots. Complications arise from the fact that these two sets of standing waves will influence each other – the very act of placing an object in the microwave oven changes the standing wave pattern in the chamber, and that change will affect the genesis of standing waves within the sample.



(a)



(b)

Figure 22 (a) Marshmallows joined by toothpicks and resting on inverted 25 mL beakers in the microwave oven (no turntable present). (b) After microwaving for a few seconds, some (not all) of the marshmallows have begun to melt.

To investigate the power distribution in the vertical direction, we use a small beaker elevated to different heights. A 50 mL beaker containing 12.5 mL water was microwave irradiated for 12 s at the elevations represented in Figure 23. (Pieces of cardstock were cut so that their widths corresponded to the elevation needed; they were curled so that they could support the weight of the beaker and its contents.)

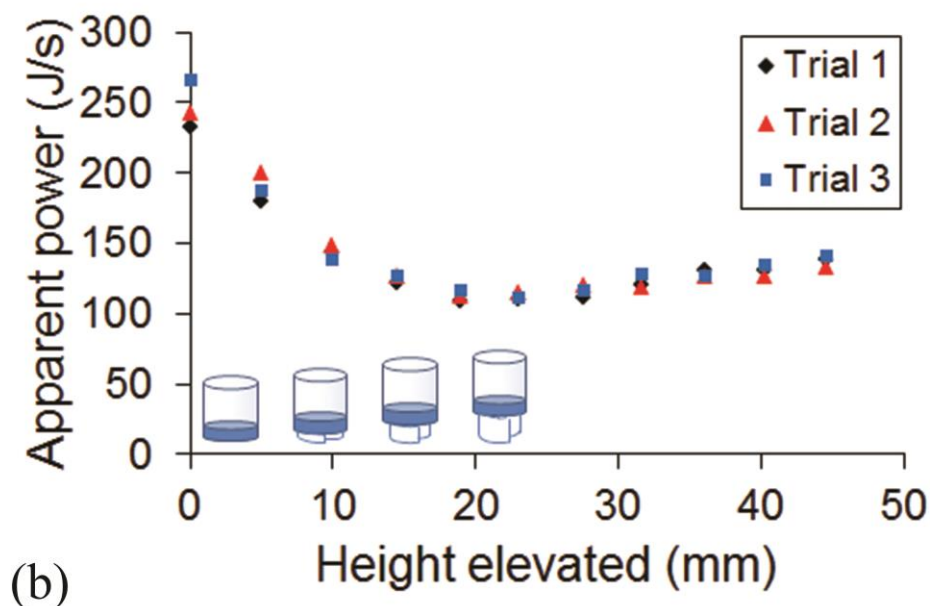
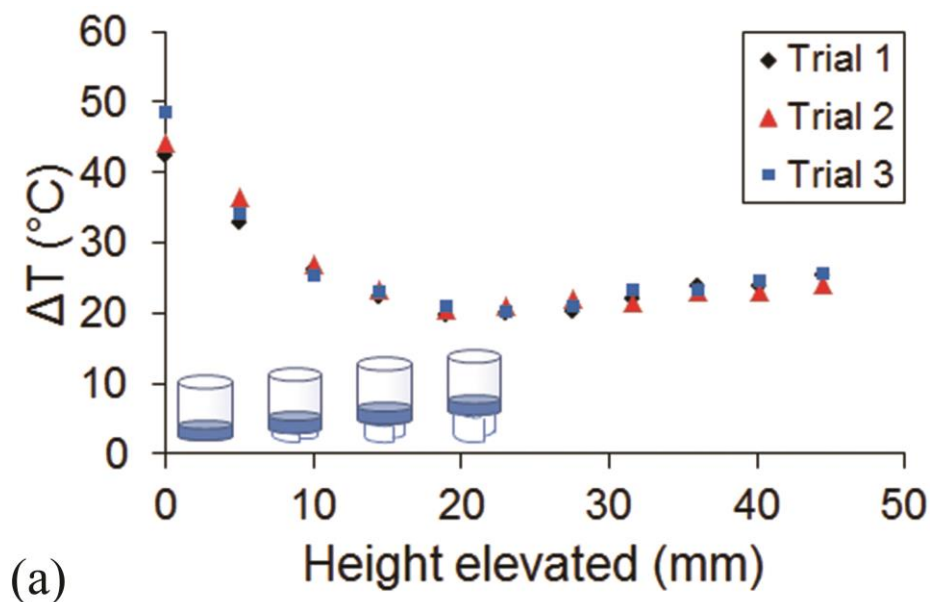


Figure 23 (a) Temperature increase caused by microwaving 12.5 mL of water in a 50 mL beaker, plotted as a function of the height of the beaker above the turntable. (b) Corresponding estimates of the microwave oven output power, obtained with Equation 1. The microwave oven timer was set to 12 s in all cases.

Results in Figure 23 show that across the elevations tested, the measured power tends to be greatest at locations close to the turntable – consistent with good engineering design for a domestic microwave oven.

Because of the significant spatial power distribution within the oven chamber, calibrations should be performed with the work piece at the same location where the material to be heated will subsequently be placed.

Chapter conclusions

- (1) Reproducible exposure of samples to microwave radiation requires measurement, not an assumption, of the magnetron start-up delay time.
- (2) Heat loss from the calibration vessel can occur *during* calibration of a microwave oven, such that the apparent power (as measured by the calibration) is less than the true output power of the oven. Microwave oven calibration standards should be refined to take account of this heat loss, in order to give a more accurate measure of the power that samples will be exposed to during a particular microwave treatment.
- (3) Use of a large volume of water in calibrations gives a more accurate measure of the output power of the microwave oven; conversely, use of a smaller volume of water leads to a larger thermal gradient during the calibration, resulting in increased heat loss and ultimately an underestimate of the oven's output power.
- (4) Calibrations performed with larger sample volumes avoid the complicating effects of standing waves of microwave energy, thus making the calibrations more reliable.
- (5) The shape and aspect ratio of the calibration vessel can have significant effects on calibration results. Thus, these should both be specified in calibration standards.
- (6) Calibration results depend on the position that the calibration vessel occupies in the microwave oven chamber. Thus the calibration vessel should consistently be placed at the same location that subsequent samples will occupy.

Chapter 6: Does *Bombyx mori* Cocoon Silk Absorb Microwave Radiation?^q

A 2004 study [103] indicated that microwave radiation enhances many of the mechanical properties of *Bombyx mori* silkworm cocoon silk and *Nephila clavipes* spider major ampullate silk. However, there was no attempt to standardize the conditions under which samples were stored prior to testing. Having investigated (in previous chapters) several conditions that can affect the results of 1) tensile experiments performed on silk (page 31), 2) microwave oven use (page 45), and 3) statistical interpretations of data (page 27), the present chapter is devoted to investigating whether microwave radiation affects the mechanical properties of silk, subject to the procedural constraints developed in previous chapters.

Chapter-specific Materials and Methods

Silk Collection

All silk was collected by the same person, following the procedure described on page 18. Care was taken to avoid unnecessarily straining the fibers during collection.

Storage conditions

After microwaving (but prior to tensile testing), all samples were stored over a silica gel desiccant in an airtight plastic container. The samples on their cardstock frames rested on paper that separated them from direct contact with the desiccant.

Effect of microwave exposure times on *B. mori* silk tensile properties

Figure 24 shows comparison plots of properties measured from silk fibers that received three different levels of microwave exposure. Twelve samples were tested to breaking (four from each level of microwave exposure). Fiber diameters in the three groups were comparable ($11.6 \mu\text{m} \pm 2.5 \mu\text{m}$), and so were the testing conditions ($20.7 \text{ }^\circ\text{C} \pm 0.6 \text{ }^\circ\text{C}$, $41\% \pm 2\%$ relative humidity). All samples were collected from the same white cocoon. Silk was microwaved in 60 second bursts, with a 200 mL water load present in the oven.

^q As presented (in part) in our paper entitled “Mechanical properties of *Bombyx mori* silkworm silk subjected to microwave radiation” (submitted 2013, [JMR](#)) and in our 2011 proceedings paper entitled “The Effect of Microwave Radiation on Tensile Properties of Silkworm (*B. mori*) Silk” (Reference [175]).

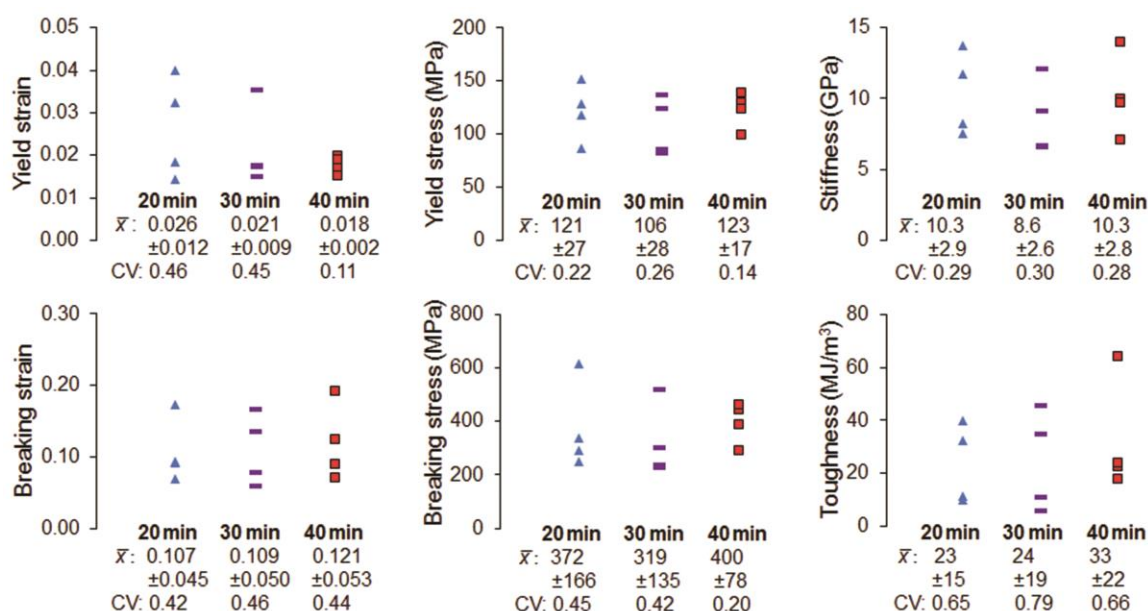


Figure 24 Comparison of tensile properties of silk samples collected from a single white cocoon and microwaved for 20 minutes, 30 minutes, or 40 minutes. The conventionally calculated mean (\bar{x}) \pm standard deviation is given below each set of samples (in the same units as the plotted data), along with the coefficient of variation (CV).

Results from the three different levels of microwave exposure were compared using a Kruskal-Wallis nonparametric statistical test [150]. At the 90% confidence level, there were no significant differences between the three groups for any of the properties represented in Figure 24.

The experiment was repeated with silk from a different (yellow) cocoon, covering a wider range of microwave exposure times: 0, 20, 40, and 60 minutes of cumulative microwave exposure. Figure 25 shows the experimental results. Fiber diameters were again comparable between groups ($17.2 \mu\text{m} \pm 3.5 \mu\text{m}$), as were testing conditions ($23.0^\circ\text{C} \pm 0.6^\circ\text{C}$ and $42 \pm 4\%$ relative humidity).

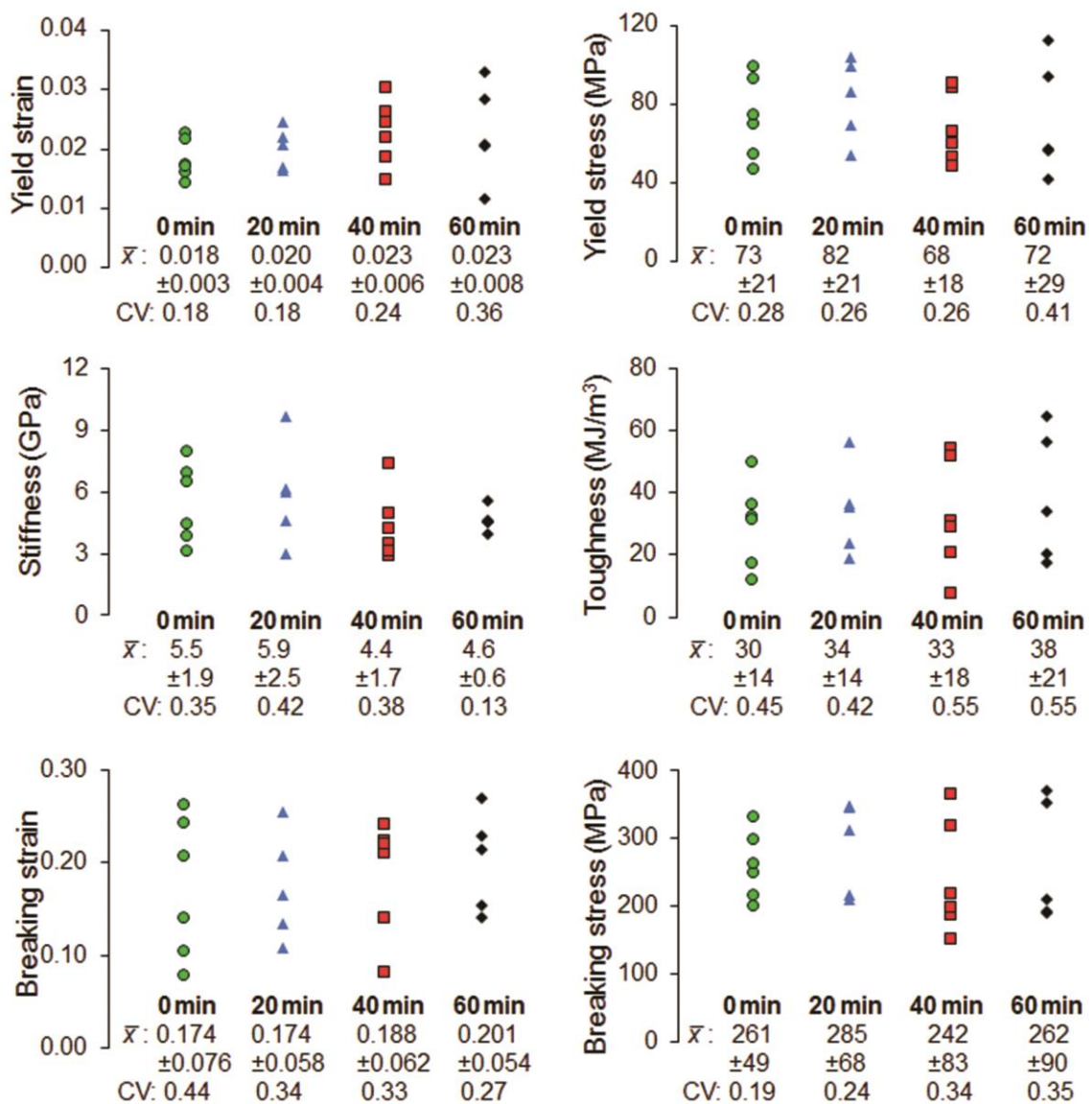


Figure 25 Comparison of tensile properties of silk samples collected from a single yellow cocoon and microwaved for 0 minutes (6 samples), 20 minutes (5 samples), 40 minutes (6 samples), and 60 minutes (5 samples). The conventionally calculated mean (\bar{x}) \pm standard deviation is given below each set of samples (in the same units as the plotted data), along with the coefficient of variation (CV).

Once again, when a Kruskal-Wallis test is used to compare results from the different levels of microwave exposure, no significant change is observed in any of the tensile properties (at the 90% confidence level).

Our initial attempts to reproduce the microwave effect reported previously [103] were unsuccessful under the prevailing conditions of our lab (Figure 24 and Figure 25). Factors

leading to the differences in results between our experiments reported here and those in which a microwave effect was observed may include:

- (1) Microwave irradiation conditions: in the experiments summarized in Figure 24 and Figure 25, a water load was included in the microwave oven – a precaution not taken during the previous study [103].
- (2) The power output of the microwave oven was not measured in the previous study, so there is no way to tell if the radiation levels in our experiments are comparable.
- (3) Tensile testing conditions: the gauge length of our samples was 55 mm, versus 100 mm in the previous study.
- (4) Ambient conditions during the experiments: humidity and temperature are known to affect the behavior of many silks [115] [86] [152] [153] [154] [156] [155], and the ambient conditions in our laboratory (Merced, CA) tend to be warmer and drier than those reported in the original study (Edinburgh, Scotland).

While we have no way of achieving the precise ambient conditions that existed in the original study, we have attempted to address (4) already by at least standardizing our own storage conditions: all samples in the present study were kept in the same desiccating environment prior to mechanical tests, and the temperature and humidity were recorded each day that tensile tests were performed. While our samples had a shorter gauge length than those in the original study (due to the size of the punch that we used for making the cardstock supports), we ensured that the strain rate during tensile tests was the same. Thus, (3) is an unlikely source of the different results obtained from the two studies. We therefore turned our attention to (1) (microwave irradiation conditions), and performed additional experiments accordingly.

Effect of water load on microwave absorption by *B. mori* silk fibers

One possible explanation for there being no significant effect of microwave radiation in the data presented in Figure 24 and Figure 25 is that the water load included in the oven may have inadvertently dominated microwave absorption. We therefore performed a set of experiments with no water load in the microwave oven for comparison (Figure 26). In addition, we reduced the duration of individual microwaving bursts from 1 minute to 30 seconds, in keeping with the 2004 study [103]. Sample diameters from different groups were comparable at: $16.5 \mu\text{m} \pm 3.2 \mu\text{m}$. Ambient conditions at the time of testing were similar for all groups: $23.0^\circ\text{C} \pm 1.2^\circ\text{C}$, $52\% \pm 4\%$ relative humidity.

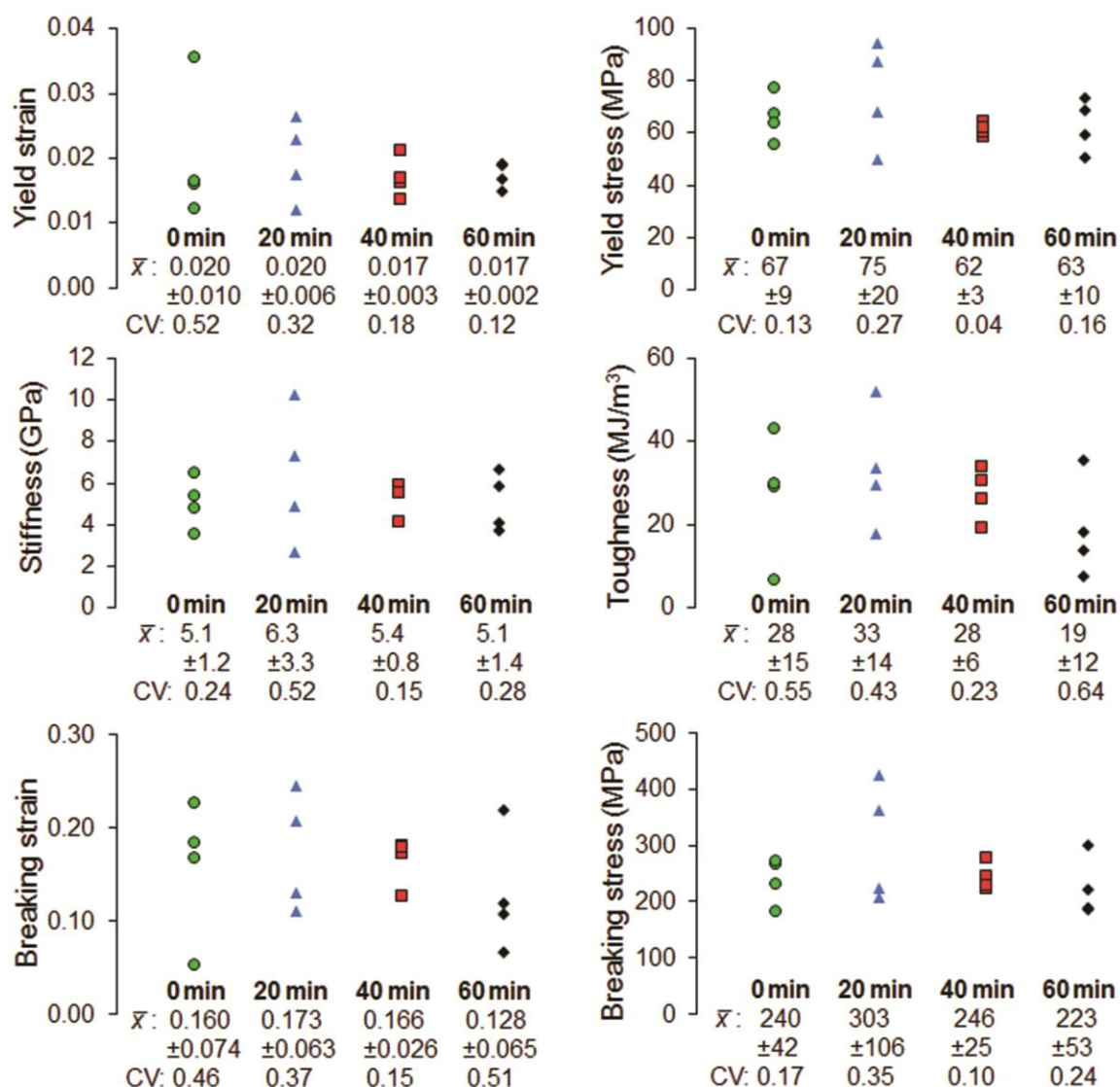


Figure 26 Comparison of tensile properties of silk samples collected from a single yellow cocoon and microwaved for 0 minutes, 20 minutes, 40 minutes, and 60 minutes (4 samples in each case). No water load was included in the microwave oven. The conventionally calculated mean (\bar{x}) \pm standard deviation is given below each set of samples (in the same units as the plotted data), along with the coefficient of variation (CV).

When a Kruskal-Wallis test is used to compare results from the different levels of microwave exposure, no significant change is observed in any of the tensile properties (at the 90% confidence level).

We performed an additional property comparison in the form of stress relaxation tests, to check whether the microwave effect reported previously for stress relaxation [103] was repeated in our data. Our results, from experiments performed on samples selected from the same batches of silk as represented in Figure 26, showed no significant dependence

on microwave exposure (Figure 27). Comparison was based on the normalized load at the end of the experiments, using a Kruskal-Wallis test at the 90% confidence level. Ambient temperature and humidity at the time of stress relaxation testing were comparable between sample groups, ($23.4\text{ }^{\circ}\text{C} \pm 0.8\text{ }^{\circ}\text{C}$ and $51\% \pm 3\%$ relative humidity, and so were sample diameters ($14.5\text{ }\mu\text{m} \pm 2.8\text{ }\mu\text{m}$).

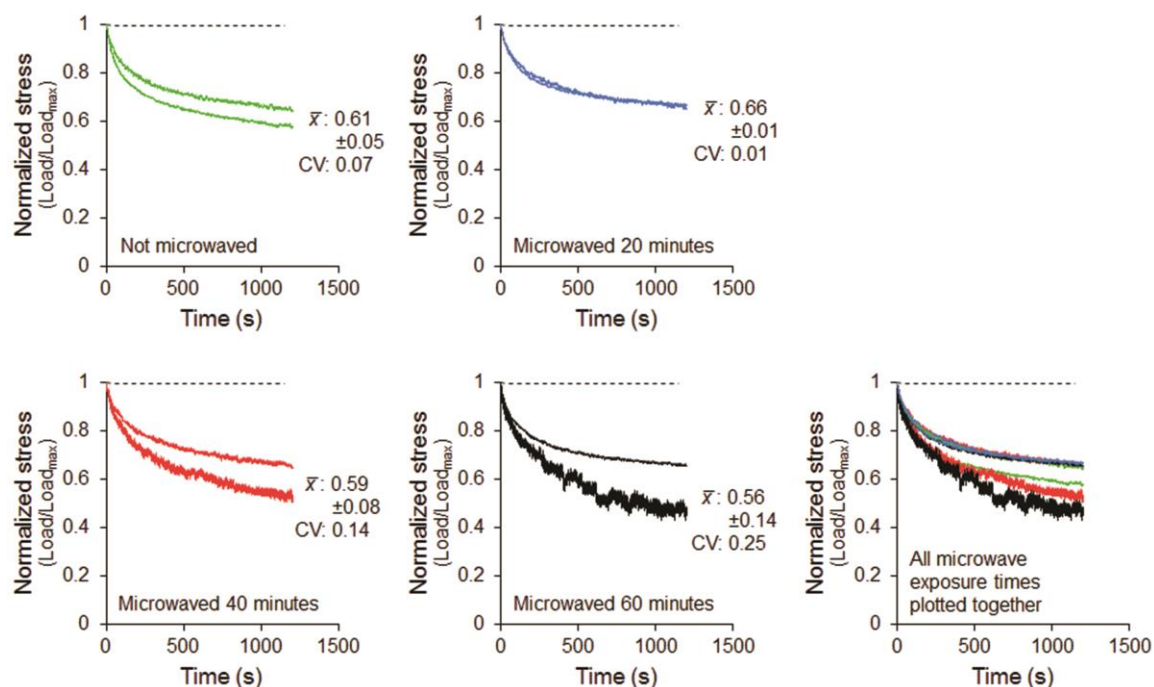


Figure 27 Stress relaxation in silkworm cocoon silk with 0 minutes, 20 minutes, 40 minutes, and 60 minutes of microwave exposure. No water load was included in the microwave oven. Two samples were tested at each level of microwave exposure. The conventionally calculated mean (\bar{x}) \pm standard deviation of the normalized stress at the end of the test is given in each case, along with the coefficient of variation (CV). The horizontal broken line was obtained from carbon fiber (a material highly resistant to stress relaxation), demonstrating that the relaxation behavior observed with silk is not an artifact of the equipment used to perform the tests.

Since different microwave exposure times in the absence of a water load did not lead to significant changes in any of the measured mechanical properties, we conclude that microwave absorption by the water load did not affect the outcome of the experiments summarized in Figure 24 and Figure 25. Subsequent recalibration of the microwave oven power output indicated that the microwave oven had not been damaged by operation without the water load.

Effect of strain rate on the apparent tensile properties of *B. mori* silk fibers

One of the effects of microwave radiation reported previously [103] was a decrease in stress relaxation when compared to samples that had not been microwaved. Samples that had not been microwaved relaxed to a normalized stress of 0.69 after 1200 s, compared to 0.87 for microwaved samples (values approximated from Figure 1 of ref [103]).

Our results presented in Figure 27 show samples (regardless of microwave exposure time) relaxing to a normalized stress of approximately 0.6 on average. Because our samples, tested under local ambient conditions, relaxed more than those reported previously, we wondered if the effects of microwave exposure were masked in our experiments by an ability of the samples to relax during the ramping step. Therefore, an additional experiment was performed in which the ramp rate to establish the initial load was doubled to 0.550 mm/min (corresponding to a strain rate of $1.67 \times 10^{-4} \text{ s}^{-1}$), to reduce the ability of samples to relax during the elongation step.

Figure 28 shows results of stress relaxation tests performed on samples deformed at the higher strain rate; the silk was taken from the same white cocoon as the samples represented in Figure 24. Microwaving was carried out in 30 second bursts, and no water load was included in the microwave oven. Ambient temperature and humidity during testing were $23.1^\circ\text{C} \pm 0.3^\circ\text{C}$ and $43\% \pm 5\%$ respectively.

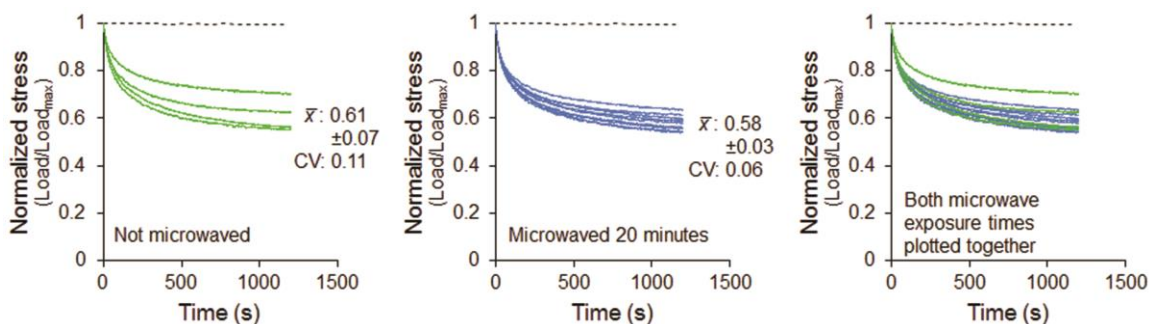


Figure 28 Stress relaxation in silkworm cocoon silk with 0 minutes (4 samples) and 20 minutes (9 samples) of microwave exposure. Initial ramp rate was doubled relative to the tests plotted in Figure 27. The conventionally calculated mean (\bar{x}) \pm standard deviation of the normalized stress at the end of the test is given for each batch of silk, along with the coefficient of variation (CV). The horizontal broken line was obtained from carbon fiber.

A statistical comparison between samples that were microwaved and those that were not was made with a two-tailed Mann-Whitney test at the 90% confidence level. The normalized loads at the ends of the tests were not significantly different in the two groups. Moreover, the normalized load at the end of the tests was still approximately 0.6.

Since doubling the ramp rate in stress relaxation tests still revealed no significant effects of microwaving, tensile tests to failure (which generally occur over a longer time scale) were not carried out at the increased strain rate. Over the course of a tensile test to

failure, samples would have even more time to relax away from any microwave induced changes, so we expect that such a test would not provide additional information.

Effect of microwave radiation on the failure predictability of *B. mori* silk fibers

While we observe no statistical change in any of the measured mechanical properties as a function of microwave exposure time, the possibility remains that the *spread* of the property values may have been affected by microwave exposure. To test this possibility, we constructed Weibull plots (Figure 29) to compare the spread of data from silk that had not been microwaved, and of silk with 20 minutes of cumulative microwave exposure.

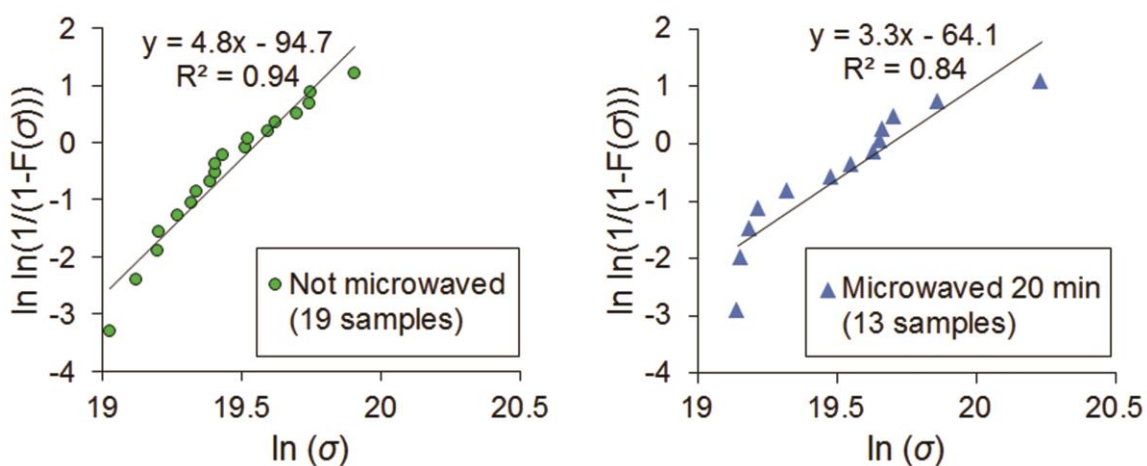


Figure 29 Weibull plots constructed with the breaking strength of samples that had not been microwaved (left), and samples with 20 minutes of microwave exposure (right).

When a straight line is fitted to the data, the plots show that β decreases from 4.8 to 3.3 upon microwaving, suggesting that microwave exposure decreases the failure predictability of silk. We note however that, especially in the case of the microwaved silk, the data do not fit well to a straight line; also, the number of samples in the microwaved set is small (13 samples, compared to the recommended minimum of 21 [113]), so confidence in the value of β estimated should be limited.

Since our comparisons of mechanical properties (Figure 24 thru Figure 28) revealed no differences between any of the microwave exposure times, we compiled an additional plot (Figure 30) with data from all the microwaved samples (40) combined.

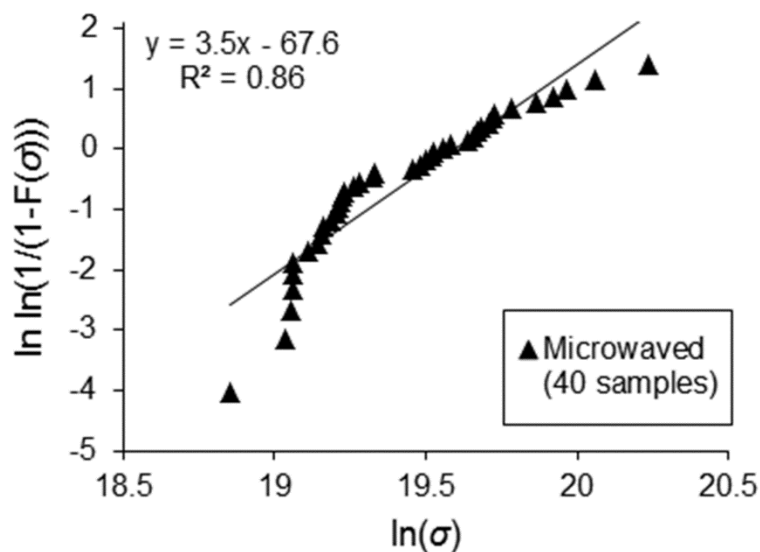


Figure 30 Weibull plot constructed with the breaking strengths of samples that had been microwaved for times ranging from 20 to 60 minutes.

While this plot confirmed the decrease in the Weibull modulus ($\beta = 3.5$) in response to microwaving, it also confirmed that the nonlinearity was not a simple random consequence of working with a small data set. Nonlinearity in a Weibull plot can indicate that a mixture of failure modes is present [113]. At least two different slopes are apparent in the Weibull plot of Figure 30, suggesting that at least two failure mechanisms may be active in the silk fibers we have tested.

Molecular dynamics simulations have shown [133] that the failure mechanism of beta-sheet nanocrystals in silk depends on the size of these nanocrystals. Larger nanocrystals fail by a bending mechanism, in which hydrogen bonds break one at a time as bending progresses. Smaller nanocrystals fail by a shearing mechanism that allows hydrogen bonds to act collectively in conferring resistance to deformation, so that the small crystals are stronger and tougher than the larger ones. These simulations may provide insight into our Weibull plots. Low breaking strengths (which are associated with a higher Weibull modulus; Figure 30) may correspond to fibers in which the response is dominated by larger beta-sheet crystals; the crystals break at a relatively predictable stress level, because hydrogen bonds only break one at a time in each nanocrystal. Higher breaking strengths may correspond to silk with small beta-sheet crystals; the stress at which these fibers break is less predictable, because it will depend on how many hydrogen bonds are present within each layer of the nanocrystal to support shear loading. Also, nanocrystals in which multiple hydrogen bonds have to break simultaneously will require a minimum threshold of stress to trigger failure, corresponding to the stress at which we observe the change in slope of the Weibull plots.

Does microwave radiation cause thermal heating of silk?

It is apparent that microwave radiation *does* interact with silk in some way (as evidenced by the change in the Weibull modulus). However, under our testing conditions, irradiation does not cause changes as drastic as those observed in the 2004 study [103]. There are two possible mechanisms by which microwave radiation may affect a material [144]: (i) the radiation may enable chemical and/or microstructural changes – and therefore property changes – in the same way that conventional heating would, or (ii) the high heating rates that are achievable by microwaving may selectively favor changes that would be masked under conventional conditions, where heating rates are low enough to give preference to changes that have a lower activation energy.

We designed an experiment to test how quickly silk heats when exposed to microwave radiation. Black silk fabric was obtained, and a small (several inches on each side) swatch cut out. Two different liquid crystal thermal paints were obtained from Edmund Scientific's, one producing color in the 95-104°F temperature range, and the other from 104-113°F. Both were painted onto the silk fabric (in different locations), and allowed to dry (Figure 31).



Figure 31 A piece of silk fabric, with one thermochromic liquid crystal paint on the left (active in the 95-104°F range), and another on the right (active in the 104-113°F range).

The visibility of the paint upon heating was tested by holding the swatch over a hot plate. The color change was obvious after just a few seconds, beginning with the lower temperature range paint (Figure 32a). When blocked from the heat, the color quickly faded, verifying that the color change was reversible (Figure 32b).

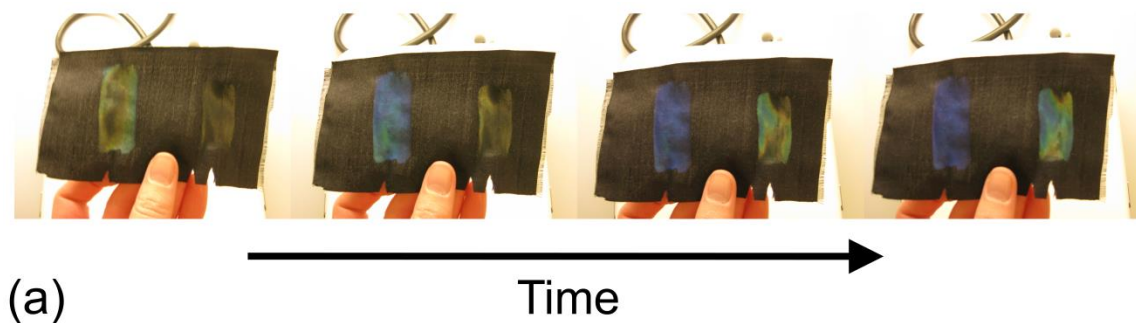


Figure 32 (a) Color changes that occur on heating a swatch of silk painted with two thermochromic liquid crystal paints. (b) The color change reverses as the silk cools back to room temperature, as shown here by blocking the source of heat.

Next the swatch was placed in the microwave oven (Figure 33a). The swatch was laid in the center of the turntable, across the rims of two small glass beakers; this was done to provide some separation between the silk and the glass turntable, which becomes warm to the touch when the microwave oven is run. By resting on the open end of the beakers, the silk-glass contact was minimized and silk-air contact maximized. The microwave oven was initiated (at $t = 0$ s), and then paused (at $t = 29$ s) once a color change was observed in the lower temperature range paint (Figure 33b). The oven was unpaused, and after an additional 31 s the higher range paint began to change color (Figure 33c).

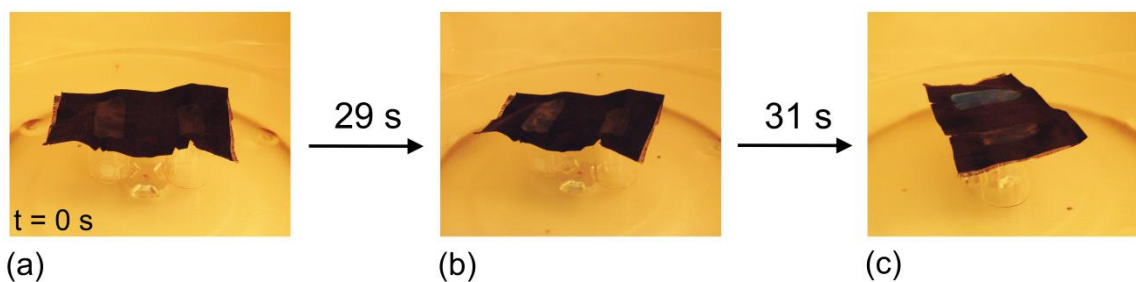


Figure 33 Thermochromic liquid crystal paints on silk fabric change color as microwave exposure time progresses.

While it is possible that individual, unpainted silk fibers may have a different thermal behavior than the present swatch with hundreds of painted fibers, results of this experiment suggest that silk does not heat rapidly when microwaved, and moreover that under the present experimental conditions, it is not an efficient absorber of microwave radiation.

Chapter conclusions

- (1) Provided that ambient conditions are comparable to those presented in this study, *B. mori* silk can be exposed to a wide range of microwave radiation doses without its mechanical properties being adversely affected. Thus, the silk can be used to reinforce materials that are subjected to microwave processing, as well as materials that are subjected to in-service microwave radiation.
- (2) While the mean values of mechanical properties were unaffected by the microwave treatments delivered in this study, the spread of breaking strength values as measured by the Weibull modulus increased with microwave exposure. The decrease in failure predictability of individual fibers suggests that silk can more appropriately be used in a composite material for situations where it will be exposed to microwave radiation, rather than relying on individual, isolated fibers for mechanical performance.
- (3) Due to the significant variations in ambient conditions when comparing results from different laboratories, standardization of storage and testing conditions is essential for meaningful inter-laboratory comparisons to become possible.
- (4) Under the experimental conditions reported here, silk is a poor absorber of microwave energy.

Chapter 7: Does Thermal Annealing Affect the Mechanical Properties of *B. mori* silk?^r

Under the present conditions, microwave radiation only appears to cause slight heating of silk (see section beginning on page 71), and doesn't produce the enhanced mechanical properties reported in 2004 [103]. Under the prevailing experimental conditions in the 2004 study, could the microwave treatment have produced thermal heating sufficient to induce microstructural changes in the silk? If so, a conventional thermal heat treatment may produce the enhanced tensile behavior. To close this loop, we characterized several mechanical properties of degummed and subsequently annealed *B. mori* silk, and compared them to the corresponding properties of degummed *B. mori* silk that was not annealed. The annealing treatment was carried out at 140 °C for 7 hours (conditions that optimally increased crystal size in an unrelated study of *B. mori* silk [172]), and then the fibers were allowed to cool gradually to room temperature over the course of an hour.

Chapter-specific Materials and Methods

Collection of silk fibers

A *B. mori* silkworm cocoon was degummed by boiling in approximately 1 liter of water for 30 minutes. Metal tweezers were used to keep the cocoon submerged in the water while boiling. The cocoon was allowed to dry overnight in air. Tweezers and gloved hands were used to gently tease single-strand sections of fiber (bave) from the dry cocoon. When a freed section reached length of ~6cm, the fiber was cut close to its point of attachment to the cocoon and transferred into a glass petri dish for annealing.

Effect of annealing on the mechanical properties of *B. mori* silk

Figure 34 shows comparison plots of properties measured from six annealed samples, and from six samples that had not been annealed. No significant differences were observed in any of the tensile properties measured (compared by a Mann-Whitney nonparametric statistical test at the 90% confidence level).

^r As presented in our 2012 proceedings paper entitled "Does Thermal Annealing Affect the Mechanical Properties of Silkworm (*Bombyx mori*) Cocoon Silk?" (Reference [176])

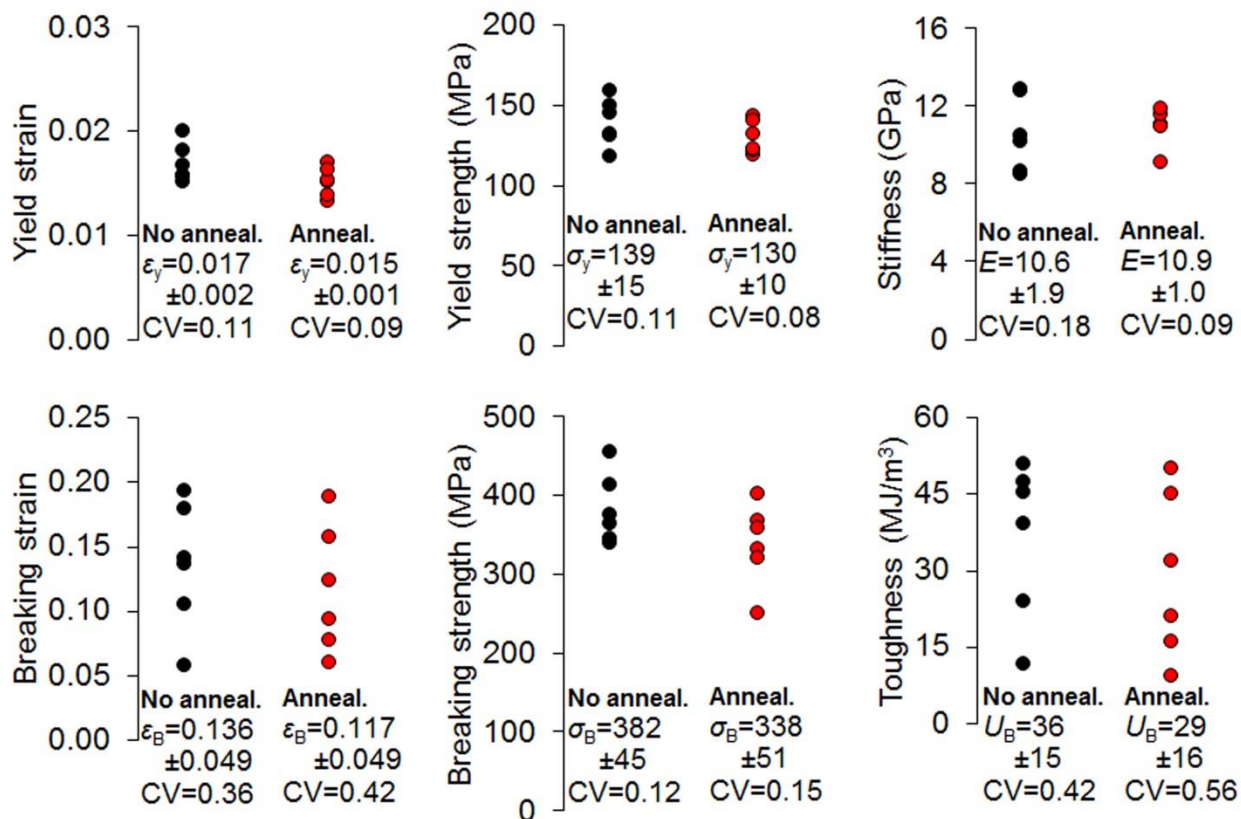


Figure 34 Comparison of tensile properties of silk samples that had not been annealed (“No anneal.”), and that had been annealed (“Anneal.”). The mean \pm standard deviation are given below each data set (in the same units as the plotted data), along with the coefficient of variation (CV). All samples were stored at ambient conditions prior to tensile tests. At the time of testing, the ambient temperature was $23.8\text{ }^{\circ}\text{C} \pm 0.4\text{ }^{\circ}\text{C}$ (“No anneal.”) and $23.7\text{ }^{\circ}\text{C} \pm 0.5\text{ }^{\circ}\text{C}$ (“Anneal.”). The ambient humidity was $42\% \pm 1\%$ and $43\% \pm 1\%$ respectively.

Figure 35 shows the comparison of stress relaxation plots between six annealed samples and six samples that had not been annealed. Again, the comparison does not reveal any significant difference in stress values after 20 minutes.

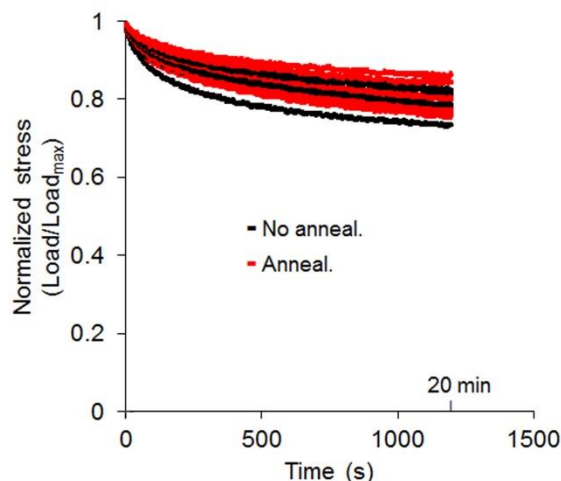


Figure 35 Comparison of stress relaxation in samples that had not been annealed (“No anneal.”), and samples that had been annealed (“Anneal.”). At the time of testing, the ambient temperature was $23.6 \text{ }^\circ\text{C} \pm 0.2 \text{ }^\circ\text{C}$ (“No anneal.”), and $23.5 \pm 0.2 \text{ }^\circ\text{C}$ (“Anneal.”). The ambient humidity was $47\% \pm 1\%$ and $46\% \pm 1\%$ respectively.

Under the experimental conditions reported here, the annealing treatment did not affect any of the mechanical properties measured. Since we followed an annealing procedure that was previously shown to have an optimal effect on increasing crystal size [172], we expected any consequence of uniform, conventional thermal annealing on mechanical properties to be reflected in our results. The fact that we observed no statistically significant changes in mechanical properties suggests that reported effects [103] of microwave radiation on such properties are not a simple result of annealing by the microwaves. In other words, any microwave-induced enhancement of mechanical properties requires the attendant microstructural or chemical changes to occur via a specific kinetic route that is not accessible via conventional heating rates [144].

Structure-property relationships

Our results bring to light another question: if the annealing treatment described here changed the microstructure of the silk fibers (by increasing crystal size), why were the mechanical properties of the fibers not affected? The fact that we observed no significant differences in our comparison is counterintuitive in view of the principle of processing–microstructure–property interdependence, and leads us to consider whether it is possible to alter the microstructure without affecting the mechanical properties in *B. mori* silk.

Experiments performed on regenerated *B. mori* silk fibers have shown that a post spin drawing step can enhance ductility (increase the breaking strain) relative to fibers that did not experience the post spin draw [122]—an example of microstructure affecting mechanical properties. Confining our discussion to naturally spun silks, we find reports

of *B. mori* fibers that experience no appreciable change in stiffness following plastic deformation [108]. An explanation of why stiffness can remain unchanged in some naturally spun silks during plastic deformation has been formulated in terms of the microstructural changes that take place within ordered and amorphous regions [158]: as ordered regions are degraded during deformation (decreasing the stiffness), chains in the amorphous regions of the silk are extended and aligned in the direction of the applied tensile stress (increasing the stiffness). Since the two mechanisms can balance each other out, there exists at least one property (stiffness) which can remain approximately constant in the face of microstructural changes associated with deformation. Other properties of *B. mori* silk (breaking strain and toughness) can be changed by deformation [111].

It is understandable that the increase in crystal sizes expected from our annealing treatment might not affect stiffness, if the overall amount of crystalline material is maintained throughout the microstructure. Further experiments are needed to determine whether this is the case, and to explore why all the other properties measured also remain unchanged. These properties will not just depend on the size and volume fraction of crystals, but also on the distribution of microstructural defects.

Effect of ambient conditions

Another consideration is that the relative humidity during our annealing treatment in Merced, CA may differ from the conditions that accompanied the annealing treatment carried out in India [172]. A more recent report has since shown that water vapor can play a key role in controlling crystal sizes in regenerated (reconstituted) *B. mori* silk [86]; therefore, it is possible that our annealing treatment did not have the same detailed microstructural consequences as the study performed in India.

Although the literature pertaining to silk research is expansive, the community of silk researchers has yet to adopt standardized procedures pertaining to sample testing conditions (including temperature, humidity, sample gauge length, and strain rate during tensile tests), as well as sample preparation methods (including storage conditions). Furthermore, the ambient conditions that did prevail during a particular experiment (and leading up to that experiment) are often not reported. The difficulties that result when trying to make inter-laboratory comparisons have been noted previously [111], and our results here in combination with the 1991 study [172] further emphasize this point.

Chapter Conclusions

- (1) In situations where microwave heating does affect the mechanical properties of silkworm (*B. mori*) silk, those effects are a result of changes that take place via a specific kinetic route that depends on rapid heating and cannot be accessed by a conventional thermal anneal.

- (2) Under our experimental conditions, tensile properties of silk collected from a *B. mori* cocoon and annealed for 7 hr at 140°C do not significantly differ from those of silk taken from the same cocoon but not annealed. Tempered with knowledge about the sensitivity of silk to humidity, this finding suggests that silk may be used in conditions well above room temperature without concern about changes in mechanical performance.
- (3) Complications arising from inter-laboratory comparisons of silk experiments can be minimized by reporting (and ideally standardizing) storage and testing conditions.

Chapter 8: Future Work

In view of the fact that the effects of microwave radiation on silk are so dependent on the environmental conditions that pertain during an experiment, there is still much work to be done in order to understand silk behavior in general, and microwaved silk in particular. Here we have made contributions to this knowledge by discovering not only how microwave irradiated, but also annealed (see the section beginning on page 74), desiccated (see the section beginning on page 33), and differently-handled silks (see the section beginning on page 38) behave when tested in the ambient conditions that prevail in our laboratory: 20.1°C to 24.2°C and 28% to 56% relative humidity (as noted throughout). We end with a brief discussion of directions for future study that tie directly to the work described here.

Microwave induced enhancements

In the present body of work we have identified a set of conditions that do *not* produce microwave enhancements to the mechanical properties of silk. The potential remains for microwave enhancements to occur, as evidenced by previously published work [103]. There are multiple variables that may contribute to whether or not enhancements occur at the time of microwaving, including:

1. Water content of the silk (which will contribute to how many and which types of hydrogen bonds are present in the silk).
2. Whether the microwave treatment occurs before or after the degumming treatment (will affect which components of silk are present for microwaves to interact with).
3. What type of degumming treatment is used (how complete is the removal of sericin, and does the degumming treatment chemically alter any of the constituents that will be exposed to the radiation).
4. The duration of the microwave treatment (there is necessarily a threshold energy required to induce changes in silk).
5. Ambient temperature at the time of microwaving (which will influence the interaction between the microwave radiation and dielectric materials it comes in contact with).
6. Ambient humidity at the time of microwaving (which will influence (1.) above).
7. Atmospheric pressure at the time of microwaving (which will influence how quickly water molecules enter or leave the silk microstructure).
8. Sample placement within the electromagnetic field (enhancement activation may require specific intensity levels of either the electric or magnetic field components of the microwave radiation)

To identify which microwaving conditions *do* result in enhancements to the mechanical properties of silk, it will be expedient to perform experiments under conditions that allow control over as many of the above mentioned variables as possible. (1) can be controlled

by conditioning silk prior to experiments. (2), (3), and (4) can be regulated through general experimental design. (5), (6), (7), and (8) require specialized equipment that allows control of ambient conditions *inside* the microwave oven chamber.

Specialized single-mode microwave applicators have been used [173] to probe the heating behavior of other materials, and would be a beneficial tool in the context of probing for conditions that enhance the mechanical properties of silk. The steady state distributions of the electric (E-) and magnetic (H-) fields in the waveguide of the applicator can be simulated with commercially available software (e.g. Wave-J ω , Photon Ltd. Kyoto, Japan). This would allow for positioning of silk samples at precise points within the electric (E-) and magnetic (H-) fields. Subsequent mechanical testing could indicate which component of the electromagnetic field (or which combination of components) is responsible for inducing changes in silk.

XRD analyses

Deciphering Weibull plots

Figure 30 (see page 70) showed a Weibull plot constructed from microwave irradiated silk, in which two different failure modes were apparent. We proposed that these two failure modes may be due to the crystalline component of fibers being dominated by one of two different types of beta sheet crystals. We hypothesized that weaker fibers contain larger beta sheet crystals which fail by a bending mechanism (in which hydrogen bonds break one at a time), whereas stronger fibers contain smaller beta sheet crystals that fail by a shearing mechanism (in which sets of hydrogen bonds act in unison to resist failure).

Our hypothetical distribution of crystal sizes could be tested through x-ray diffraction experiments to analyze the crystalline component of fibers (as has been done before [172] [174]) following mechanical testing. Such an experiment could be designed as follows:

1. Following the same nominal procedures we have described here (pages 17-20, 62), obtain silk fibers from a degummed cocoon and prepare each for mechanical testing. Collect enough fibers to allow a statistically significant Weibull plot to be generated later (this generally means 21 samples [113], but because we are interested in observing *two* failure modes, a minimum of 42 fibers should be obtained).
2. Assign each sample its own unique ID (label both ends of the cardstock support with this ID).
3. Test the mechanical properties of each fiber to breaking. (Keep the broken samples for later use)
4. Construct a Weibull plot based on the breaking strengths of all fibers tested.
5. Identify which samples fall into (A) the lower strength (higher Weibull modulus) regime, and which ones fall into (B) the higher strength (lower Weibull modulus) regime.

6. Sort the broken samples (from step 3) into either category (A) or (B), as identified in step 5.
7. Prepare the two groups of samples (A and B) for XRD analysis. Because all of the fibers in a particular group belong to the same failure regime, diffraction can be carried out in bulk on these samples. Therefore, a total of two diffraction analyses are all that's required—one for (A) and one for (B).
8. Compare XRD results of (A) and (B) to determine if one group has smaller crystal sizes than the other.

Effects of annealing on crystal size

On page 74 we describe an annealing experiment carried out to alter the microstructure of silk. The procedure we carried out was designed to allow the crystals within silk to grow, as has been done previously [172]. However, the mechanical properties of the annealed silk were not significantly different from silk that had not been annealed according to our measurements. Therefore, we questioned whether it is possible to alter the microstructure of silk without affecting its mechanical properties. Alternatively, our annealing treatment may not have resulted in the crystal growth we expected. XRD could be used as a straightforward means of testing whether the annealing treatment we performed really did alter the crystal structure of silk, by comparing the analysis of annealed fibers with that of fibers that have not been annealed.

References

- [1] D. L. Kaplan, "Fibrous proteins-- silk as a model system," *Polymer Degradation and Stability*, vol. 59, pp. 25-32, 1998.
- [2] R. V. Lewis, "Spider Silk: Ancient Ideas for New Biomaterials," *Chemical Reviews*, vol. 106, no. 9, pp. 3762-3774, 2006.
- [3] H. R. Hepburn and S. P. Kurtstjens, "The combs of honeybees as composite materials," *Apidologie*, vol. 19, no. 1, pp. 25-36, 1988.
- [4] K. Zhang, H. Duan, B. L. Karihaloo and J. Wang, "Hierarchical, multilayered cell walls reinforced by recycled silk cocoons enhance the structural integrity of honeybee combs," *PNAS*, vol. 107, no. 21, pp. 9502-9506, 2010.
- [5] C. L. Craig, "Evolution of Arthropod Silks," *Annu. Rev. Entomol.*, vol. 42, pp. 231-267, 1997.
- [6] P. E. Marek, W. A. Shear and J. E. Bond, "A redescription of the leggiest animal, the millipede *Illacme plenipes*, with notes on its natural history and biogeography (Diplopoda, Siphonophorida, Siphonorhinidae)," *ZooKeys*, vol. 241, pp. 77-112, 2012.
- [7] J. S. Edgerly, J. A. Davilla and N. Schoenfeld, "Silk Spinning Behavior and Domicile Construction in Webspinners," *Journal of Insect Behavior*, vol. 15, no. 2, pp. 219-242, 2002.
- [8] M. A. Collin, J. E. Garb, J. S. Edgerly and C. Y. Hayashi, "Characterization of silk spun by the embiopteran, *Antipaluria urichi*," *Insect Biochemistry and Molecular Biology*, vol. 39, pp. 75-82, 2009.
- [9] W. Dorow, U. Maschwitz and S. Rapp, "The natural history of *Polyrhachis (Myrmhopla) muelleri* Forel 1893 (Formicidae Formicinae), a weaver ant with mimetic larvae and an unusual nesting behaviour," *Tropical Zoology*, vol. 3, pp. 181-190, 1990.
- [10] T. E. Sutherland, J. H. Young, S. Weisman, C. Y. Hayashi and D. J. Merritt, "Insect Silk: One Name, Many Materials," *Annual Review of Entomology*, vol. 55, pp. 171-188, 2010.
- [11] X.-X. Qin, K. J. Coyne and J. H. Waite, "Tough Tendons. Mussel Byssus has Collagen with Silk-like Domains," *The Journal of Biological Chemistry*, vol. 272, no. 51, pp. 32623-32627, 1997.
- [12] J. Gosline, M. Lillie, E. Carrington, P. Guerette, C. Ortlepp and K. Savage, "Elastic proteins: biological roles and mechanical properties," *Phil. Trans. R. Soc. Lond. B*, vol. 357, pp. 121-132, 2002.
- [13] J. S. Edgerly, S. M. Shenoy and V. G. Werner, "Relating the Cost of Spinning Silk to the Tendency to Share It for Three Embiids with Different Lifestyles (Order Embiidina: Clothodidae, Notoligotomidae, and Australembiidae)," *Environmental Entomology*, vol. 35, no. 2, pp. 448-457, 2006.
- [14] F. Chen, D. Porter and F. Vollrath, "Morphology and structure of silkworm cocoons," *Materials Science and Engineering C*, vol. 32, pp. 772-778, 2012.

- [15] J. M. Gosline, P. A. Guerette, C. S. Ortlepp and K. N. Savage, "The Mechanical Design of Spider Silks: from Fibroin Sequence to Mechanical Function," *The Journal of Experimental Biology*, vol. 202, pp. 3295-3303, 1999.
- [16] R. W. Merritt and J. B. Wallace, "Filter-feeding Insects," *Scientific American*, vol. 244, no. 4, pp. 132-144, 1981.
- [17] N. Yonemura, F. Sehnal, K. Mita and T. Tamura, "Protein Composition of Silk Filaments Spun under Water by Caddisfly Larvae," *Biomacromolecules*, vol. 7, pp. 3370-3378, 2006.
- [18] J. Zhang, R. Rajkhowa, J. L. Li, X. Y. Liu and X. G. Wang, "Silkworm cocoon as natural material and structure for thermal insulation," *Materials and Design*, vol. 49, pp. 842-849, 2013.
- [19] A. Lang, "Silk investment in gifts by males of the nuptial feeding spider *Pisaura mirabilis* (Araneae: Pisauridae)," *Behaviour*, vol. 133, pp. 697-716, 1996.
- [20] M. J. Albo, L. E. Costa-Schmidt and F. G. Costa, "To feed or to wrap? Female silk cues elicit male nuptial gift construction in a semiaquatic trechaleid spider," *Journal of Zoology*, vol. 277, pp. 284-290, 2009.
- [21] R. Lewis, "Unraveling the Weave of Spider Silk," *BioScience*, vol. 46, no. 9, pp. 636-638, 1996.
- [22] J. S. Rovner and S. J. Knost, "Post-immobilization wrapping of prey by lycosid spiders of the herbaceous stratum," *Psyche*, vol. 81, pp. 398-415, 1974.
- [23] R. H. Harwood, "Predatory Behavior of *Argiope aurantia* (Lucas)," *American Midland Naturalist*, vol. 91, no. 1, pp. 130-139, 1974.
- [24] E. A. Greenquist and J. S. Rovner, "Lycosid spiders on artificial foliage: stratum choice, orientation preferences, and prey-wrapping," *Psyche*, vol. 83, pp. 196-209, 1976.
- [25] K. V. Yeargan, "Biology of Bolas Spiders," *Annu. Rev. Entomol.*, vol. 39, pp. 81-99, 1994.
- [26] N. P. Horrocks, F. Vollrath and C. Dicko, "The silkmoth cocoon as humidity trap and waterproof barrier," *Comparative Biochemistry and Physiology, Part A*, vol. 164, pp. 645-652, 2013.
- [27] R. S. Seymour and S. K. Hetz, "The diving bell and the spider: the physical gill of *Argyroneta aquatica*," *The Journal of Experimental Biology*, vol. 214, pp. 2175-2181, 2011.
- [28] H.-P. Zhao, X.-Q. Feng and H.-J. Shi, "Variability in mechanical properties of *Bombyx mori* silk," *Materials Science and Engineering C*, vol. 27, pp. 675-683, 2007.
- [29] I. Agnarsson, M. Kuntner and T. A. Blackledge, "Bioprospecting Finds the Toughest Biological Material: Extraordinary Silk from a Giant Riverine Orb Spider," *PLoS ONE*, vol. 5, no. 9, pp. 1-8, 2010.
- [30] J. T. Prince, K. P. McGrath, C. M. DiGirolamo and D. L. Kaplan, "Construction, Cloning, and Expression of Synthetic Genes Encoding Spider Dragline Silk," *Biochemistry*, vol. 34, pp. 10879-10885, 1995.
- [31] F. Teulé, A. R. Cooper, W. A. Furin, D. Bittencourt, E. L. Rech, A. Brooks and R. V. Lewis, "A protocol for the production of recombinant spider silk-like proteins for artificial fiber spinning,"

Nature Protocols, vol. 4, no. 3, pp. 341-355, 2009.

- [32] J. Scheller, K.-H. Gührs, F. Grosse and U. Conrad, "Production of spider silk proteins in tobacco and potato," *Nature Biotechnology*, vol. 19, pp. 573-577, 2001.
- [33] Y. Zhang, J. Hu, Y. Miao, A. Zhao, T. Zhao, D. Wu, L. Liang, A. Miikura, K. Shiomi, Z. Kajiura and M. Nakagaki, "Expression of EGFP-spider dragline silk fusion protein in BmN cells and larvae of silkworm showed the solubility is primary limit for dragline proteins yield," *Mol Biol Rep*, vol. 35, pp. 329-335, 2008.
- [34] H. Wen, X. Lan, Y. Zhang, T. Zhao, Y. Wang, Z. Kajiura and M. Nakagaki, "Transgenic silkworms (*Bombyx mori*) produce recombinant spider dragline silk in cocoons," *Mol Biol Rep*, vol. 37, pp. 1815-1821, 2010.
- [35] F. Teulé, Y.-G. Miao, B.-H. Sohn, Y.-S. Kim, J. J. Hull, M. J. Fraser, Jr., R. V. Lewis and D. L. Jarvis, "Silkworms transformed with chimeric silkworm/spider silk genes spin composite silk fibers with improved mechanical properties," *PNAS*, vol. 109, no. 3, pp. 923-928, 2012.
- [36] A. Lazaris, S. Arcidiacono, Y. Huang, J.-F. Zhou, F. Duguay, N. Chretien, E. A. Welsh, J. W. Soares and C. N. Karatzas, "Spider Silk Fibers Spun from Soluble Recombinant Silk Produced in Mammalian Cells," *Science*, vol. 295, pp. 472-476, 2002.
- [37] H.-T. Xu, B.-L. Fan, S.-Y. Yu, Y.-H. Huang, Z.-H. Zhao, Z.-X. Lian, Y.-P. Dai, L.-L. Wang, Z.-L. Liu, J. Fei and N. Li, "Construct synthetic gene encoding artificial spider dragline silk protein and its expression in milk of transgenic mice," *Animal Biotechnology*, vol. 18, pp. 1-12, 2007.
- [38] M. Mondal, K. Trivedy and S. N. Kumar, "The silk proteins, sericin and fibroin in silkworm, *Bombyx mori* Linn., - a review," *Caspian Journal of Environmental Sciences*, vol. 5, no. 2, pp. 63-76, 2007.
- [39] C.-Z. Zhou, F. Confalonieri, N. Medina, Y. Zivanovic, C. Esnault, T. Yang, M. Jacquet, J. Janin, M. Duguet, R. Perasso and Z.-G. Li, "Fine organization of *Bombyx mori* fibroin heavy chain gene," *Nucleic Acids Research*, vol. 28, no. 12, pp. 2413-2419, 2000.
- [40] K. Yamaguchi, Y. Kikuchi, T. Takagi, A. Kikuchi, F. Oyama, K. Shimura and S. Mizuno, "Primary Structure of the Silk Fibroin Light Chain Determined by cDNA Sequencing and Peptide Analysis," *J. Mol. Biol.*, vol. 210, pp. 127-139, 1989.
- [41] P. Zhang, K. Yamamoto, Y. Aso, Y. Banno, D. Sakano, Y. Wang and H. Fujii, "Proteomic Studies of Isoforms of the P25 Component of *Bombyx mori* Fibroin," *Biosci. Biotechnol. Biochem.*, vol. 69, no. 11, pp. 2086-2093, 2005.
- [42] S. Inoue, K. Tanaka, F. Arisaka, S. Kimura, K. Ohtomo and S. Mizuno, "Silk Fibroin of *Bombyx mori* Is Secreted, Assembling a High Molecular Mass Elementary Unit Consisting of H-chain, L-chain, and P25, with a 6:6:1 Molar Ratio," *The Journal of Biological Chemistry*, vol. 275, no. 51, pp. 40517-40528, 2000.
- [43] K. Tanaka, N. Kajiyama, K. Ishikura, S. Waga, A. Kikuchi, K. Ohtomo, T. Takagi and S. Mizuno, "Determination of the site of disulfide linkage between heavy and light chains of silk fibroin produced by *Bombyx mori*," *Biochimica et Biophysica Acta*, vol. 1432, pp. 92-103, 1999.
- [44] K. Tanaka, K. Mori and S. Mizuno, "Immunological Identification of the Major Disulfide-Linked

- Light Component of Silk Fibroin," *J. Biochem.*, vol. 114, pp. 1-4, 1993.
- [45] K. Kerkam, C. Viney, D. Kaplan and S. Lombardi, "Liquid crystallinity of natural silk secretions," *Nature*, vol. 349, pp. 596-598, 1991.
- [46] Q. Lu, H. Zhu, C. Zhang, F. Zhang, B. Zhang and D. L. Kaplan, "Silk Self-Assembly Mechanisms and Control From Thermodynamics to Kinetics," *Biomacromolecules*, vol. 13, pp. 826-832, 2012.
- [47] H. Teramoto and M. Miyazawa, "Molecular Orientation Behavior of Silk Sericin Film as Revealed by ATR Infrared Spectroscopy," *Biomacromolecules*, vol. 6, pp. 2049-2057, 2005.
- [48] S. W. Watt, I. J. McEwen and C. Viney, "Stability of Molecular Order in Silkworm Silk," *Macromolecules*, vol. 32, pp. 8671-8673, 1999.
- [49] M.-p. Ho, H. Wang and K.-t. Lau, "Effect of degumming time on silkworm silk fibre for biodegradable polymer composites," *Applied Surface Science*, vol. 258, pp. 3948-3955, 2012.
- [50] J. Pérez-Rigueiro, M. Elices, J. Llorca and C. Viney, "Effect of Degumming on the Tensile Properties of Silkworm (*Bombyx mori*) Silk Fiber," *Journal of Applied Polymer Science*, vol. 84, pp. 1431-1437, 2002.
- [51] J. Pérez-Rigueiro, M. Elices, J. Llorca and C. Viney, "Tensile properties of silkworm silk obtained by forced silking," *Journal of Applied Polymer Science*, vol. 82, no. 8, pp. 1928-1935, 2001.
- [52] P. Jiang, H. Liu, C. Wang, L. Wu, J. Huang and C. Guo, "Tensile behavior and morphology of differently degummed silkworm (*Bombyx mori*) cocoon silk fibers," *Materials Letters*, vol. 60, pp. 919-925, 2006.
- [53] E. M. Pritchard, X. Hu, V. Finley, C. K. Kuo and D. L. Kaplan, "Effect of Silk Protein Processing on Drug Delivery from Silk Films," *Macromolecular Bioscience*, vol. 13, pp. 311-320, 2013.
- [54] H.-Y. Wang and Y.-Q. Zhang, "Effect of regeneration of liquid silk fibroin on its structure and characterization," *Soft Matter*, vol. 9, pp. 138-145, 2013.
- [55] B. L. Thiel, K. B. Guess and C. Viney, "Non-periodic lattice crystals in the hierarchical microstructure of spider (major ampullate) silk," *Biopolymers*, vol. 41, no. 7, pp. 703-719, 1997.
- [56] F. Paquet-Mercier, T. Lefèvre, M. Auger and M. Pérolet, "Evidence by infrared spectroscopy of the presence of two types of β -sheets in major ampullate spider silk and silkworm silk," *Soft Matter*, vol. 9, pp. 208-215, 2013.
- [57] I. Krasnov, I. Diddens, N. Hauptmann, G. Helms, M. Ogurreck, T. Seydel, S. S. Funari and M. Müller, "Mechanical Properties of Silk: Interplay of Deformation on Macroscopic and Molecular Length Scales," *Physical Review Letters*, vol. 100, pp. 1-4, 2008.
- [58] R. E. Marsh, R. B. Corey and L. Pauling, "An Investigation of the Structure of Silk Fibroin," *Biochimica et Biophysica Acta*, vol. 16, pp. 1-34, 1955.
- [59] K. Mita, S. Ichimura and T. C. James, "Highly Repetitive Structure and Its Organization of the Silk Fibroin Gene," *Journal of Molecular Evolution*, vol. 38, pp. 583-592, 1994.

- [60] G. Liu, X. Huang, Y. Wang, Y.-Q. Zhang and X. Wang, "Thermal transport in single silkworm silks and the behavior under stretching," *Soft Matter*, vol. 8, pp. 9792-9799, 2012.
- [61] C. Viney, "From Natural Silks to New Polymer Fibres," *Journal of The Textile Institute*, vol. 91, no. 3, pp. 2-23, 2000.
- [62] D. F. Williams, "On the nature of biomaterials," *Biomaterials*, vol. 30, pp. 5897-5909, 2009.
- [63] G. H. Altman, F. Diaz, C. Jakuba, T. Calabro, R. L. Horan, J. Chen, H. Lu, J. Richmond and D. L. Kaplan, "Silk-based biomaterials," *Biomaterials*, vol. 24, pp. 401-416, 2003.
- [64] J. G. Hardy, L. M. Römer and T. R. Scheibel, "Polymeric materials based on silk proteins," *Polymer*, vol. 49, pp. 4309-4327, 2008.
- [65] J. G. Hardy and T. R. Scheibel, "Composite materials based on silk proteins," *Progress in Polymer Science*, vol. 35, pp. 1093-1115, 2010.
- [66] S. Takeda, "New field of insect science: Research on the use of insect properties," *Entomological Science*, vol. 16, pp. 125-135, 2013.
- [67] B. Panilaitis, G. H. Altman, J. Chen, H.-J. Jin, V. Karageorgiou and D. L. Kaplan, "Macrophage responses to silk," *Biomaterials*, vol. 24, pp. 3079-3085, 2003.
- [68] O. J. Lee, J. M. Lee, J. H. Kim, J. Kim, H. Kweon, Y. Y. Jo and C. H. Park, "Biodegradation behavior of silk fibroin membranes in repairing tympanic membrane perforations," *Journal of Biomedical Materials Research A*, vol. 100A, no. 8, pp. 2018-2026, 2012.
- [69] H. Liu, Z. Ge, Y. Wang, S. L. Toh, V. Sutthikhum and J. C. H. Goh, "Modification of Sericin-free Silk Fibers for Ligament Tissue Engineering Application," *J Biomed Mater Res Part B: Appl Biomater*, vol. 82B, pp. 129-138, 2007.
- [70] F. Vollrath, D. Porter and C. Holland, "The science of silks," *MRS Bulletin*, vol. 38, pp. 73-80, 2013.
- [71] U.-J. Kim, J. Park, H. J. Kim, M. Wada and D. L. Kaplan, "Three-dimensional aqueous-derived biomaterial scaffolds from silk fibroin," *Biomaterials*, vol. 26, pp. 2775-2785, 2005.
- [72] A. G. Mikos and J. S. Temenoff, "Formation of highly porous biodegradable scaffolds for tissue engineering," *Electronic Journal of Biotechnology*, vol. 3, no. 2, pp. 1-6, 2000.
- [73] G. Li, H. Liu, T. Li and J. Wang, "Surface modification and functionalization of silk fibroin fibers/fabric toward high performance applications," *Materials Science and Engineering C*, vol. 32, pp. 627-636, 2012.
- [74] S. Periyasamy, D. Gupta and M. L. Gulrajani, "Modification of one side of mulberry silk fabric by monochromatic VUV excimer lamp," *European Polymer Journal*, vol. 43, pp. 4573-4581, 2007.
- [75] J. Shao, J. Zheng, J. Liu and C. M. Carr, "Fourier Transform Raman and Fourier Transform Infrared Spectroscopy Studies of Silk Fibroin," *Journal of Applied Polymer Science*, vol. 96, pp. 1999-2004, 2005.
- [76] A. Kaneko, S. Hirai, Y. Tamada and T. Kuzuya, "Evaluation of Calcium Phosphate-Coated Silk Fabric Produced by Sol-Gel Processing as a Wound Cover Material," *SENI GAKKAISHI*, vol. 65,

no. 3, pp. 97-102, 2009.

- [77] P. Uttayarat, S. Jetawattana, P. Suwanmala, J. Eamsiri, T. Tangthong and S. Pongpat, "Antimicrobial Electrospun Silk Fibroin Mats with Silver Nanoparticles for Wound Dressing Application," *Fibers and Polymers*, vol. 13, no. 8, pp. 999-1006, 2012.
- [78] T. Toshiaki, T. Chantal, R. Corinne, K. Toshio, A. Eappen, K. Mari, K. Natuo, T. Jean-Luc, M. Bernard, C. Gérard, S. Paul, F. Malcolm, P. Jean-Claude and C. Pierre, "Germline transformation of the silkworm *Bombyx mori* L. using a piggyBac transposon-derived vector," *Nature Biotechnology*, vol. 18, pp. 81-84, 2000.
- [79] A. Nagano, Y. Tanioka, N. Sakurai, H. Sezutsu, N. Kuboyama, H. Kiba, Y. Tanimoto, N. Nishiyama and T. Asakura, "Regeneration of the femoral epicondyle on calcium-binding silk scaffolds developed using transgenic silk fibroin produced by transgenic silkworm," *Acta Biomaterialia*, vol. 7, pp. 1192-1201, 2011.
- [80] Z. Megeed, J. Cappello and H. Ghandehari, "Genetically engineered silk-elastinlike protein polymers for controlled drug delivery," *Advanced Drug Delivery Reviews*, vol. 54, pp. 1075-1091, 2002.
- [81] A. Das, C. N. Saikia and S. Hussain, "Grafting of Methyl Methacrylate (MMA) onto *Antheraea assama* Silk Fiber," *Journal of Applied Polymer Science*, vol. 81, pp. 2633-2641, 2001.
- [82] S. Sofia, M. B. McCarthy, G. Gronowicz and D. L. Kaplan, "Functionalized silk-based biomaterials for bone formation," *Journal of Biomedical Materials Research*, vol. 54, pp. 139-148, 2001.
- [83] Y. Nomura, V. Sharma, A. Yamamura and Y. Yokobayashi, "Selection of silk-binding peptides by phage display," *Biotechnology Letters*, vol. 33, pp. 1069-1073, 2011.
- [84] Y. Cao and B. Wang, "Biodegradation of Silk Biomaterials," *International Journal of Molecular Sciences*, vol. 10, pp. 1514-1524, 2009.
- [85] S. Karlsson and A.-C. Albertsson, "Biodegradable Polymers and Environmental Interaction," *Polymer Engineering and Science*, vol. 38, no. 8, pp. 1251-1253, 1998.
- [86] X. Hu, K. Shmelev, L. Sun, E.-S. Gil, S.-H. Park, P. Cebe and D. L. Kaplan, "Regulation of Silk Material Structure by Temperature-Controlled Water Vapor Annealing," *Biomacromolecules*, vol. 12, pp. 1686-1696, 2011.
- [87] H. Liu, H. Fan, Y. Wang, S. L. Toh and J. C. H. Goh, "The interaction between a combined knitted silk scaffold and microporous silk sponge with human mesenchymal stem cells for ligament tissue engineering," *Biomaterials*, vol. 29, pp. 662-674, 2008.
- [88] L. J. Bray, K. A. George, S. L. Ainscough, D. W. Hutmacher, T. V. Chirila and D. G. Harkin, "Human corneal epithelial equivalents constructed on *Bombyx mori* silk fibroin membranes," *Biomaterials*, vol. 32, pp. 5086-5091, 2011.
- [89] P. W. Madden, J. N. Lai, K. A. George, T. Giovenco, D. G. Harkin and T. V. Chirila, "Human corneal endothelial cell growth on a silk fibroin membrane," *Biomaterials*, vol. 32, pp. 4076-4084, 2011.
- [90] B. D. Lawrence, M. Cronin-Golomb, I. Georgakoudi, D. L. Kaplan and F. G. Omenetto, "Bioactive Silk Protein Biomaterial Systems for Optical Devices," *Biomacromolecules*, vol. 9, pp. 1214-1220,

2008.

- [91] I. Karakutuk, F. Ak and O. Okay, "Diepoxide-Triggered Conformational Transition of Silk Fibroin: Formation of Hydrogels," *Biomacromolecules*, vol. 13, pp. 1122-1128, 2012.
- [92] A. Sionkowska and A. Płancka, "Preparation and characterization of silk fibroin/chitosan composite sponges for tissue engineering," *Journal of Molecular Liquids*, vol. 178, pp. 5-14, 2013.
- [93] H.-J. Jin, J. Chen, V. Karageorgiou, G. H. Altman and D. L. Kaplan, "Human bone marrow stromal cell responses on electrospun silk fibroin mats," *Biomaterials*, vol. 25, pp. 1039-1047, 2004.
- [94] G. H. Altman, R. L. Horan, H. H. Lu, J. Moreau, I. Martin, J. C. Richmond and D. L. Kaplan, "Silk matrix for tissue engineered anterior cruciate ligaments," *Biomaterials*, vol. 23, pp. 4131-4141, 2002.
- [95] H. Zhang, L.-l. Li, F.-y. Dai, H.-h. Zhang, B. Ni, W. Zhou, X. Yang and Y.-z. Wu, "Preparation and characterization of silk fibroin as a biomaterial with potential for drug delivery," *Journal of Translational Medicine*, vol. 10, no. 117, pp. 1-9, 2012.
- [96] M. Tomita, "Transgenic silkworms that weave recombinant proteins into silk cocoons," *Biotechnol Lett*, vol. 33, pp. 645-654, 2011.
- [97] K. Numata and D. L. Kaplan, "Silk-based delivery systems of bioactive molecules," *Advanced Drug Delivery Reviews*, vol. 62, pp. 1497-1508, 2010.
- [98] S. Kubik, "High-Performance Fibers from Spider Silk," *Angew. Chem. Int. Ed.*, vol. 41, no. 15, pp. 2721-2723, 2002.
- [99] P. N. Khanam, M. M. Reddy, K. Raghu, K. John and S. V. Naidu, "Tensile, Flexural and Compressive Properties of Sisal/Silk Hybrid Composites," *Journal of Reinforced Plastics and Composites*, vol. 26, no. 10, pp. 1065-1070, 2007.
- [100] H.-y. Cheung, M.-p. Ho, K.-t. Lau, F. Cardona and D. Hui, "Natural fibre-reinforced composites for bioengineering and environmental engineering applications," *Composites: Part B*, vol. 40, pp. 655-663, 2009.
- [101] P. M. Cunniff, S. A. Fossey, M. A. Auerbach and J. W. Song, "Mechanical Properties of Major Ampulate Gland Silk Fibers Extracted from *Nephila clavipes* Spiders," in *Silk Polymers*, D. Kaplan and et al., Eds., Washington, DC, American Chemical Society, 1994.
- [102] P. Bajaj and Sriram, "Ballistic protective clothing: An overview," *Indian Journal of Fibre & Textile Research*, vol. 22, pp. 274-291, 1997.
- [103] N. A. Morrison, F. I. Bell, A. Beautrait, J. Ritchie, C. Smith, I. J. McEwen and C. Viney, "Do Natural Silks Make Good Engineering Materials?," in *Mat. Res. Soc. Symp. Proc.*, 2004.
- [104] C. Müller, M. Hamedi, R. Karlsson, R. Jansson, R. Marcilla, M. Hedhammar and O. Inganäs, "Woven Electrochemical Transistors on Silk Fibers," *Advanced Materials*, vol. 23, pp. 898-901, 2011.
- [105] M. Gandhi, H. Yang, L. Shor and F. Ko, "Post-spinning modification of electrospun nanofiber nanocomposite from *Bombyx mori* silk and carbon nanotubes," *Polymer*, vol. 50, pp. 1918-1924,

2009.

- [106] H. Tao, M. A. Brenckle, M. Yang, J. Zhang, M. Liu, S. M. Siebert, R. D. Averitt, M. S. Mannoor, M. C. McAlpine, J. A. Rogers, D. L. Kaplan and F. G. Omenetto, "Silk-Based Conformal, Adhesive, Edible Food Sensors," *Advanced Materials*, vol. 24, pp. 1067-1072, 2012.
- [107] C. Viney, "Silk Fibers: Origins, Nature and Consequences of Structure," in *Structural Biological Materials*, Oxford, Pergamon/Elsevier Science, 2000, pp. 293-333.
- [108] J. Pérez-Rigueiro, C. Viney, J. Llorca and M. Elices, "Silkworm Silk as an Engineering Material," *Journal of Applied Polymer Science*, vol. 70, pp. 2439-2447, 1998.
- [109] H.-P. Zhao, X.-Q. Feng, S.-W. Yu, W.-Z. Cui and F.-Z. Zou, "Mechanical properties of silkworm cocoons," *Polymer*, vol. 46, pp. 9192-9201, 2005.
- [110] H.-P. Zhao, X.-Q. Feng, W.-Z. Cui and F.-Z. Zou, "Mechanical properties of silkworm cocoon pelades," *Engineering Fracture Mechanics*, vol. 74, pp. 1953-1962, 2007.
- [111] E. J. Reed, L. L. Bianchini and C. Viney, "Sample Selection, Preparation Methods, and the Apparent Tensile Properties of Silkworm (*B. mori*) Cocoon Silk," *Biopolymers*, vol. 97, no. 6, pp. 397-407, 2012.
- [112] H.-Y. Cheung, K.-T. Lau, M.-P. Ho and A. Mosallam, "Study on the Mechanical Properties of Different Silkworm Silk Fibers," *Journal of Composite Materials*, vol. 43, no. 22, pp. 2521-2531, 2009.
- [113] R. B. Abernethy, *The new Weibull handbook: reliability & statistical analysis for predicting life, safety, survivability, risk, cost and warranty claims*, 5th ed., North Palm Beach, Florida: Robert B. Abernethy, 2006.
- [114] M. Ghosh, A. Mukhopadhyay and U. K. Mukhopadhyay, "Effect of air pollution on physiology and yield of mulberry silkworm, *Bombyx mori* L.," *Research Journal of Chemistry and Environment*, vol. 17, no. 5, pp. 60-68, 2013.
- [115] C. Fu, D. Porter and Z. Shao, "Moisture Effects on *Antheraea pernyi* Silk's Mechanical Property," *Macromolecules*, vol. 42, pp. 7877-7880, 2009.
- [116] G. R. Plaza, P. Corsini, J. Pérez-Rigueiro, E. Marsano, G. V. Guinea and M. Elices, "Effect of Water on *Bombyx mori* Regenerated Silk Fibers and Its Application in Modifying Their Mechanical Properties," *Journal of Applied Polymer Science*, vol. 109, pp. 1793-1801, 2008.
- [117] T. Seydel, W. Knoll, I. Greving, C. Dicko, M. M. Koza, I. Krasnov and M. Müller, "Increased molecular mobility in humid silk fibers under tensile stress," *Physical Review*, vol. 83, pp. 1-9, 2011.
- [118] P. Colomban, H. M. Dinh, A. Bunsell and B. Mauchamp, "Origin of the variability of the mechanical properties of silk fibres: 1 - The relationship between disorder, hydration and stress/strain behaviour," *Journal of Raman Spectroscopy*, vol. 43, pp. 425-432, 2012.
- [119] B. Mortimer, D. R. Drodge, K. I. Dragnevski, C. R. Siviour and C. Holland, "In situ tensile tests of single silk fibres in an environmental scanning electron microscope (ESEM)," *J Mater Sci*, vol. 48, pp. 5055-5062, 2013.

- [120] S. Das and A. Ghosh, "Study of Creep, Stress Relaxation, and Inverse Relaxation in Mulberry (*Bombyx mori*) and Tasar (*Antheraea mylitta*) Silk," *Journal of Applied Polymer Science*, vol. 99, pp. 3077-3084, 2006.
- [121] J. Ritchie, C. Smith, F. I. Bell, I. J. McEwen and C. Viney, "Effects of Wetting and Desiccation on the Creep Properties of Spider Dragline Silk," in *Mater. Res. Soc. Symp. Proc.*, 2005.
- [122] J. Pérez-Rigueiro, L. Biancotto, P. Corsini, E. Marsano, M. Elices, G. R. Plaza and G. V. Guinea, "Supramolecular organization of regenerated silkworm silk fibers," *International Journal of Biological Macromolecules*, vol. 44, pp. 195-202, 2009.
- [123] G. R. Plaza, P. Corsini, E. Marsano, J. Pérez-Rigueiro, M. Elices, C. Riekkel, C. Vendrely and G. V. Guinea, "Correlation Between Processing Conditions, Microstructure and Mechanical Behavior in Regenerated Silkworm Silk Fibers," *Journal of Polymer Science Part B: Polymer Physics*, vol. 50, pp. 455-465, 2012.
- [124] W. Wei, Y. Zhang, Y. Zhao, J. Luo, H. Shao and X. Hu, "Bio-inspired capillary dry spinning of regenerated silk fibroin aqueous solution," *Materials Science and Engineering C*, vol. 31, pp. 1602-1608, 2011.
- [125] M. Sun, Y. Zhang, Y. Zhao, H. Shao and X. Hu, "The structure-property relationships of artificial silk fabricated by dry-spinning process," *Journal of Materials Chemistry*, vol. 22, pp. 18372-18379, 2012.
- [126] J. Luo, Y. Zhang, Y. Huang, H. Shao and X. Hu, "A bio-inspired microfluidic concentrator for regenerated silk fibroin solution," *Sensors and Actuators B*, vol. 162, pp. 435-440, 2012.
- [127] C. Viney and F. I. Bell, "Inspiration versus duplication with biomolecular fibrous materials: learning nature's lessons without copying nature's limitations," *Current Opinion in Solid State and Materials Science*, vol. 8, pp. 165-171, 2004.
- [128] Z. Shao and F. Vollrath, "Surprising strength of silkworm silk," *Nature*, vol. 418, p. 741, 2002.
- [129] Y. Tanaka, Y.-J. Hua, L. Roller and S. Tanaka, "Corazonin reduces the spinning rate in the silkworm, *Bombyx mori*," *Journal of Insect Physiology*, vol. 48, pp. 707-714, 2002.
- [130] J. A. Veenstra, "Isolation and structure of corazonin, a cardioactive peptide from the American cockroach," *Federation of European Biochemical Societies*, vol. 250, no. 2, pp. 231-234, 1989.
- [131] G. R. Plaza, P. Corsini, E. Marsano, J. Pérez-Rigueiro, L. Biancotto, M. Elices, C. Riekkel, F. Agulló-Rueda, E. Gallardo, J. M. Calleja and G. V. Guinea, "Old Silks Endowed with New Properties," *Macromolecules*, vol. 42, pp. 8977-8982, 2009.
- [132] S. Keten and M. J. Buehler, "Geometric Confinement Governs the Rupture Strength of H-bond Assemblies at a Critical Length Scale," *Nano Letters*, vol. 8, no. 2, pp. 743-748, 2008.
- [133] S. Keten, Z. Xu, B. Ihle and M. J. Buehler, "Nanoconfinement controls stiffness, strength and mechanical toughness of β -sheet crystals in silk," *Nature Materials*, vol. 9, pp. 359-367, 2010.
- [134] O. Ahumada, M. Cocca, G. Gentile, E. Martuscelli and L. D'Orazio, "Uniaxial Tensile Properties of Yarns: Effects of Moisture Level on the Shape of Stress-Strain Curves," *Textile Research Journal*,

- vol. 74, no. 11, pp. 1001-1006, 2004.
- [135] A. U. Ude, A. K. Ariffin, K. Sopian and C. H. Azhari, "Energy attenuation capability of woven natural silk/epoxy composite plates subjected to drop-weight impacts," *ARPJ Journal of Engineering and Applied Sciences*, vol. 5, no. 8, pp. 75-87, 2010.
- [136] A. U. Ude, A. K. Ariffin and C. H. Azhari, "An Experimental Investigation of the Response of Woven Natural Silk Fiber/Epoxy Sandwich Composite Panels Under Low Velocity Impact," *Fibers and Polymers*, vol. 14, no. 1, pp. 127-132, 2013.
- [137] S. P. Priya, H. V. Ramakrishna, S. K. Rai and A. V. Rajulu, "Tensile, Flexural, and Chemical Resistance Properties of Waste Silk Fabric-reinforced Epoxy Laminates," *Journal of Reinforced Plastics and Composites*, vol. 24, no. 6, pp. 643-648, 2005.
- [138] J. Mijović and J. Wijaya, "Review of Cure of Polymers and Composites by Microwave Energy," *Polymer Composites*, vol. 11, no. 3, pp. 184-191, 1990.
- [139] K.-Y. Lee, B. J. Park, D. H. Lee, I.-S. Lee, S. O. Hyun, K.-H. Chung and J.-C. Park, "Sterilization of *Escherichia coli* and MRSA using microwave-induced argon plasma at atmospheric pressure," *Surface & Coatings Technology*, vol. 193, pp. 35-38, 2005.
- [140] B. J. Park, K. Takatori, Y. Sugita-Konishi, I.-H. Kim, M.-H. Lee, D.-W. Han, K.-H. Chung, S. O. Hyun and J.-C. Park, "Degradation of mycotoxins using microwave-induced argon plasma at atmospheric pressure," *Surface & Coatings Technology*, vol. 201, pp. 5733-5737, 2007.
- [141] D. E. Clark and W. H. Sutton, "Microwave processing of materials," *Annu. Rev. Mater. Sci.*, vol. 26, pp. 299-331, 1996.
- [142] L. Zhou, N. Yan, H. Zhang, X. Zhou, Q. Pu and Z. Hu, "Microwave-accelerated derivatization for capillary electrophoresis with laser-induced fluorescence detection: A case study for determination of histidine, 1- and 3-methylhistidine in human urine," *Talanta*, vol. 82, pp. 72-77, 2010.
- [143] C. O. Kappe and A. Stadler, *Microwaves in Organic and Medicinal Chemistry*, vol. 25, R. Mannhold, H. Kubinyi and G. Folkers, Eds., Weinheim: WILEY-VCH Verlag GmbH & Co. KGaA, 2005.
- [144] D. Stuerge, "Microwave-Material Interactions and Dielectric Properties, Key Ingredients for Mastery of Chemical Microwave Processes," in *Microwaves in Organic Synthesis, Second edition*, A. Loupy, Ed., WILEY-VCH Verlag GmbH & Co. KGaA, Weinheim, 2006.
- [145] R. D. Knight, *Physics for Scientists and Engineers: a Strategic Approach*, San Francisco: Addison Wesley, 2004, p. 631.
- [146] G. R. Login, J. B. Leonard and A. M. Dvorak, "Calibration and Standardization of Microwave Ovens for Fixation of Brain and Peripheral Nerve Tissue," *Methods: A Companion to Methods in Enzymology*, vol. 15, pp. 107-117, 1998.
- [147] R. D. Knight, *Physics for Scientists and Engineers: a Strategic Approach*, San Francisco: Addison Wesley, 2004, p. 527.
- [148] A. F. Mills, *Basic Heat and Mass Transfer*, 2nd ed., Upper Saddle River: Prentice Hall, 1999, p. 926.

- [149] D. L. Dunaway, B. L. Thiel, S. G. Srinivasan and C. Viney, "Characterizing the cross-sectional geometry of thin, non-cylindrical, twisted fibres (spider silk)," *Journal of Materials Science*, vol. 30, pp. 4161-4170, 1995.
- [150] M. I. Sullivan, *Statistics: Informed Decisions Using Data*, Upper Saddle River, New Jersey: Pearson Prentice Hall, 2007.
- [151] J. C. Fothergill, "Estimating the Cumulative Probability of Failure Data Points to be Plotted on Weibull and other Probability Paper," *IEEE Transactions on Electrical Insulation*, vol. 25, no. 3, pp. 489-492, 1990.
- [152] R. W. Work, "A Comparative Study of the Supercontraction of Major Ampullate Silk Fibers of Orb-Web-Building Spiders (Araneae)," *Journal of Arachnology*, vol. 9, no. 3, pp. 299-308, 1981.
- [153] F. I. Bell, I. J. McEwen and C. Viney, "Supercontraction stress in wet spider dragline," *Nature*, vol. 416, p. 37, 2002.
- [154] J. Pérez-Rigueiro, M. Elices and G. V. Guinea, "Controlled supercontraction tailors the tensile behaviour of spider silk," *Polymer*, vol. 44, pp. 3733-3736, 2003.
- [155] K. N. Savage, P. A. Guerette and J. M. Gosline, "Supercontraction Stress in Spider Webs," *Biomacromolecules*, vol. 5, pp. 675-679, 2004.
- [156] J. Pérez-Rigueiro, C. Viney, J. Llorca and M. Elices, "Mechanical properties of silkworm silk in liquid media," *Polymer*, vol. 41, pp. 8433-8439, 2000.
- [157] K. Nakamura, T. Hatakeyama and H. Hatakeyama, "Effect of Bound Water on Tensile Properties of Native Cellulose," *Textile Research Journal*, vol. 53, pp. 682-688, 1983.
- [158] S. Carmichael and C. Viney, "Molecular Order in Spider Major Ampullate Silk (Dragline): Effects of Spinning Rate and Post-Spin Drawing," *Journal of Applied Polymer Science*, vol. 72, pp. 895-903, 1999.
- [159] M. A. Garrido, M. Elices, C. Viney and J. Pérez-Rigueiro, "The variability and interdependence of spider drag line tensile properties," *Polymer*, vol. 43, pp. 4495-4502, 2002.
- [160] H. Tabunoki, S. Higurashi, O. Ninagi, H. Fujii, Y. Banno, M. Nozaki, M. Kitajima, N. Miura, S. Atsumi, K. Tsuchida, H. Maekawa and R. Sato, "A carotenoid-binding protein (CBP) plays a crucial role in cocoon pigmentation of silkworm (*Bombyx mori*) larvae," *FEBS Letters*, vol. 567, pp. 175-178, 2004.
- [161] Y. Tamura, K.-i. Nakajima, K.-i. Nagayasu and C. Takabayashi, "Flavonoid 5-glucosides from the cocoon shell of the silkworm, *Bombyx mori*," *Phytochemistry*, vol. 59, pp. 275-278, 2002.
- [162] A. Kurioka and M. Yamazaki, "Purification and Identification of Flavonoids from the Yellow Green Cocoon Shell (Sasamayu) of the Silkworm, *Bombyx mori*," *Biosci. Biotechnol. Biochem.*, vol. 66, no. 6, pp. 1396-1399, 2002.
- [163] T. Sakudoh, H. Sezutsu, T. Nakashima, I. Kobayashi, H. Fujimoto, K. Uchino, Y. Banno, H. Iwano, H. Maekawa, T. Tamura, H. Kataoka and K. Tsuchida, "Carotenoid silk coloration is controlled by a carotenoid-binding protein, a product of the Yellow blood gene," *Proc Natl Acad Sci USA*, vol. 104,

- no. 21, pp. 8941-8946, 2007.
- [164] S. Putthanasarat, P. Tapadia, S. Zarkoob, L. D. Miller, R. K. Eby and W. W. Adams, "The color of dragline silk produced in captivity by the spider *Nephila clavipes*," *Polymer*, vol. 45, pp. 1933-1937, 2004.
- [165] K. Tsuchida, Z. E. Jouni, J. Gardetto, Y. Kobayashi, H. Tabunoki, M. Azuma, H. Sugiyama, N. Takada, H. Maekawa, Y. Banno, H. Fujii, H. Iwano and M. A. Wells, "Characterization of the carotenoid-binding protein of the Y-gene dominant mutants of *Bombyx mori*," *Journal of Insect Physiology*, vol. 50, pp. 363-372, 2004.
- [166] ASTM International, "Standard Test Method for Calibration of Microwave Ovens, ASTM F 1317 - 98 (Reapproved 2007 and 2012)," 100 Barr Harbor Drive, P.O. Box C700, West Conshohocken, PA.
- [167] S. A. Barringer, E. A. Davis, J. Gordon, K. G. Ayappa and H. T. Davis, "Effect of Sample Size on the Microwave Heating Rate: Oil vs. Water," *AIChE Journal*, vol. 40, no. 9, pp. 1433-1439, September 1994.
- [168] S. A. Barringer, E. A. Davis, J. Gordon, K. G. Ayappa and H. T. Davis, "Microwave-Heating Temperature Profiles for This Slabs Compared to Maxwell and Lambert Law Predictions," *Journal of Food Science*, vol. 60, no. 5, pp. 1137-1142, 1995.
- [169] R. D. Knight, *Physics for Scientists and Engineers: a Strategic Approach*, San Francisco: Addison Wesley, 2004, p. 653.
- [170] W. M. Haynes, Ed., *CRC Handbook of Chemistry and Physics*, 93rd ed., Boca Raton, FL: Taylor & Francis Group, 2012, pp. 6-14.
- [171] M. V. Goldman, "Microwave Ovens," [Online]. Available: <http://www.colorado.edu/physics/2000/microwaves/mwintro.html>. [Accessed March 7, 2013].
- [172] R. Somashekar and R. G. Urs, "Effect of annealing on crystal size in pure Mysore silk fibres," *Bull. Mater. Sci.*, vol. 14, no. 1, pp. 87 - 91, February 1991.
- [173] N. Yoshikawa, E. Ishizuka and S. Taniguchi, "Heating of Metal Particles in a Single-Mode Microwave Applicator," *Materials Transactions*, vol. 47, no. 3, pp. 898-902, 2006.
- [174] R. G. K. Urs, G. Subramanya and R. Somashekar, "Crystal Size and Minimum Enthalpy of Various Races of Silk Fibers," *Textile Res. J.*, vol. 63, no. 10, pp. 610-613, 1993.
- [175] E. J. Reed and C. Viney, "The Effect of Microwave Radiation on Tensile Properties of Silkworm (*B. mori*) Silk," in *Mater. Res. Soc. Symp. Proc. Vol. 1301*, 2011.
- [176] E. J. Reed and C. Viney, "Does Thermal Annealing Affect the Mechanical Properties of Silkworm (*Bombyx mori*) Cocoon Silk?," in *Mater. Res. Soc. Symp. Proc. Vol. 1465*, 2012.